JIMMA UNIVERSITY

JIMMA INSTITUTE OF TECHNOLOGY

SCHOOL OF GRADUATE STUDIES

CIVIL ENGINEERING DEPARTMENT

EVALUATION OF STRUT AND TIE MODEL FOR RC DEEP BEAMS USING NONLINEAR FINITE ELEMENT ANALYSIS

A Thesis Submitted to School of Graduate Studies in Partial Fulfillment of the Requirements for Degree of Master of Science; in Civil Engineering with Specialty in Structural Engineering

By
Meseret Shimelis

December, 2017

JIMMA UNIVERSITY

JIMMA INSTITUTE OF TECHNOLOGY

SCHOOL OF GRADUATE STUDIES

CIVIL ENGINEERING DEPARTMENT

EVALUATION OF STRUT AND TIE METHOD FOR RC DEEP BEAMS USING NONLINEAR FINITE ELEMENT ANALYSIS

A Thesis Submitted to School of Graduate Studies in Partial Fulfillment of the Requirements for Degree of Master of Science; in Civil Engineering with Specialty in Structural Engineering

By

Meseret Shimelis

Main advisor: Temesgen Wondimu (PhD)

Co-advisor: Diosdado John Corpuz (MSc.), Asso. Prof.

Declaration

This thesis report is my original work and I have made all the necessary effort as it has not been presented for a Master degree in any other university, and that all sources of material used for the research paper have been duly acknowledged.

By

Meseret Shimelis _____ _____

Signature Date

Approved by Board of Examiners

Temesgen Wondimu (PhD) _____ _____

Main Advisor Signature Date

Diosdado John Corpuz (MSc.) _____ _____

Co-advisor Signature Date

_____ _____ _____

External Examiner Signature Date

_____ _____ _____

Internal Examiner Signature Date

_____ _____ _____

Chairman Signature Date

ACKNOWLEDGEMENT

First of all I would like to thank almighty God for giving the energy and patience in accomplishing this thesis work. Likewise I would like to thank my advisors Dr. Temesgen Wondimu and Mr. Diosdado John Corpuz (MSc.) for their special help during the preparation of this document starting from consulting on my title selection and objective developments, development until assemblage of the final document.

ABSTRACT

This work proposes alternative analytical method for the prediction of ultimate load carrying capacity of reinforced concrete deep beams to that of strut-and-tie method. Three categories each category with five reinforced concrete deep beam specimens of shear span to depth ratio 1.00, 1.25, 1.50, 1.75 and 2.00 are studied. The beams are studied first analytically and then results from analytical method are validated by using nonlinear finite element analysis. It is confirmed that the result from analytical method for ultimate load capacity is in best agreement with nonlinear finite element analysis and this shows that the analytic approach used to predict ultimate load capacity is applicable.

In the next session of the work a case study is carried out to determine the influence of some parameters on the predictive capacity of the proposed analytic method. Generally the effect of main reinforcement and web reinforcement ratios are covered in the parametric study part. For all categories the results from parametric study indicates that the increase in main reinforcement ratio has showed significant increase up to ultimate load and further increase will not affect the ultimate load capacity. In the same manner the increase in web reinforcement ratio either vertical or horizontal reinforcement ratio for all categories resulted in a linear load capacity increase especially for deep beams with shear span to depth ratio 1.00, 1.25 and 1.50. But for deep beams with shear span to depth ratios of 1.75 and 2.00 significant increases in load carrying capacity is not recorded. Also the diagrams for ultimate load versus vertical and horizontal reinforcement ratio for all categories indicate that vertical web reinforcement ratio is effective in increase ultimate load carrying capacity than for the same increase in horizontal web reinforcement ratio.

Keywords: CONCRETE SOFTENING, STRUT, TIE, DISCRETIZATION, CONSTRAINT:

TABLE OF CONTENT

Contents

LIST OF TABLES

LIST OF FIGURES

LIST OF SYMBOLS AND ABREVATIONS

β : Dilation angle

m : Eccentricity of the plastic potential surface

γ : The parameter used in yield surface called the ratio of second stress invariant on the tensile meridian to that on the compressive meridian

μ : Viscous parameter used in concrete damage plasticity model

$f_{ck,cube}$: Cylindrical cube characteristic compressive strength

f'_c: 28th day characteristic compressive strength of concrete

f_t: Tensile strength contribution from reinforcement and concrete

σ_c : Compressive stress of concrete

ε_c : Compressive strain of concrete

ε_{c1} : The strain at peak stress in the stress-strain relationship

ε_{cu1} : Nominal ultimate strain of concrete

η : A parameter used to the ratio compressive strain of concrete

v: Ultimate shear strength reduction factor derived in this research paper

f_{ct}: Tensile strength of concrete

f_{ctk}: Characteristic compressive strength of concrete

G_f: Fracture energy parameter

f_{cm}: Mean compressive strength of concrete according to EN2/1992

f_y: Yield strength of steel reinforcement

w_t: Width of tie in STM

w_c: Width of compressive strut balancing flexural reinforcement

k: Nonlinear stress distribution factor

f_1: Tensile stress in the diagonal strut in perpendicular direction

f_2: Compressive stress in the strut and parallel to it

A_{str}: Cross-sectional area of diagonal compressive strut

l_b: Length of bearing plate at support

E_s: Modulus of elasticity of steel reinforcement

E_c: Modulus of elasticity of concrete

E_{cm}: Mean modulus of elasticity of concrete

A_s: Area of main steel reinforcement

A_{sv}: Area of vertical web steel reinforcement

A_{sh}: Area of horizontal web steel reinforcement

f_{yd}: Design yield strength of steel reinforcement

θ_s : Angle of the compressive strut from horizontal

a_v: Shear span of a deep beam

V_n: Ultimate shear strength

T_s: The tensile force present in the tie of strut and tie model

jd: flexural lever arm

h: Total depth of a beam

A_c: Cross sectional area of the beam

b_w: width of the beam

w_t: Width of tie in struts and tie model

w_c: With of compressive strut in strut and tie model

d_t: Tension damage

d_c: Compression damage

G: The flow potential in the Drucker-prager hyperbolic function Equation

ρ_s : Main steel reinforcement ratio

ρ_v : Vertical web steel reinforcement ratio

ρ_h : Horizontal steel reinforcement ratio

P_{pre}: Analytically predicted ultimate load

P_{FEA}: Finite element analysis ultimate load

BVPs: Boundary value problems

NLFEA: Nonlinear Finite Element Analysis

FEA: Finite Element Analysis

RC: Reinforced Concrete

CMSD: The crack mouth sliding displacement

MPa: Mega Pascal (SI unit of stress)

GPa: Giga Pascal (SI unit of stress)

ACI: American Concrete Institution

AASHTO: American Association State Highway Transportation Officials

EN: Euro Norm for Euro Code

STM: Strut-and-Tie Model/Method

LRFD: Load Resistance Factor Design

CPD: Concrete plasticity damage

CDM: Concrete damage model

CDPM: Concrete damage plasticity model

C3D8R: An 8-node linear brick element, with reduced integration, hourglass control.

T3D3H: A 3-node quadratic 3-D truss element, with hybrid integration.

MCF: Modified compression field theory

CV: Coefficient of Variance

SD: Standard deviation

1. INTRODUCTION

1.1. Background of the Study

Deep beams play a very significant role in design of large as well as small structures. Some times for architectural purposes buildings are designed without using any column for a very large span. In such case if ordinary beams are provided they can cause failure such as flexural failure. In addition, most widely popular application of deep beams in construction industry is in construction of transfer girders in offshore structures and foundations, walls of bunkers, load bearing walls in buildings, plate elements in folded plates, pile caps, floor diaphragm and shear walls are the most important once [1].

The structural behavior of reinforced concrete deep beams has been proved to be different when compared with slender or short beams. One of the important parameters controlling this change is its shear span to depth ratio which depends on the depth of the beam [1]. Since this ratio is small in deep beams, there is a significant change in the strain distribution across the deep beam's depth. This variation of strain is non-linear and is not seen in ordinary slender beams. Shear deformation which is insignificant in ordinary beams is considered to be substantial in deep beams and hence it cannot be ignored as this factor is also associated with the depth and span of the beam. In such cases it has been recognized that the finite element method can provide realistic and satisfactory solutions for nonlinear behavior of reinforced concrete structures [2].

The analysis follows the truss analogy approach, in which parallel inclined cracks are assumed and expected to be formed in the regions of high shear. Essentially the reinforcement in strut-and-tie model acts as a tie and, hence reinforced concrete deep beams are analogous to steel trusses. Deep beams are also classified as disturbed regions, which are characterized by nonlinear strain distribution [3]. Elastic solutions of deep beams provide a good description of their behavior before cracking [3]. However, after cracking major redistribution of strains and stresses takes place and the beam strength must be predicted by nonlinear analysis [4]. Basically this research paper is aimed at employing this nonlinear analysis method in such a way that major stress redistribution

will take place after elastic capacity range and to give consideration to the importance of reserved capacity after elastic stage.

1.1.1. Current Conditions and Expected Output

Currently, Strut-and-Tie model based design is considered as the most simple and applicable method which can be used to simplify analysis and design of deep beams [5]. A lot of researchers are devoted to investigate a parametric study on the effect of ultimate load capacity [5]. Significant or impressive parameters on shear behavior of deep beams have been identified including concrete compressive strength, shear span to depth ratio, amount and arrangement of shear reinforcement and amount of main reinforcement [5]. Even though these and other parameters are expected to affect the behavior of deep beams under ultimate condition, and this is also investigated by parametric studies, it is interesting to incorporate these parameters in the determination of strength of strut-and-tie components. But this is not incorporated in ACI318-08 design code and it is tried to incorporate these parameters such as main and web reinforcement terms in the ultimate strength prediction equation is seen as interesting.

Therefore, incorporation of parameters mainly main and web reinforcement ratios into strength prediction expressions of strut-and-tie model components is expected to be achievement of this research paper. A test conducted on deep beam specimens by [5] and the result has shown that vertical and horizontal shear reinforcements are efficient in shear capacity of deep beams, also the orthogonal shear reinforcement was the most efficient was the most efficient when placed perpendicular to major axis of diagonal crack. Also concentrating of shear reinforcement within middle region of shear span can improve the ultimate shear strength of deep beam. The test results were compared with the predicted ultimate strengths using the ACI318-08 provision, ACI code tended to unsafe or scatter results and the performed investigations deduced that the ACI code provisions need to be revised [5].

The study of behavior of concrete structures especially deep beams when subjected to loads is open ended. This is evidenced by findings made and inconsistencies solution approaches and design procedures followed by design codes even when applying the same method, such as [6] and [7]. The variation by the design codes arises due to the

empirical nature of equations used to predict the capacity of the member. Therefore, the analytic method is supposed to best predict the ultimate capacity of deep reinforced concrete sections covered in this work.

1.2. Statement of the Problem

The use of deep beams at lower levels in tall buildings for both residential and commercial purpose as well in the construction of bridges as transfer girders has increased rapidly because of their convenience and economic efficiency [8]. Due to this increased demand of the structural members in the growing construction technology necessitates the in depth investigation of analytical procedures that can accurately predict the ultimate capacity of the members so that the premature failure that hinders the service life of the utility is maintained at serviceability limit state condition.

Due to this growing demand using this structural member a simple and refined method of design approach is always needed. This inconsistency is seen from literatures done by different authors at different time and in different design codes as in [9] and [10]. Though the STM is effective for the design of D-regions, the method has not yet been widely implemented due to many reasons such as;

a) The difficulty in fixing an optimum truss configurations for a given structural member with given loading
b) The complexity and approximation of the solution and the inability of the STM to predict the failure mode of deep beams

In addition since the behavior of reinforced concrete deep beams under ultimate load is very complex it is seen that the study on deep reinforced concrete beams as interesting field of study by varying ultimate load influencing parameters and this is expected to lead in the most consistent and accurate approach with more refined methods of solution such as finite element method.

Therefore, this has initiated further study for ultimate loading condition and establishing consistent analytic expression capable of predicting unique ultimate load capacity which was the main drawback of strut and tie method lacking prediction of unique solution; and

this is assumed to be achieved with the help of nonlinear finite element analysis by using Abaqus/Standard as numerical simulating software.

1.3. Research Questions

This research paper in more general term tries to answer the question of determining the ultimate load carrying capacity of representative categories of reinforced concrete deep beams by conducting a case study in most refined approach than previous studies. Particularly, the following major issues are given special consideration.

i. What simpler and refined analytic expression can predict the behavior of reinforced concrete deep beams under ultimate load condition in a particularly selected truss configuration under STM?
ii. How the main parameters that affect the ultimate load capacity of reinforced concrete deep beam?
iii. How the web (vertical and horizontal) reinforcement ratio affect the ultimate load carrying capacity of reinforced concrete deep beams?

1.4. Research Objectives

1.4.1. General Objective

The general objective of this research is:

- To evaluate the Strut-and-Tie method for reinforced concrete deep beam by using nonlinear finite element analysis and to establish analytic expression that capable of predicting the ultimate load carrying capacity of reinforced concrete deep beam specimens by means of case study taking advantage of nonlinear finite element numerical simulation results as validation tool.

1.4.2. Specific Objectives

The specific objectives of this research are:

- To establish analytic expression that predicts the ultimate load capacity of reinforced concrete deep beams that is in best agreement with the nonlinear finite element numerical simulation results.

- To determine the failure mode of failure of reinforced concrete deep beams under ultimate loads
- To examine and determine the influence or effect of longitudinal and web reinforcement ratios on ultimate load carrying capacity of reinforced concrete deep beams by conducting parametric study.

1.5. Significance of the Study

The wide range of alternatives in the selection of the path of forces which represent the compressive struts and the tension ties to determine the truss configuration to apply STM intersecting at nodes and the choice of locations where the corresponding reinforcement is to be placed is the primary objective. But, it is improbable to find a unique solution for a single problem at hand. While selecting the truss configuration there can be several possible truss configurations for a single problem which is subject of designer experience, leading to as many possible solutions and for unique solution experience plays a key role. Otherwise this approach is more an art than an engineering science in the selection of the models. But of many possible solutions suggested by designers even for a single problem there has to be only one solution exactly fitting the problem at hand. This unique solution for a single problem has to satisfy the basic assumptions and requirements which grant the application of the method employed. As to have ductile design this research paper is said to be significant in that it assess the yield condition of main reinforcement prior to concrete crushing takes place. This is achieved by conducting nonlinear finite element numerical simulation of selected categories of deep beams. It could be advised that unless otherwise a more refined approach of problem solving such as nonlinear finite element analysis is carried out great precaution is required in selecting optimal truss configurations since infinite solutions are applicable and consequently leading to brittle design.

Therefore, this research is significant in that for any force path or STM selected for a particular problem nonlinear finite element numerical analysis will lead to a unique solution and un experienced designers achieve confidence of designing and analyzing deep reinforced concrete sections in a ductile fashion and used to correlate results with

analytic solutions. This is obtained to be ductile failure as assumed in STM design method which is shown by yielding of flexural reinforcement.

1.6. Basic Assumptions Made in This Research Paper

As far as the strut-and-tie method based analysis is going to be assessed in this research paper it is seen as appropriate to take into consideration the following assumptions.

i. The mechanism of shear resistance of reinforced concrete beam which is used for the analytic derivation of ultimate load prediction equation is at equivalent collapse stage of the same reinforced concrete deep beam analyzed by nonlinear finite element analysis. This implies reinforced concrete beam at ultimate load forms mechanism condition both analytically and finite element analysis for equal ultimate load.
ii. The assumption of embedded constraint in defining concrete rebar interaction would enable fully bonded condition and this is not practically achieved.
iii. The assumption of reinforcement as perfect-elastic-plastic material both in tension and compression is not practically correct.

1.7. Scope and Limitations Involved in This Research Paper

a) Computation of ultimate load capacity using the equation derived in this research paper is limited to the deep beams studied in the case study. Therefore for its general applicability further studies need to be conducted on other types of deep beams not studied in this research paper.
b) The ultimate load prediction equation derived in this research is confined to only two dimensional strut-and-tie truss configurations.
c) The proposed analytical approach is validated only by nonlinear finite element analysis numerical outputs. No further validation methods are employed.

2. LITERATURE REVIEW

2.1. Literatures Review and Existence of RC Deep Beams Investigation

The study on deep beams is not a recent task by investigators. To mention some of literatures which are in connection with this study and showing advancements in the field of study is considered to be important. Therefore when searching for available literatures which have played a profound role in the developments of methods and approaches to solve problems related to deep reinforced concrete section are described in the next successive paragraphs.

The study on deep beams is started by experimental studies conducted on wall type beams behavior by [11] in 1965 and [12] in 1966. They carried out the study in the form of numerical methods and this has contributed further the numerical study on deep beam is as a significant. After these, significant numbers of experimental studies have been reported on RC deep beam behavior with or without flange, with or without opening in the web, beams under different load condition as well as simple or continuous deep beams [13]. All these experimentations and analytical approaches has been contributing as an international references for practicing civil and structural design activities in different universities and institutions.

In addition to experimental studies on RC deep beams behavior, numerical simulation with finite element method is another important issue here to discuss about. Since 1962 which finite element method was first applied in analysis of concrete structures, it was rapidly developed in both theory and application. One of the earliest attempts [14] to analyze a reinforced concrete beams by means of discrete crack model. In this approach the crack location as well as the inclination is already defined and structure will be separated to two parts once crack takes place in the designated location. In this respect new element and new nodes should be generated to satisfy new situation of finite elements after cracking. Nevertheless the most important problem was that the model as a whole was not fit to the nature of finite element method, which is based on continuum mechanics. In order to circumvent the problem of geometry discontinuity, [15] proposed another method so-called smeared crack model, which deals with material discontinuity

in constitutive level and fits well with finite element nature. Since then this model has achieved great popularity among researchers and has been developed enormously.

However with the advent of those methods in modeling RC structures and computer rapid progress as a tool to analyze those engineers and researchers used to be facing certain problems in numerical modeling of concrete structures. In a way concrete structures usually do not behave as continuum as those we assume in continuum mechanics. A recent attempt in response to that problem was to take advantages of fracture mechanics in modeling concrete members. Fortunately finite element method is sufficiently general to model fracture nature of concrete as discrete or continuum phenomena. Since then this method has enjoyed enormous development to minimize fracture zone size effect in analytical results and several robust theories such as crack band model [16], non-local theory [17] and embedded crack model have been proposed and successfully applied in numerical simulation of concrete structures. Smeared crack model basically is based on average strain approach which is smeared out in entire element surface and divided to two main categories called ‘the fixed crack model’ and ‘the rotating crack model’. In the fixed crack theory the crack forms once principal tensile stress of concrete violates tensile strength of concrete. The crack direction will be fixed constant for the following steps. Consequent to this basic assumption a shear component will be produced due to rotation of the principal stress direction. In other words principal stress and principal strain direction need not to be coincide and shear and normal stress transfer will be modeled independently. The early version of smeared crack theory is based on this approach. On the other hand in the rotating crack approach the crack direction coincides with the principal direction of average stain therefore crack direction rotates following stress condition in each loading step. In this theory no shear transfer component will be produced and only normal stress-strain is needed to be modeled. Modified compression field theory [18] and softened truss theory [19].

The idea of using fracture mechanics in analyzing concrete structures initiated after realizing softening nature of concrete in tension by some researchers such as [20]. They found that better and realistic results can be obtained if concrete stress reduces gradually instead of sudden drop to zero. ACI Committee 446 in its latest approved report [21]

states five reasons that fracture mechanics need to be taken into account in concrete structures analysis including finite element method.

By far, information regarding the general principles of strut-and-tie modeling is the most extensively reported. Generally, these types of articles outline the procedure for determining B-and D-regions, determining boundary conditions, developing a truss model, solving for member forces, choosing and detailing reinforcement, and checking the stress conditions of nodes and struts. In addition to outlining the strut-and-tie model procedure, these documents also give suggestions for strut and node strengths and show some basic models for simple structural elements. These documents were some of the building blocks for in-depth research and reports that more closely examined items such as strut and node strengths, detailing and anchorage requirements for reinforcement, and strut-and-tie models for increasingly complex structural members. The literature search for articles dealing with the strength of struts and nodes also yielded a large amount of data. Determining the appropriate effective compressive strengths for different types of nodes and struts has been of interest to many researchers. Researchers have tried to determine the strengths for the different types of nodes and struts through both laboratory testing and analytical research. Despite the vast amount of research done in this area, there is no clear consensus among researchers on the strength of struts and nodes.

Simplified assumptions in design have been made in different design codes when applying strut-and-tie model to this structural element. These simplifications are necessitated because of the wide range of alternatives in the selection of the path of forces which represent the compressive struts and the tension ties intersecting at nodes and the choice of locations where the corresponding reinforcement is to be placed.

Therefore, depending on the interpretation of the designer, simplification of the paths of forces that are chosen to represent the real structure can considerably differ. Since this load-path modeling is plastic method with stress concentration conditions and load concentration, it does not provide a check for the serviceability levels inherent in the semi plastic methods but represents strength limit states at the critical sections. Thus, after excessive deformation and cracking which is observable at failure stage, the idealizations made in the choice of the force paths render this method less accurate for design

purposes, particularly no unique design solutions are possible. This approach is more an art than an engineering science in the selection of the models. Significant over design is therefore required and extensive full scale tests needed for different structural systems. Hence great precaution is required in selecting optimum truss configurations since infinite solutions are applicable and it does not provide a check on serviceability.

Existing methods of predicting deep beam behavior at failure involves either elastic theory or semi-empirical equation, neither of which entirely satisfactory [22]. The basic assumption that plane sections remain plane after loading and that the material is homogeneous and elastic do not hold for deep beams. Finite element method offers a powerful and general analytical tool for studying the behavior of reinforced concrete deep beams [23]. Finite element method as a tool can provide realistic and satisfactory solutions for linear and nonlinear behavior of deep beam structural elements [24].

Finite element method uses many elements in analyzing any continuum which makes it difficult for manual analysis. As the number of elements used increases, the computational effort required to prepare the output and interpret the results increase. For this reason computer based programs help to reduce the effect and complexity involved by analyzing a continuum using manual analysis. But some programs may contain limitation to process a large number of finite elements and which further depends on the machine performance used and capacity to process the desired output as required. Unlikely the accuracy of the program sometimes affects the accuracy of the result and modeling of the actual condition also required to obtain the desired output such that approximate analysis is carried out.

The reason for introducing or limiting the ultimate load condition as a function of ultimate load influencing parameters (variables) designated as strut strength reduction factor ν in this research of Eq. (1) below is to account for the limited ductility of concrete and to absorb other shortcomings of applying the theory of plasticity to concrete. In general ν for mean effective compressive strength f_{cm} of concrete can be determined by considering factors that reduce the compressive strength when concrete is subjected to

loads. These loads can be either of compressive or tensile, but responsible for compressive strength reduction and also tensile strength reduction.

Empirically, this can be set as in terms of mean cylindrical compressive strength f_{cm} and reduction factor *v* as in Eq. (1) by [25].

$$f_c = \nu f'_{cm} \quad \text{---------- (1)}$$

Where f_c is the reduced compressive strength

According to various codes and standards, the strut-and-tie model (STM) is a rational approach to analyze deep beams. The crushing strength of concrete strut in STM is evaluated based on the strut effectiveness factor *v* to take account of cracked condition. According to [26] available codes and standards are classified into two groups depending on the method utilized to calculate the strut strength reduction factor.

The first group comprises AASHTO LRFD, CSA-S6-06, CSA A23.3, and AS 3600, which define the strut strength reduction factor as a function of the principal tensile strain on the strut [27], [28] and [29]. This is mainly derived from research on modified compression-field (MCF) theory, which proposed the stress-strain relationship for cracked concrete in compression.

The second group comprises ACI 318-11, DIN 1045-1, NZS 3101, and model code 2010, which recommend a value for the strut strength reduction factor [30], [31], [32], and [33] depending on the grade of concrete and the satisfaction of the required minimum web reinforcement.

Since this research paper is programmed to alleviate the nonlinearity of concrete material model by using a suitable analytical model that takes account of concrete softening effect to support the codes and standards which are based on the modified compression field and Mohr-Coulomb failure theory. This is achieved by considering the concrete softening effect which is nonlinear behavior and a linear compression-tension interaction condition will be assumed.

2.2. Techniques Used to Determine Reduced Capacity in the Form of Effective Compressive Strength Reduction Coefficient

Different techniques were suggested by different authors for evaluating the effectiveness factor of concrete. The value of the effectiveness factor obtained is a function of the shape of the real stress strain curve, compressive strength and the ultimate strain of concrete. In addition [25] proposed a formula for the effectiveness factor of concrete beams failing in shear as a function of cylinder compressive strength of Eq. (2).

$$v = 0.8 - \frac{f_c'}{200} \quad \text{---------- (2)}$$

Where f_c' is in MPa

The above formula indicates that increasing the concrete strength reduces the value of the effectiveness factor as the lower the concrete strength. Although the plastic behavior of reinforced concrete structures is mainly influenced by the amount of reinforcement, it is better to propose a formula which considers the amount of reinforcement [34]. Based on statistical analysis for the strength reduction factor of concrete in continuous deep beams, proposed a formula for the strength reduction factor of concrete in continuous deep beams expressed in terms of concrete strength and amount of reinforcement below Eq. (3) [34].

$$v = 0.7 - \frac{f_c'}{110} - \frac{\rho}{0.85} \quad \text{---------- (3)}$$

Where f_c' is in $\frac{N}{mm^2}$

Where ρ is a weighted-reinforcement ratio for the horizontal and vertical reinforcement based on their relative contribution to the load capacity of continuous deep beams. Based on tests of concrete panels under shear, the shear strength reduction factor to the tensile strain normal to the principal compressive strain as expressed below by Eq. (4).

$$v = \frac{1}{1.0 + k_c k_f} \quad \text{---------- (4)}$$

Where $k_c = 0.35(-\frac{\varepsilon_1}{\varepsilon_3} - 0.28)^{0.8} \geq 1.0$ and $k_f = 0.1825\sqrt{f_c'} \geq 1.0$ and $\varepsilon_1, \varepsilon_3$ are principal tensile and compressive strains, respectively.

According to the value v of concrete is simply calculated by calibrating the failure loads obtained from the plasticity analysis against those from experiments [35]. This leads to conclude as this technique shows significant variation of v for different reinforced concrete structure [35]. The value of the factor for concrete wall structures failing in shear varies between 0.16 and 0.49 [36]. [37] Proposed values for the strength reduction factor varying from 0.25 to 0.85 depending on the concrete element in the plastic truss model used to predict the capacity of continuous deep beams. This is concluded that the best mean value of the strength reduction factor of reinforced concrete deep beams with fixed ends is 0.5 [38].

Following this [39] evaluated different v factor formulae used in strut-and-tie models of non-flexural members such as deep beams, corbels and nibs. He concluded that effectiveness factor models based primarily on concrete strength are found to have poor correlation with test results of 135 non flexural structural elements. He recommended that reduction factor models that account for the angle of the strut relative to the longitudinal axis of the structural member combined with models based on the modified compression field theory Eq.(4) above are found to give best correlation with the experimental results.

It is stated that shear strength of reinforced concrete beams without web reinforcement appears to decrease as the beam depth increases [40] and [41] and this size effect is less significant for beams with web reinforcement. It is that [42] modified the strength v proposed as in Eq. (4) by a size effect factor which is a function of deep beam effective depth and maximum size of aggregate. On the other hand, [43] suggested that size effect depends on factors such as the geometry of strut (width and length) and strut boundary conditions due to transverse web reinforcement (spacing and diameter). He proposed a modified strut and tie model that accurately predicts the size effect trends for deep beams, with a uniform safety margin for different member sizes considered.

The deformation capacity of the assumed truss configuration is the other questionable term. So due giving prime concern is seen as important, by authors [44] the validity of the chosen truss model for a reinforced concrete deep beam depends on whether the truss model represents the true situation reasonably close or not as reinforced concrete deep beams can undergo only a limited amount of redistribution of internal forces. Therefore,

if the chosen truss requires excessive deformation to reach the fully plastic state assumed, the beam may fail prematurely at a load lower than that predicted by the truss. Therefore to prevent the premature brittle failure type stated as in above it is necessary to determine the deformation capacity of the structure required by Lower Bound Theorem, which states the capacity obtained from all statically admissible stress fields is lower than or equal to the actual collapse load. In this research this could be assumed to be achievable by giving concern yielding of the main (tie) reinforcement. This will be proven by results from numerical simulation of deep reinforced concrete beams conducted on case study, so that failure is governed by yielding of main or longitudinal reinforcement.

Therefore this research is Strut-and-tie model worth in that it assess the behavior of failure of selected categories of reinforced concrete deep beams by using nonlinear finite element analysis to checkout yielding of main reinforcement and ductile failure is achieved at ultimate load condition and this further establishes confidence on applicability of strut and tie method in any deep concrete sections for the chosen truss configuration.

The prediction of ultimate load carrying capacity of continuous reinforced concrete deep beams in design manuals [45] is not clearly stated. The comparison of shear capacity test conducted on continuous specimens of deep beams using ACI318-08 and Egyptian concrete code of practice from the contributions of concrete, horizontal, and vertical shear reinforcement [45]. Both design methods showed that the amount of shear resisted by horizontal steel is higher than that resisted by vertical steel (contrary to testing results). This prediction indicates that ACI as well as Egyptian codes underestimate the shear capacity for continuous deep beams and this discrepancy in codes predictions may be attribute to the fact that the shear strength equations in both design methods for continuous deep beams are derive from simple spans [45].

2.3. Basics of Nonlinear Finite Element Analysis

The facts associated for choosing nonlinear finite element analysis as validation tool can be verified in the following paragraphs.

In this study, the damage plasticity model as implemented in the general purpose finite element software as a validation tool for the alternative analytical approach for the reinforced concrete deep beams ABAQUS [46] is used to study the behavior of reinforced concrete deep beams under ultimate load condition. The beam tested for validation of finite element analysis showed the ability to capture the whole concrete behavior up to failure with reliable accuracy when compared to the experimental results from [47]. The model uses the concepts of isotropic damaged elasticity in combination with isotropic tensile and compressive plasticity to represent the inelastic behavior of concrete. It assumes that the main two failure mechanisms are tensile cracking and compressive crushing of the concrete material. As seen from the Fig. 1 if the concrete at any point the softening branch, the elastic stiffness is reduced. The effect of the damage is different in tension and compression, and the degraded response of concrete is taken into account by introducing two independent scalar damage variables for tension and compression respectively.

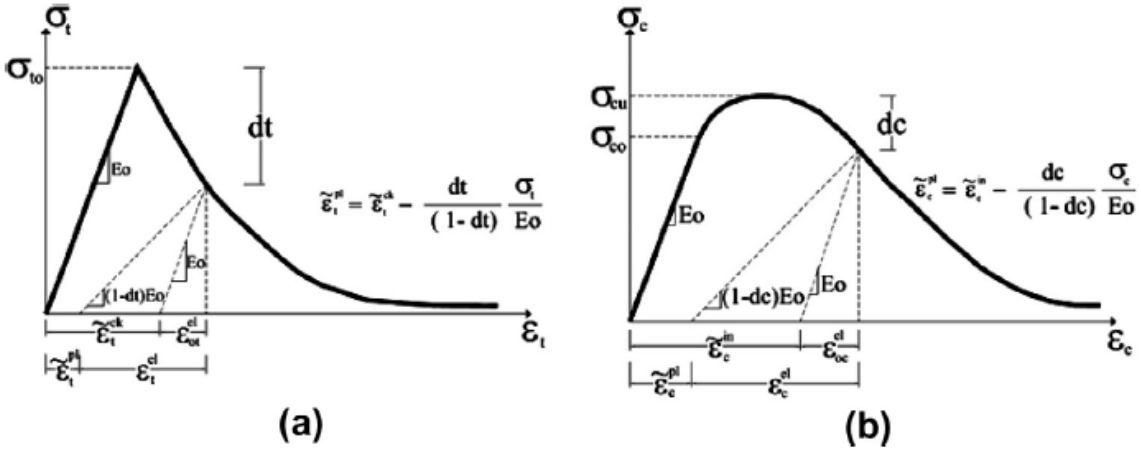

Figure 1: Response of concrete due to (a) uniaxial tension, (b) uniaxial compression [46]

In the mechanics of fracture theory it is mandatory to have material model which can nearly or almost representing the actual condition taking place. Therefore selection of the appropriate material model especially when software is used to analyze concrete members is the prime concern. Based on this fact, for validation of analytical solution in this research concrete damage plasticity model (CDPM) is used during the nonlinear finite numerical simulation stage. This is done based on the study conducted by [48] a

work conducted to identify parameters of concrete damage plasticity constitutive model and correlation of the model with experimental or laboratory results from literatures.

Based on [48] two standard applications have been shown that test the constitutive model of the concrete. These are described by [48] the first one as the analysis of the three point bending single-edge notched concrete beam specimen and the second the four point bending single edge notched concrete beam specimen under static loadings. According to his study the laboratory tests that are necessary for the identification process of constitutive parameters β, m and γ presented and the parameters β and m are used to describe the shape of flow potential function, while f and γ are responsible the shape of the yield function. The study identification procedure is realized for concrete class B50 [48]. The source of experimental results are the works [49], [50], [51] and experiments (uniaxial compression tests) elaborated at home institute and curves for both uniaxial compression and tension tests and for multi-axial tests are presented in Figs. (1-3) below [51].

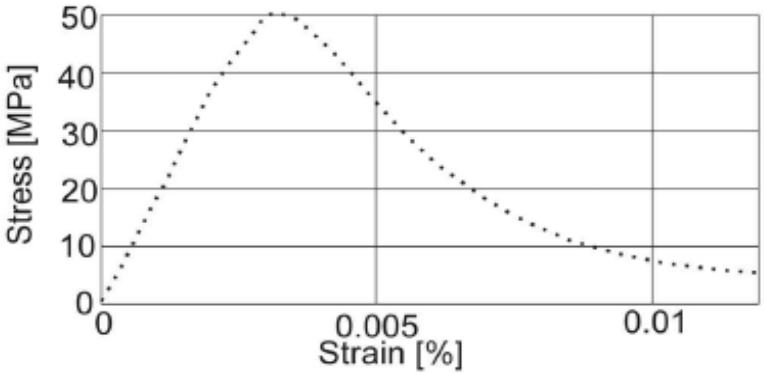

Figure 2: Uniaxial compression test of concrete, class B50-experimental (Home Institute)

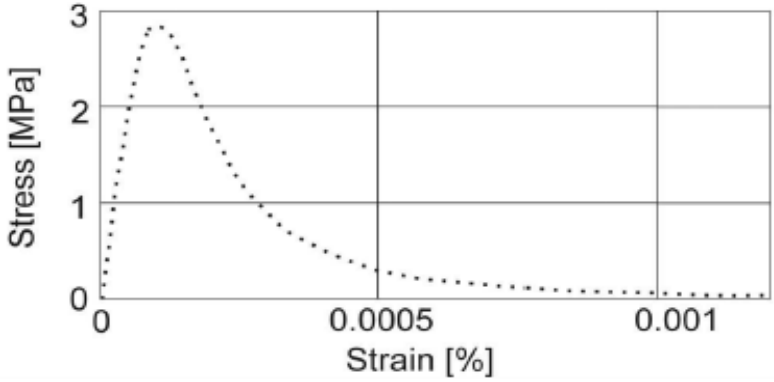

Figure 3: Uniaxial tension test of concrete, classB50-experimental curve (Home

Institute)

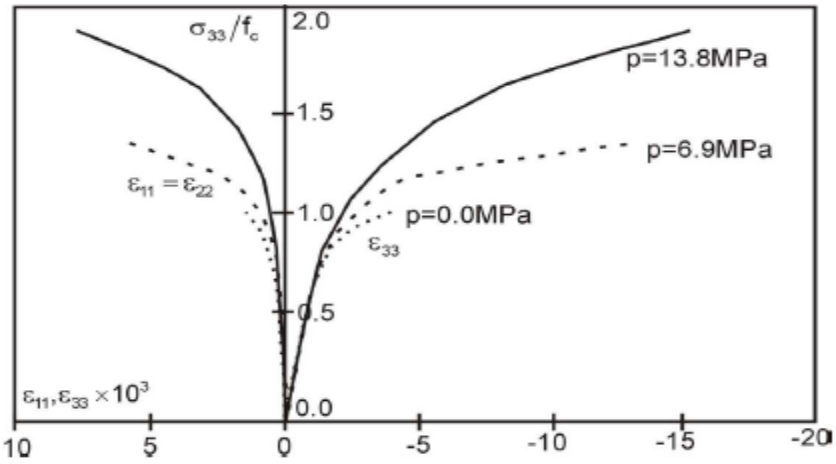

Figure 4: Triaxial compression of concrete, classB50-experimental curve [51]

For the comparison of test results [48] used Kupfer's curve for concrete B50 [49] and the stress strain curves in triaxial state of stress which are shown in Fig. (3) and the last test is superposition of two states: 1) hydrostatic state of stress (effective compressive stresses p equal to 0.0, 0.6 and 13.8MPa) and 2) uni-axial compression in the direction of σ_{33} [48].

In the procedure of constitutive parameters identification for CPD model, the fundamental group of the constitutive parameters consisted of four values which identify the shape of the flow potential surface and the yield surface and this model for the flow potential G, the Drucker-Prager hyperbolic function is accepted as in Eq.(5) below [48].

$$G = \sqrt{(f_c - mf_t \tan\beta)^2 + \bar{q}^2} - \bar{p}\tan\beta - \sigma \text{ ---------- (5)}$$

The hardening and softening rule and the evolution of the scalar damage variable for compression and tension are presented in Table (1) below as presented by [48] for concrete grade of B50 and both depend on the crushing and cracking strains.

Table 1: The material parameters of CPD model for concrete class B50 according to [48]

Material's parameters	B50	The parameters of CPD model	
		β	*38deg*
Concrete elasticity		m	1
E(Mpa)	19.7	$f=f_{b0}/f_c$	1.12
ν	0.19	ν	0.666
Concrete compression hardening		Concrete compression damage	
Stress (MPa)	Crushing strain (-)	DamageC(-)	Crushing strain(-)
15	0.0	0.0	0.0
20.197804	0.0000747307	0.0	0.0000747307
30.000609	9.88479E-05	0.0	9.88479E-05
40.303781	0.000154123	0.0	0.000154123
50.007692	0.000761538	0.0	0.000761538
40.23609	0.002557559	0.195402	0.002557559
20.23609	0.005675431	0.596382	0.005675431
5.257557	0.011733119	0.894865	0.011733119
Concrete tension stiffening		Concrete tension damage	
Stress (MPa)	Crashing strain (-)	DamageT(-)	Cracking strain(-)
1.99893	0.0	0	0.0
2.842	0.00003333	0	0.00003333
1.86981	0.000160427	0.406411	0.000160427
0.862723	0.000279763	0.69638	0.000279763
0.226254	0.000684593	0.920389	0.000684593
0.056576	0.00108673	0.980093	0.00108673

Finally, for the comparison of CPD constitutive parameters [48] identified the following laboratory tests as necessary ingredient of his work.

- The uniaxial compression
- The uniaxial tension
- The biaxial failure in plane state of stress (the Kupfer's curve for concrete grade B50)
- The triaxial test of concrete (superposition of the hydrostatic state of stress and the uniaxial compression stress).

For the validation of the work [48] conducted the standard application Abaqus/Explicit. As verification of his model he used experimental works of [49] and [51] for the estimation of the nucleation and the evolution of fracture in bending beams with notches (three-point and four-point bending). The scalar damage variable in tension is used to compare crack patterns for the numerical and experimental models [48].

a) Case of Three-point Bending Beam as used by [48]

The application of CDM model to the selected BVPs requires a comparison with experimental works for furthe applications. For the case of validation of the model by numerical results with laboratory test [49] worked on three-point bending single-edge notch concrete beam studid experimentally by [49]. The geometries of the beam are given in the Fig.(5) and are all in mm [49].

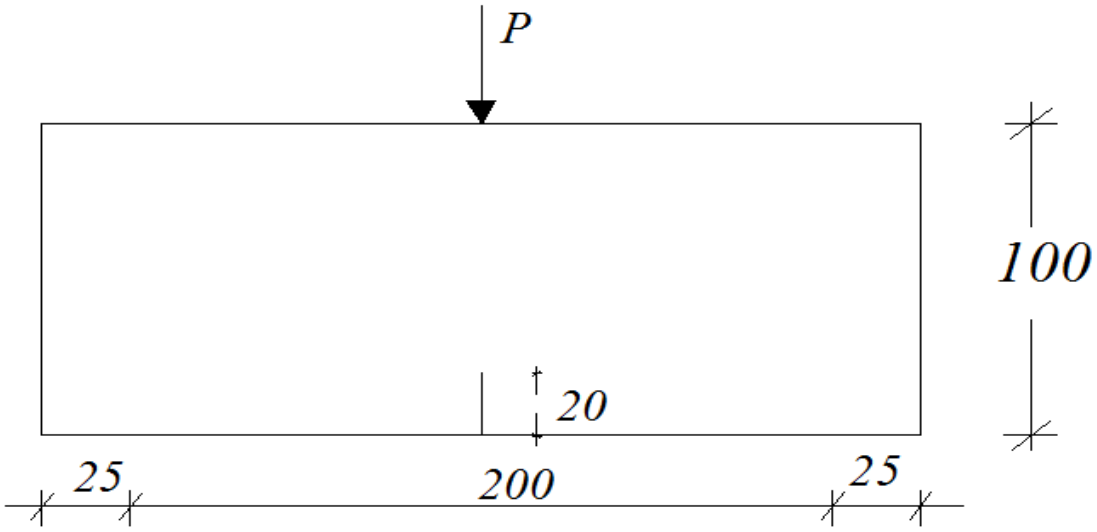

Figure 5: The geometry of three-point bending single edge notched concrete beam [49]

The finite element portion of the work conducted by [48] is also presented in Fig.(5) below.

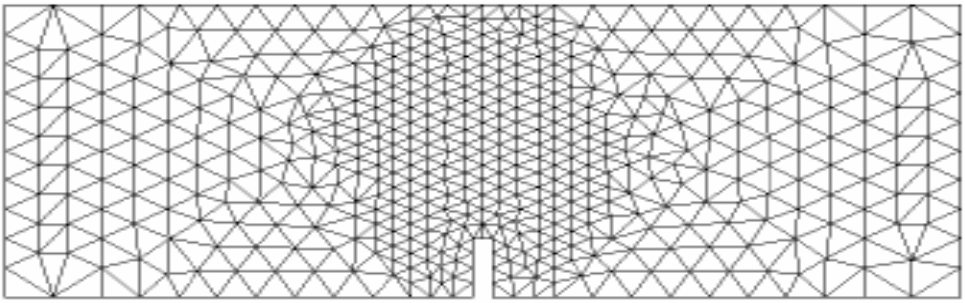

Figure 6: The finite element mesh

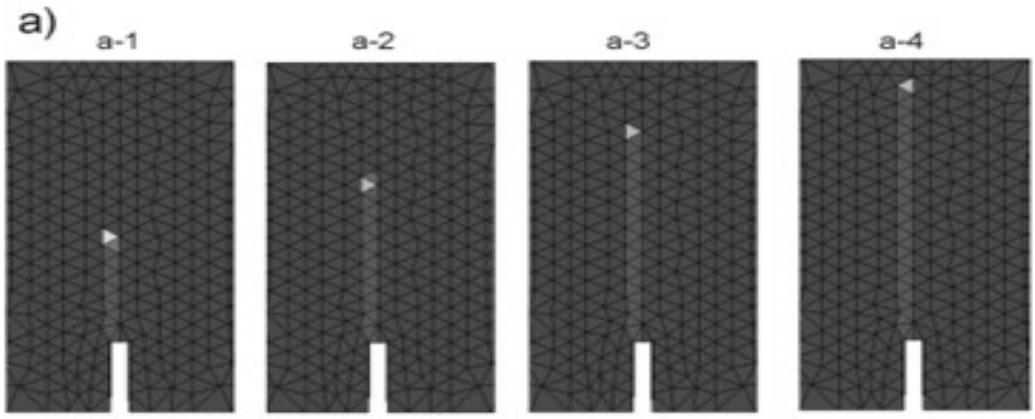

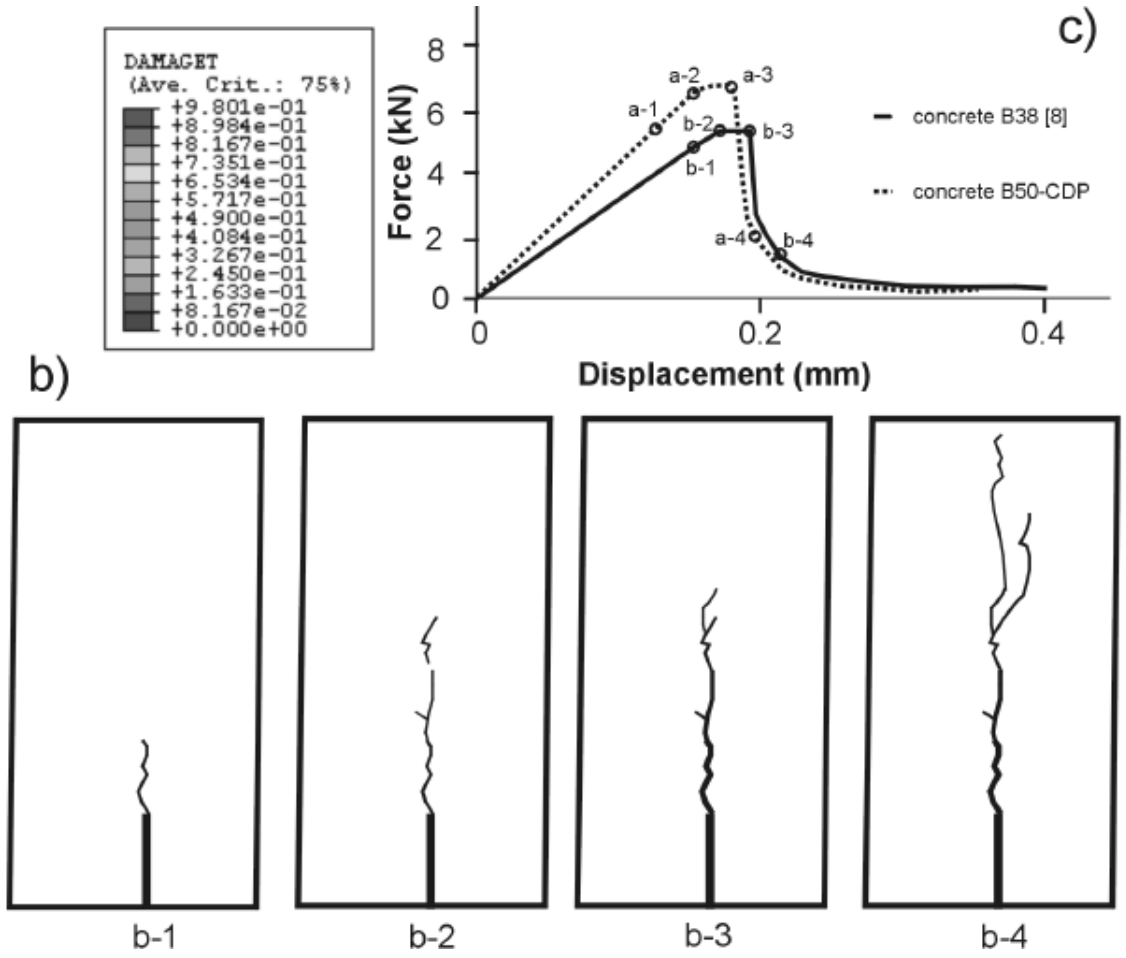

Figure 7: The comparison of crack patterns for three-point bending single-edge notched beam,

(a) beam with CPD numerical model, (b) the fracture path, which is observed in experiment [52], (c) the qualitative comparison of the plots: force-displacement curves

According to the findings of [48] concluded that the crack pattern is similar to that observed in the experimental model he used for result correlation. The qualitative comparison of the results is also presented by [48] as in the above Fig.(6c) and the single dominant crack appeared in the concrete three-point bending specimen and the shape of fracture zone location is shown in Fig.(6a) [49]. In the experimental work the crack pattern is similar to the obtained numerical results, Fig.(6b) and the results which are presented in Fig.6(a and b), correspond to the respective level of load and are shown in Fig.(6c) [49].

b) Case of Four-point Bending Beam as used by [48]

The second case of four-point bending beam test is use to verify the concrete CPD model for the case of dominant shearing and the one point loading is distributed in specific way as shown in Fig.(7) and as used in [48]. It is also described the interval between the force and the internal support is ten times shorter than between the force and the left support [54].

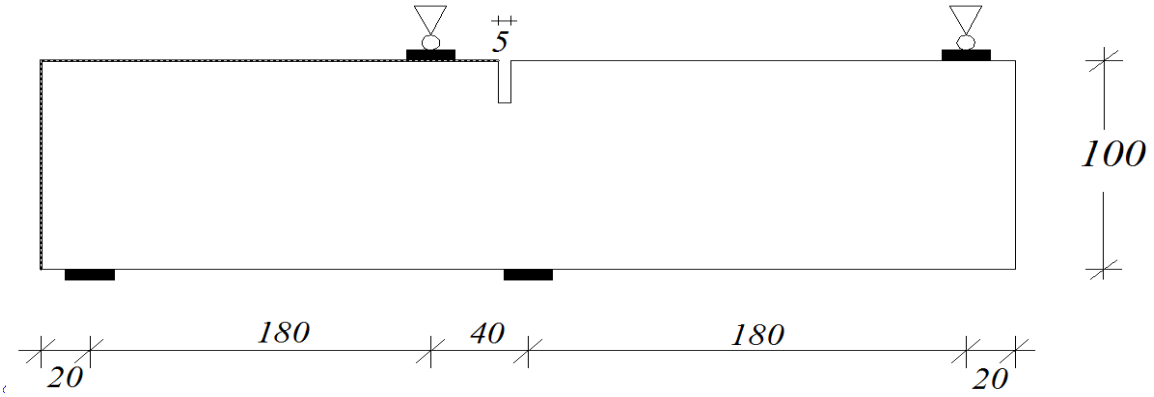

Figure 8: The geometry of four-point bending single-edge notched concrete beam [53]

It is concluded that the crack pattern, which was observed in the experiment is presented in Fig.(7) and the failure in beam specimen propagates from the notch to the place of the force application [48].

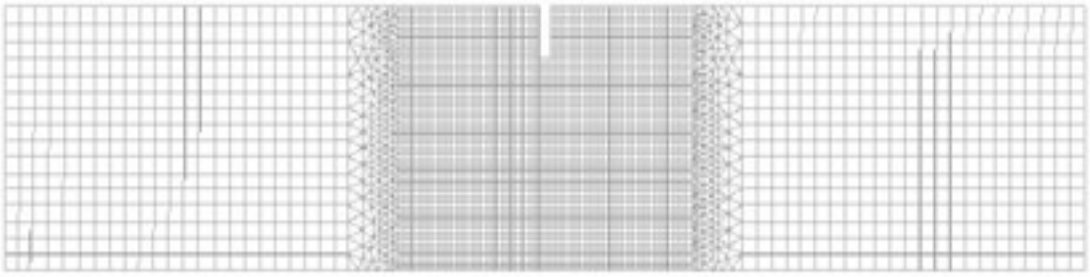

Figure 9: The finite element mesh four-node plane stress element [48]

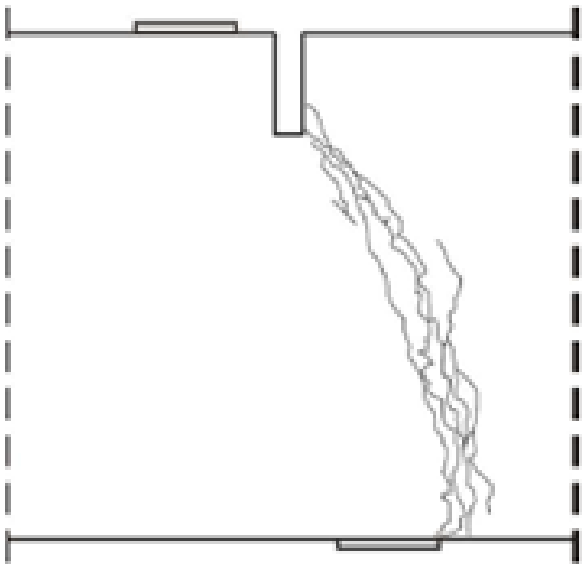

Figure 10: The experiment of [51]

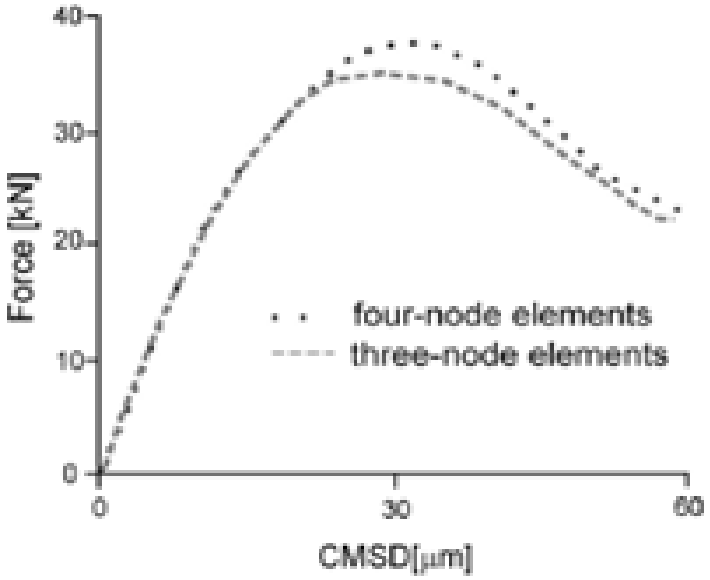

Figure 11: The comparison of the results for the different space mesh [48]

As a conclusion [48] forwarded the comparison of the numerical results obtained for both meshes is presented in Fig.(8). The crack patterns for both numerical models are similar to that of the experimental beam and important is the solution is unique and it does not depend on mesh size., in the Fig.(11) the comparison of force-CMSD (the crack mouth sliding displacement) plots for two different meshes are shown also by [48] works.

For both cases [48] concludes his observation as using CPD model enables a proper definition of the failure mechanism in concrete elements and the CPD can be used to model the behavior of concrete and the reinforced concrete structures and the other prestressed concrete structures even in advanced state of loadings. He also conclude that based on the criteria defined in the above cases it is possible to identify the constitutive parameters of CPD model of concrete and it also serves as a link between the real behavior of concrete and its numerical modeling.

It is the basic ground that the use of CDP model in the nonlinear finite element analysis part of this research and concrete material is modeled in the Abaqus/Standard for numerical simulation of reinforced concrete deep beams studied accordingly.

3. RESEARCH METHODS AND PROCEDURES

3.1. Research Methods

In this research two methods of predicting ultimate load carrying capacity are investigated. The first one is up on considering mechanism of shear resistance of reinforced concrete deep beam reinforced with both longitudinal and transverse shear reinforcements by STM studied by [48] for dynamic loading, analytically a refined ultimate shear strength or ultimate load capacity predicting expression will be derived. By the second method the analytic expression in the first method is validated with the help of nonlinear finite element numerical simulation to correlate results. Finally a parametric study will be carried out by means of numerical simulation to arrive on a working principle.

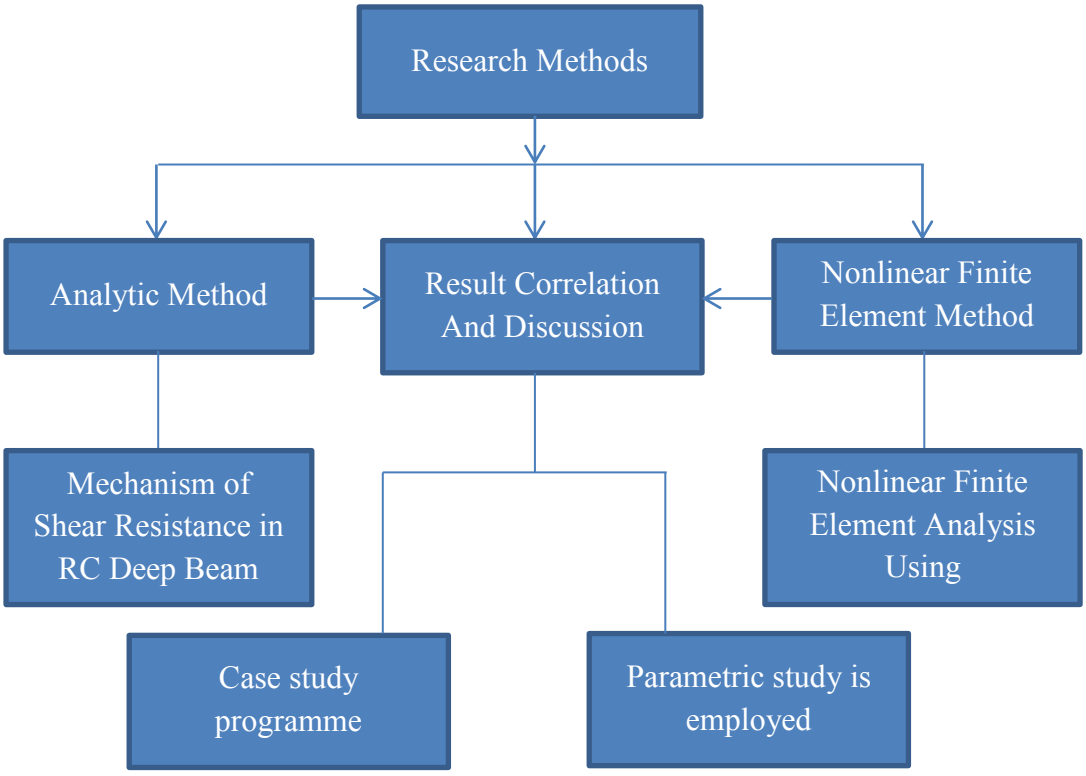

Figure 12: Flow chart showing methodology used

3.2. Research Procedures

Primarily by using the traditional strut and tie method is assessed analytically using the equilibrium of the proposed truss configuration under mechanism condition. In the first

stage a material model should be suggested in the form of constitutive law of stress strain relationship. At its stage the consideration of mechanism of reinforced concrete deep beam is used in the analytical derivation of the strut's failure condition at equilibrium, and also in the derivation of ultimate shear strength reduction factor v. The conventions in modeling of concrete and steel reinforcements are used. The second stage of this research paper is intended to validate the analytical ultimate shear strength or ultimate load capacity obtained using analytic expression in the first stage. This is enabled by using results from nonlinear finite element analysis and while conducting this nonlinear analysis stage the standard nonlinear numerical simulation software ABAQUS/Standard is employed. For this numerical simulation stage material models are used as input data including all softening parameters such as compressive and tensile damage parameters. For modeling of concrete material in the software concrete damage plasticity model is used among other fracture mechanics models based on its capability to capture the accurate behavior of reinforced concrete beams under ultimate load as investigated by [5] and [8], and reinforcing steel is modeled as perfect elastic plastic material which does not take account of hardening effects. In the analytical stage consideration of equilibrium conditions of bottom and top nodal zones it will be arrived at a new proposed analytic strut-and-tie method equation that analytically capable of predicting the ultimate load capacity. After all a parametric study to verify the general applicability of the analytical approach is conducted. Further this is intended to further establish parametric effects on ultimate load carrying capacity and helps to construct design implications of parameters.

Further to give witness to the nonlinear finite element result so that the capacity reached is at ultimate and collapse is occurring, load displacement and longitudinal (main) steel reinforcement stress strain curves to show yielding of main reinforcement prior to collapse as assumed in strut-and-tie method and failure progress showing plots with respective contour key for reinforced concrete deep beams with shear span to depth ratio 1.00 from all categories are presented next to the description of cross-sections and reinforcement details in the form of reinforcement ratio of each category. Failure progresses of deep beams which are not included in the body of this work are included in the appendix.

Finally, a parametric study is implemented to assess the response of reinforced concrete deep beams specimens for parametric variation and to investigate the influence of parameters on ultimate load capacity. This parametric study will be conducted under the following procedures.

i. When studying the effect of main or longitudinal reinforcement ratio on ultimate capacity/strength the amount or ratio of main reinforcement varied and the web is reinforced with minimum web reinforcement ratio.
ii. When studying the effect of web reinforcement the beams in each category are reinforced with constant main reinforcement ratio and the web reinforcement is set to vary independently for vertical and horizontal reinforcing each category beam. This means for example when studying the effect of vertical reinforcement on ultimate strength main reinforcement ratio is set to constant value without horizontal reinforcement and vertical reinforcement ratio effect will be studied by varying vertical reinforcement ratio and the same procedure is applied to that of horizontal reinforcement ratio effect.

3.3. Material Modeling

Reinforced concrete deep beam making materials are modeled both in tension and compression in the form of constitutive stress-strain relation as in Figs. (16), (17) and (18) below.

3.3.1. Stress – Strain Relationship of Concrete and Steel Reinforcing

To be consistent with results material models in Euro Code [10] will be used for concrete and reinforcing steel as reinforced concrete making materials are modeled in the form of their constitutive behavior as in just Euro Code 2 design manual and used as in below.

3.3.1.1. Material Model for Concrete

i. Concrete Model in Compression

The concrete material used in this study is with characteristic compressive cylinder strength of C25/30 as in tabulated Eurocode2Table 3.1[10]. This choice has been made because this concrete grade in most popular and also the study is directed toward the most applicable situations in most structural works. Most structures are made with

concrete in this range. The characteristics for this concrete are taken from Table 3.1 of the Euro code [10] and all values are in MPa**.**

Table 2: Concrete material for C25/30 according to EN1992/2 of Table 3.1

Concrete properties according to table 3.1 (Euro code)						
f_{ck}	$f_{ck,cube}$	f_{cm}	f_{ctm}	$f_{ctk,0.05}$	$f_{ctk,0.95}$	E_{cm}
25	30	33	2.6	1.8	3.3	31480

The proposed material model for non-linear structural analysis of concrete in structural works is graphically shown as in below of Fig. (13).

$$\frac{\sigma_c}{f_{cm}} = \frac{k\eta - \eta^2}{1 + (k-2)\eta} \quad \text{---------- (6)}$$

Where: $\eta = \varepsilon_c / \varepsilon_{c1}$

ε_{c1} is the strain at peak stress according to Table 3.1

$k = 1.05\mathrm{E_{cm}} \times |\varepsilon_{c1}| / f_{cm}$ (f_{cm} according to Table 3.1 of EN, 1992)

The above expression is valid for $0 < |\varepsilon_{c1}| < |\varepsilon_{cu1}|$ where ε_{cu1} is the nominal ultimate strain.

According to [40] the above expression is valid for $0 < |\varepsilon_{c1}| < |\varepsilon_{cu1}|$ where ε_{cu1} is the nominal ultimate strain.

In addition to the above as an alternative EN2/1992 of article 3.1.5(2) states other idealized stress-strain relations may be applied, if they adequately represent the behavior of the concrete considered [10]. From Fig.(16) below of stress strain curve the peak stress is at f_{cm} with value of 33MPa and the strain at this peak strain is taken to be ε_{c1} with value of 0.0021 taken from Table 3.1 of the same manual [10] for the specified grade of concrete in this research. Also from the curve it is seen the elastic property of concrete lasts at a compressive value of $0.4 f_{cm}$ with value of 13.2Mpa and inelastic strains going to be formed after this point. Once the value of maximum mean compressive stress f_{cm} is reached necking of the curve is introduced and this implies the softening behavior is reducing the compressive strength. It is assumed that this softening effect will result when the compressive strain developed reached ε_{cu1} the nominal ultimate strain and this with a value of 0.0035 and this value is as in EN2/1992 of Table 3.1 of the same manual. The angle of the curve tangent to the curve at $0.4 f_{cm}$ is described as $\tan\alpha = E_{cm}$ with

value of 31.48GPa for the specified grade of concrete used in this research and according to [40] of Table 3.1.

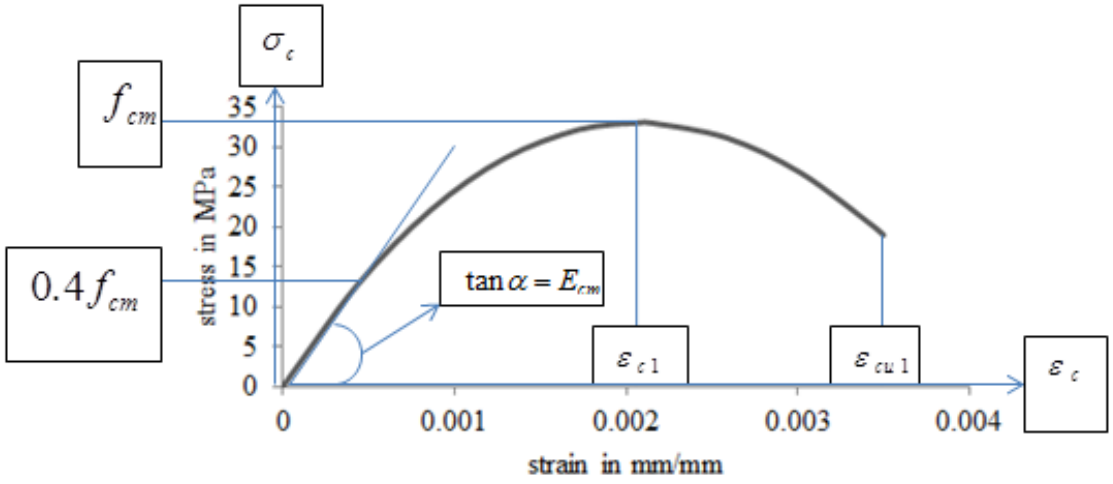

Figure 13: Stress Strain Curve for concrete in compression material model

ii. Concrete material model in tension

Tensile strength of concrete for use throughout this paper and also tensile fracture energy G_f can be approximated using the Euro code 2 recommendations of Eq. (7) below.

$$f_{ctm} = 0.3 f_{ck}^{2/3} \leq C50/60 \quad \text{---------- (7)}$$

Where f_{ctm} = is the mean tensile strength of concrete material and f_{ck} is as defined in concrete material modeling in compression sub topic.

From the curve shown below the value of fracture energy parameter energy G_f is computed in 137.9N/m and the maximum crack opening is obtained when the tensile strength of concrete fully lost and shown in the Fig. (14). Without the application of tensile stress to the core of the specimen the tensile strength is also obtained for the specific grade of concrete used in this research and its value is as shown on the curve below.

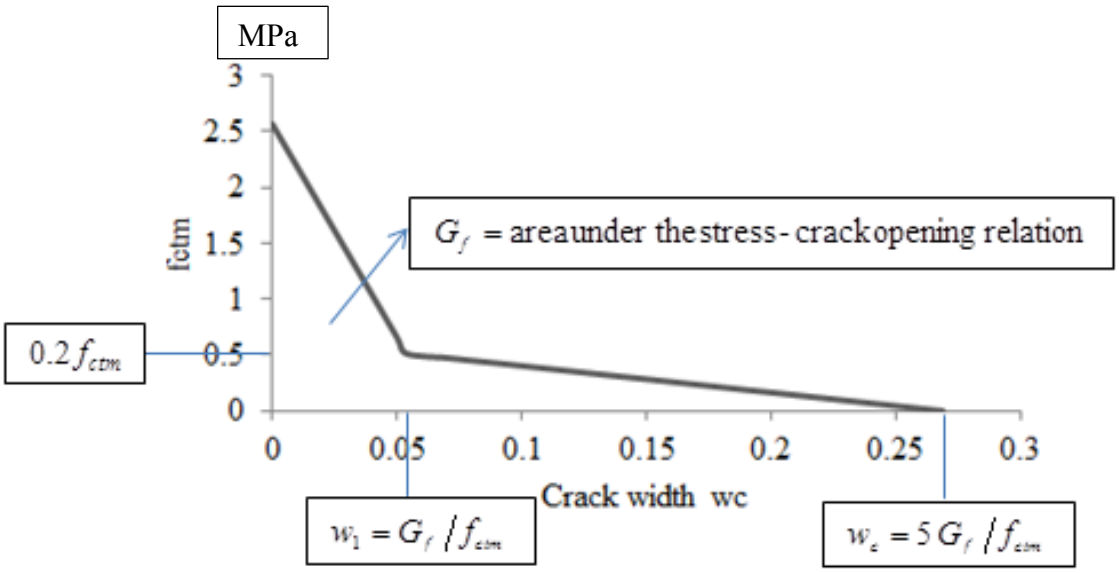

Figure 14: Tensile Stress Crack width curve for concrete in tension material model

3.3.1.2. Material Model for Reinforcing Steel

Steel reinforcements are modeled as an elastic perfect plastic material both in tension and compression with no hardening after yield point. This model is shown in the figure below. This is basically due to the material test results which showed almost no hardening behavior for reinforcement after the yield point.

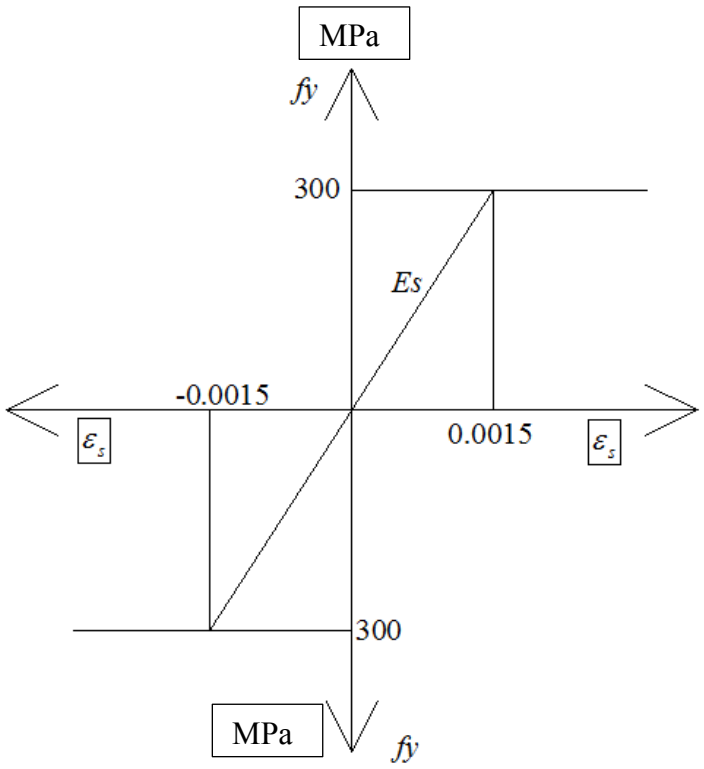

Figure 15: Material model for reinforcement for both tension and compression

4. ANALYTIC APPROACH

The application of knowledge and principles of equilibrium has still remained the backbone of any engineering science as long as load and stability is concerned. The derivation of equilibrium equations in this research paper which takes account of all constituents; such as longitudinal reinforcement, web reinforcement (vertical and horizontal) and compressive and tensile strength of concrete are assumed to play a significant role on the ultimate load capacity of reinforced concrete deep beam section. In this section of the research two analytic approaches to the problem are covered. This is achieved first by first investigation of the mechanism of shear resistance of reinforced concrete deep beam in [38] and a nonlinear finite element numerical simulation in the second stage.

4.1. Mechanism of Shear Resistance in Reinforced Concrete Deep Beam

4.1.1. Basic Assumption in Mechanism of Shear Resistance of RC Deep Beams

The major assumptions employed in the derivation of analytic expression to evaluate strut-and-tie design method in refined way using mechanism of shear resistance in Fig.(19) are listed below.

1. Compressive stress f_2 is created through a direction between load and support [54]. This stress causes the possible formation of a concrete crushing failure in the diagonal strut, which has to be resisted by the reduced mean concrete compressive strength vf_{cm}.
2. Transverse tensile stress f_1 is created in a direction perpendicular to the diagonal strut. Consequently, the deep beam may fail by concrete splitting, which can be resisted by the longitudinal steel, transverse reinforcement, and concrete tensile strength [54].

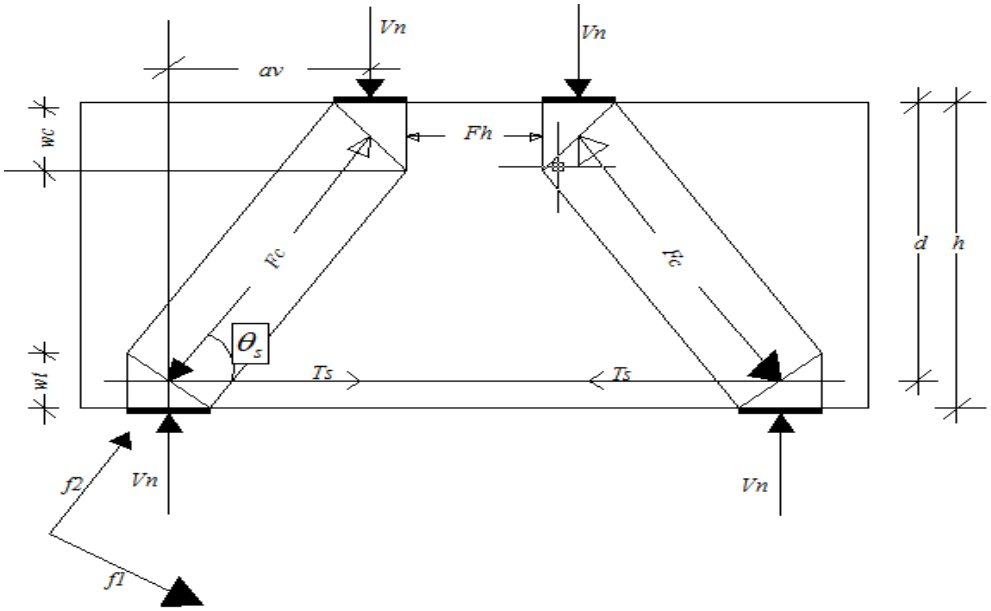

Figure 16: Strut-and-Tie Model for two point loaded simply supported deep beam [54]

The equilibrium forces at the bottom nodal zone of the diagonal strut based on orientation of elements in Fig. (16) are concluded as used in through the following relationships.

$$\sum F_y = 0; \qquad F_c = \frac{V_n}{\sin\theta_s} \text{ ---------- (8)}$$

$$\sum F_x = 0; \qquad T_s = \frac{V_n}{\tan\theta_s} \text{ ---------- (9)}$$

Where T_s the tensile force present in the strut-and-tie model of tie

$$\tan\theta_s = \frac{jd}{a_v} \text{ ---------- (10)}$$

$\theta_s =$ refers to the angle of inclination of the strut defined as in Fig. (16).

Where a_v is the horizontal distance between the applied load and the support center, and jd the lever arm of the longitudinal reinforcement (tie) to the center of the upper strut can be defined as follow.

$$jd = h - \frac{w_t}{2} - \frac{w_c}{2}$$

Where w_t and w_c are the depth of top and bottom nodal zones, respectively.

The compressive stress calculated from the equilibrium of the strut under mechanism condition as in below,

$$f_2 = \frac{F_c}{A_{str}} = \frac{V_n}{A_{str}\sin\theta_s} \text{ ---------- (11)}$$

Where A_{str} the diagonal strut's cross-sectional area and V_n is the ultimate shear strength that equilibrates the applied collapse/ultimate load P_u.

To determine the tensile stress f_t perpendicular to the diagonal strut at the bottom nodal zone, first consider the deep beam shown in the above Fig. (15) for equilibrium derivation [45].

$$f_1 = \frac{kT_s\sin\theta_s}{A_c/\sin\theta_s} = kP \text{ ---------- (12)}$$

Where: A_c is the deep beam cross-sectional area, and

$\frac{kT_s\sin\theta_s}{A_c/\sin\theta_s}$ is the average tensile stress across the diagonal strut due to the component of tensile force induced by tie reinforcement in the principal tensile direction of the bottom nodal zone and k is the nonlinear tensile stress distribution factor.

The stress distribution is nonlinear and cannot be determined directly by the assumption of beam theory, therefore assumptions are needed to find the stress distribution factors k_1 and k_2, where respectively refers top and bottom nodal zone distribution factors. Previous studies [55] and [56] found that the values of stress distribution factors k_1 and k_2 are of 2 and 0, respectively. By those studies these values have been proven best agreement with experimental results of reinforced concrete deep beams under static loading conditions. The bottom nodal zone experiences a biaxial tension-compression stress state, and the compressive strength of concrete is reduced due to the softening effect of the tensile stress. Based on the modified from Mohr-Coulomb theory [57], in this study the failure criterion at the bottom nodal zone is assumed as a linear interactive relationship between transverse principal tensile and compressive stresses [54].

For the determination of tensile stress and compressive stress components into their respective principal directions it is shown that all the contributing elements including

main and vertical reinforcing main and web reinforcements in orthogonal directions as in Fig. (20) below.

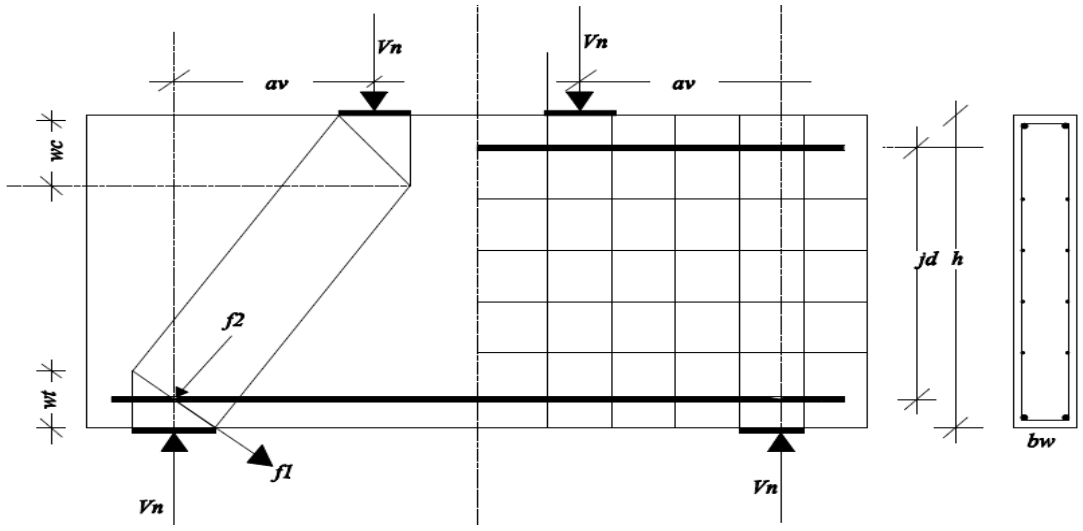

Figure 17: Determination of Tensile stress in the tie reinforcement in the direction of f_1 [54]

In the above Fig. (17) the beam is assumed reinforced with both vertical and horizontal web reinforcements in addition to main flexural reinforcement. The figure also shows that the direction of principal tensile and principal compressive stress designated by (f_1) and (f_2) respectively. It is evident that the contribution of vertical and horizontal web reinforcements are taken into account to contribute to the ultimate load capacity of the beam.

4.1.2. Consideration of Concrete Softening Effect

From previous findings it is possible to classify the concept of concrete softening effect to take into account in the determination of ultimate load capacities of deep reinforced concrete section under biaxial tension-compression stress state. Generally they are classified into three as in [54] and listed below.

a) Many of the codes, including [58], and [59], adopt the concrete strength efficiency factors, thereby resulting in statistical test results. However, an argument exists in evaluating the factors. Moreover, for some specific conditions, these factors may be over or underestimated because they are defined as empirical values.

b) Function expressions, such as $\beta = f(\varepsilon_1)$, are used to consider the influence of principal strain on the compressive strength [60]. This method seems to be more accurate, but adds complexity because of the simultaneous application of equilibrium conditions, compatibility equations, and stress-strain relationships.

c) Linear interactive failure criteria, such as modified Mohr-Coulomb theory [61], are utilized to account for the softening effect directly. Thus, the relationship of [54] below will be utilized.

$$\frac{f_1}{f_t} + \frac{f_2}{f'_c} = 1 \quad \text{---------- (13)}$$

Where f_1 and f_2 are principal tensile and compressive stresses at the nodal zone, and they represent the actual stress state; f'_c is the 28th day cylindrical compressive strength, and it represents the maximum compressive capacity in the f_2 direction; but later on to create a convention with the Euro Code [40] designation of compressive strength designation is represented by f_{cm} to mean that the mean compressive strength used in this paper and from now on this convention will be established, consequently the equation representing the Mohr Coulomb linear interaction is re-written as in below and f_t is the tensile strength contribution of reinforcement, and concrete, and it represents the maximum tensile capacity in the f_1 direction.

$$\frac{f_1}{f_t} + \frac{f_2}{f_{cm}} = 1 \quad \text{---------- (14)}$$

Consequently, this equation is applicable at the bottom nodal zone as the bottom nodal zone experiences a biaxial tension-compression stress state. To avoid complexities of reaching at conclusion and based on assumptions of nodal stress condition it is appropriate to impose a limitation on the compressive stress f_2 along the diagonal strut so that this should not exceed f_{cm}. Thus, the relation in Eq. (15) below is appropriate assumption as in [54].

$$f_2 \le f_{cm} \quad \text{---------- (15)}$$

In addition, the top nodal zone experiences a biaxial compression-compression stress state. Therefore, if the width of the top-loaded region is comparable to that of the bottom

support region, Eq. (15) is sufficient to safeguard failure of this top nodal zone. Thus, no further consideration is given to the top node.

The denominator of first term f_t in Eq. (14) is the combined tensile strength contribution of reinforcement, and concrete and it is given by,

$$f_t = \frac{kA_s f_{yd} \sin\theta_s}{A_c / \sin\theta_s} + \left(\frac{A_{sv} f_{ydw} \sin 2\theta_s}{2A_c} + \frac{A_{sh} f_{ydw} \sin^2 \theta_s}{A_c}\right)\frac{d}{h} + f_{ct} \text{ ---------- (16)}$$

Where A_s, A_{sv} and A_{sh} are respective total areas of longitudinal, vertical and horizontal web reinforcement; f_{yd}, f_{ydv} and f_{ydh} are yield strengths of longitudinal, vertical and horizontal web reinforcement, and f_{ct} is tensile strength of concrete as modeled in concrete material modeling subtopic.

The first term in Eq. (16) represents the tensile capacity of longitudinal steel reinforcement and is derived in a similar fashion as the term f_1 in Eq. (12), except that the full strength of longitudinal reinforcement is used in place of T. Furthermore, the effect of longitudinal reinforcement ($A_s f_{yd} \cos\theta_s$) in the f_2 direction has been ignored for simplicity. For a deep beam with a very small a/d ratio, this component will be insignificant, as $\cos\theta_s$ approaches zero. On the other hand, if the a/d is relatively high, the deep beam is likely to fail due to excessive tensile stress in the f_1 direction. In this case, failure is governed by the first term in Eq. (14), and thus the term have f'_c little influence on the ultimate shear strength. Therefore, it is justifiable to neglect the contribution of longitudinal reinforcement to the compressive capacity in the f_2 direction [54]. The same assumption is made for web reinforcement.

The second term in Eq. (16) represents the tensile capacity of inclined web reinforcement. It takes account of orthogonal arrangements of web reinforcement, be it vertical, or horizontal. From the geometry of the strut-and-tie model, the tensile strength contribution of web reinforcement in the f_1 direction of practical arrangement of web reinforcement into vertical and horizontal can be expressed as $\frac{A_{sv} f_{ydw} \sin 2\theta_s}{2A_c}$ and

$\frac{A_{sh} f_{ydw} \sin^2 \theta_s}{A_c}$, respectively [38]. Where A_{sv} and A_{sh} refer the areas of vertical and horizontal web reinforcement within the distance of shear span.

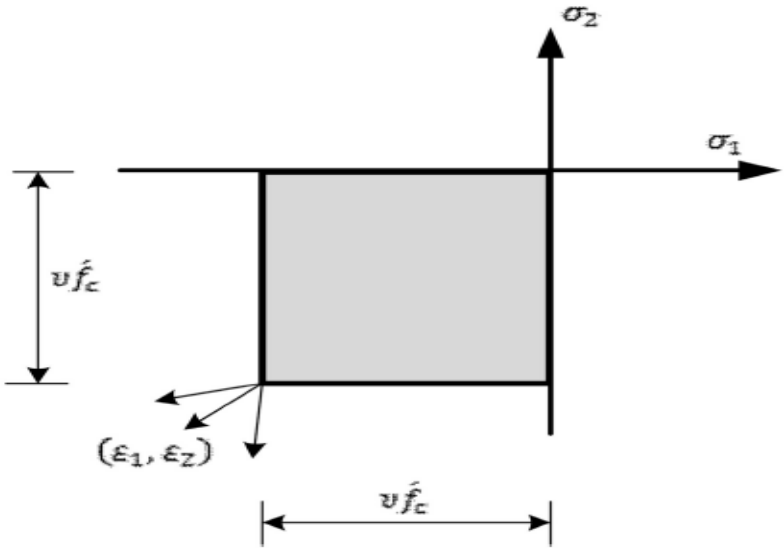

Figure 18: Modified Coulomb Failure Criteria [54]

If the bottom nodal zone is subjected to the biaxial tension-compression stress state, the following equation can be derived from Eq. (15):

$$V_n \le A_{str} f'_c \sin\theta_s \quad \text{---------- (17)}$$

4.1.3. Strut Strength Reduction Factor Derivation

After all we need to designate an assumed strength reduction factor by v. Therefore based on the proposed truss configuration, the equation that yields the concrete strut strength reduction factor v Fig. (12) can be expressed as:

$$\frac{F_c}{A_{str}} = v f'_c \quad \text{---------- (18)}$$

Substituting Eq. (11, 12, and 18 into 14), the following equation can be obtained first by equating Eq. (11) and (18) solve for V_n

$\frac{V_n}{A_{str}\sin\theta_s} = \nu f'_c$ Solving for $V_n = \nu A_{str} f'_c \sin\theta_s$ now substitute Eq. (12) and this value of ultimate shear strength into the linear interaction proposed by Modified Coulomb Theory of Eq. (14) to solve for assumed reduction factor ν.

$$\frac{(\frac{kT_s\sin\theta_s}{A_c})}{\frac{\sin\theta_s}{f_t}} + \frac{\nu f'_c A_{str}\sin\theta_s}{A_{str}\sin\theta_s f'_c} = 1$$

Rearranging and solving for unknown gives

$$\nu = (1 - \frac{kT_s\sin^2\theta_s}{A_c f_t}) \quad \text{---------- (19)}$$

Where T_s refers to the tension force in the bottom steel reinforcement. It is also that the second term in Eq. (19) represents the contribution of the tension force of the bottom steel resolved in the direction of the diagonal strut.

Here the basic assumption is that the tensile force in the longitudinal reinforcement is assumed to be equivalent with the yield force in the longitudinal reinforcement. In the strut-and-tie model the yielding of main/longitudinal reinforcement is assumed to take place prior to concrete crushing in compression. Therefore at ultimate condition we can assume the yielding force in the main/longitudinal reinforcement to be equivalent to the concrete crushing force including softening parameters. As a result we can represent the tensile force in the longitudinal reinforcement as equivalent to the compressive stress in the compression strut at ultimate load condition and manipulating the proposed material model for concrete compressive stress as a function of mean cylindrical compressive strength f_{cm} in accordance with [38] as used in the above concrete material modeling subtopic,

$$\frac{\sigma_c}{f_{cm}} = \frac{k\eta - \eta^2}{1 + (k-2)\eta} \quad \text{---------- (20)}$$

And where all notations are with similar meaning with concrete material modeling subtopic, and T_s

$$T_s = \sigma_c b_w w_t \quad \text{---------- (21)}$$

Resolving component of this tensile force present in the longitudinal reinforcement into the principal direction of f_1 will gives,

$$f_1 = T_s \sin\theta_s = \sigma_c b_w w_t \sin\theta_s \quad \text{---------- (22)}$$

Therefore substituting Eq. (22) back into Eq. (19) gives the expression for the unknown strength reduction factor

$$v = (1 - \frac{k\sigma_c b_w w_t \sin^2 \theta_s}{A_c f_t}) \quad \text{---------- (23)}$$

The ultimate shear strength V_n can be derived by substituting in terms assumed reduction factor will be given as the same to that of [38] for deep beams under dynamic loading:

$$V_n = vA_{str} f'_c \sin\theta_s \quad \text{---------- (24)}$$

4.1.4. Strut Parameters and Dimensioning its Geometry

The cross-sectional area of the strut A_{str} is calculated by the following:

$$A_{str} = b_w(w_t \cos\theta_s + l_b \sin\theta_s) \quad \text{---------- (25)}$$

Where b_w the width of the beam, w_t is the bottom tie depth, and l_b is the support-bearing plate length.

The depth of the top node w_c can be determined considering the limit equilibrium of the top node. If a stress limit of f_{cm} is imposed on the top node, the depth w_c can be determined from Eq. (26) below.

$$w_c = \frac{V_n}{f_{cm} b_w \tan\theta_s} \quad \text{---------- (26)}$$

The w_c value cannot be calculated at first. For the determination of the top compressive strut width it is better required step. In this research paper it is devised that the steps involved in the determination of compressive strut width as below.

i. Assume material parameters for concrete and steel reinforcement
ii. Determine width of tie reinforcement w_t
iii. For first iteration assume that width of the compressive strut w_{c1} equals with w_t

iv. Calculate the angle of inclination of the diagonal strut by using values of w_t and w_{c1} already found as above in step (ii) and (iii).

v. Calculate the tensile stress resistance of contribution from main reinforcement, web reinforcement and tensile strength of concrete using Eq.(16)

vi. Compute cross-sectional area of diagonal compressive strut A_{str} by using Eq. (25)

vii. Compute the Ultimate shear strength reduction factor designated as v in this research paper using Eq. (23)

viii. Compute the ultimate shear strength v_n by using Eq. (24)

ix. Compute the required compressive strut width w_c using Eq. (26)

x. Check that if w_c from step (ix) equals with the one assumed as w_{c1} in step (iii) if ok, adopt the value as the desired compressive strut width

xi. If step (x) not satisfied, assume another value for w_{c1} in step (iii) and carryout second iteration and so on until the desired criteria satisfied, i.e. w_c equals w_{cn} at n^{th} step.

It is understood that for optimal assessing of ultimate load carrying capacity, the effect of tensile strength of concrete f_{ct} , and web reinforcement is taken in consideration.

4.2. Finite Element Analysis

It is already stated in different design manuals and codes [61] and [63] the application of finite element analysis supposed to be preferable than any other approximate method of analysis. But this requires the effort of simulating and modeling of the actual condition. In practice modeling such condition representing what is really on the ground is not possible. Therefore from the stand point of this difficulty in modeling and simulating the real behavior of problem at hand, the solution expected will be so approximate. Therefore when applying finite element analysis, modeling and simulation require great precaution so that the result should not be much far from true or correct value. That means the results obtained from such analysis should be within acceptable tolerance limit.

4.2.1. Nonlinear Finite Element Simulation

For optimal assessment of reinforced concrete structures the application of nonlinear finite element analysis is chosen as best fitting. Of all available nonlinearity conditions only material nonlinearity is simulated in this research paper. Especially, nonlinear behavior of concrete is given prime importance and hence used due. The reinforcement is modeled as perfectly elastic plastic material both in tension and compression as stated in material modeling subtopic.

4.2.2. Element Discretization

The reinforced deep beam member constitutes three part instances. Namely, solid three dimensional deformable homogenous concrete part instances, three dimensional deformable wire truss reinforcement part instance and solid three dimensional deformable homogenous steel plate part instance.

Solid concrete continuum part instance is meshed into sizes of 100 elements of C3D8R elements. The solid steel plate both at support and loadings is also discretized as C3D8R elements. The reinforcement is also discretized as T3D3H elements. The designation of elements by C3D8R and T3D3H to mean that continuum three dimensional eight node brick element with reduced integration of the stiffness matrix and three dimensional truss element with hybrid integration of the stiffness matrix. The concrete and steel plate is used linear stress formulation and the reinforcement is used quadratic formulation.

Constraints are applied for mutual action of reinforcement and concrete. Embedded constraining is applied for reinforcement and concrete. Both at support and loadings steel plates with dimension mentioned in respective case study categories are constrained as tie. In Figure (19) below discretized assembly with shear span to depth ratio of 1.50 from the three categories as an example are shown.

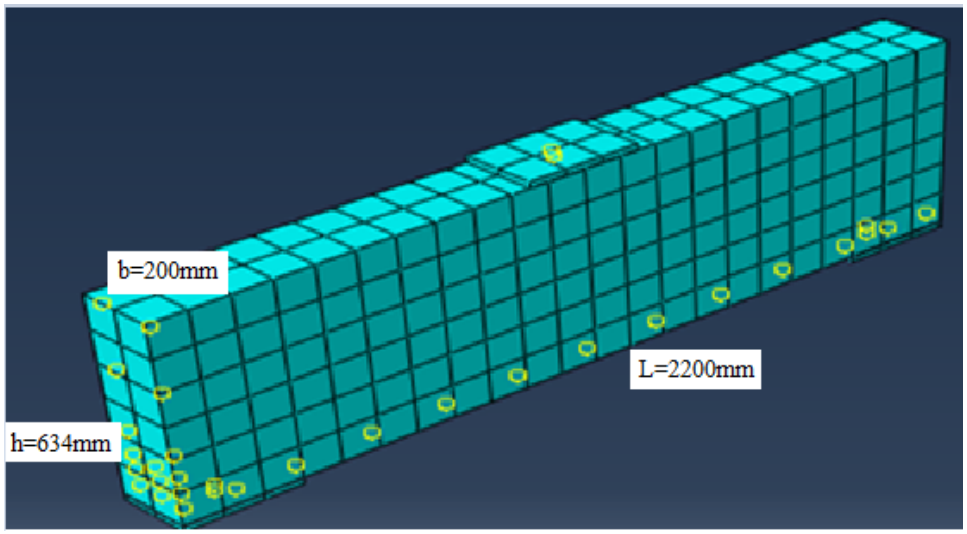

(a) One point concentrated load loaded deep beam

The geometry of the beam in Fig. (19a) is overall span of 2200mm, width 200mm and depth of 634mm.

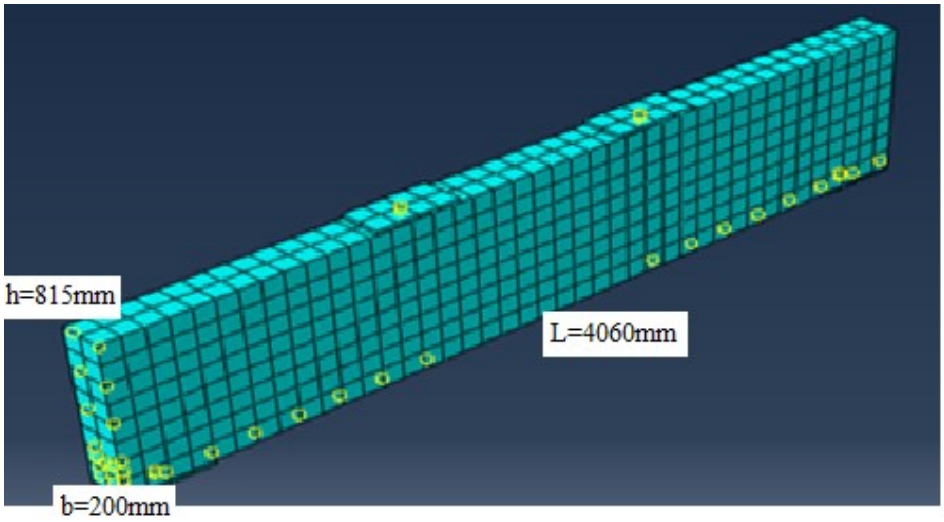

(b) Two point concentrated load loaded deep beam

The geometries of the beam in FEA model in Fig. (19b) above are overall span length of 4060mm, width 200mm and depth of 815mm.

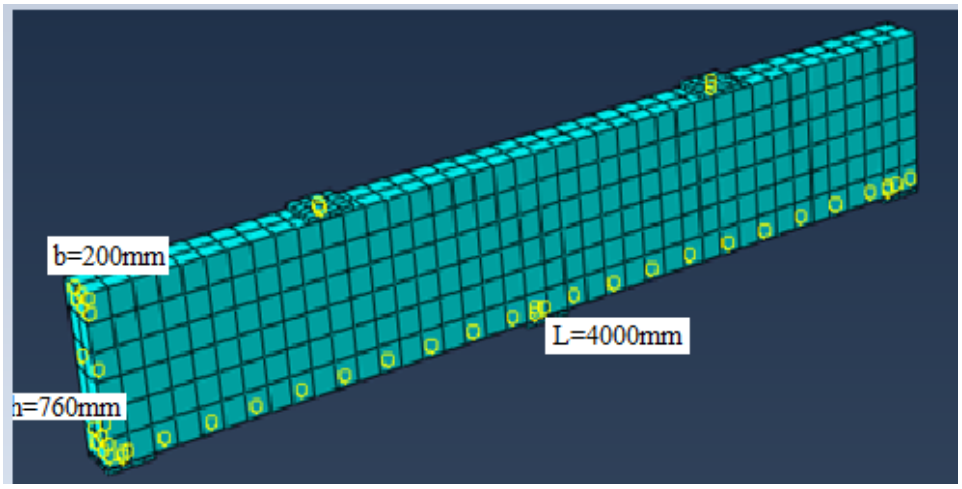

(c) Symmetrically two point concentrated load loaded two span continuous deep beam

The beam model in Fig. (19c) above is modeled in FEA with overall span length of 4000mm, width 200mm and depth of 760mm.

Figure 19: Representative finite element discretization of deep beam specimens with shear span to depth ratio 1.50 from all categories

4.2.3. Material Data Used in the Nonlinear Finite Element Simulation

4.2.3.1. Concrete and Reinforcing Steel Material Data

Abaqus/Standard software is implemented in the nonlinear numerical simulation of reinforced concrete deep beams considered in the case study stage. Parameters used to model concrete such as in concrete damage plasticity used in this research to model concrete plasticity parameters used in the determination of biaxial failure (yield) surface such as dilatation angle, eccentricity, viscosity parameters are inputted the default values. For modeling the nonlinear behavior both in compression and tension the following Table (3) below is provided for C25/C30 concrete grade used in this research.

Table 3: Concrete compressive and tensile material behavior for software input

Concrete in Compression			Concrete in Tension		
Yield stress $\sigma_c = f_{cm}\frac{k\eta-\eta^2}{1+(k-2)\eta}$	Inelastic strain $\varepsilon_{in} = \varepsilon_c - \varepsilon_{c1}$	Compression damage dc $d_c = 1-\frac{\sigma_c}{f_{cm}}$	Yield stress $f_{ct} = f_{cm}(1-\frac{0.8w_c}{w_{c1}})$	Displacement $w = w_c$	Tensile damage $d_t = 1-\frac{f_{ct}}{f_{ctm}}$
12.036	0.00000	0.0000	2.565	0.000	0.0000
12.622	0.00003	0.0000	2.183	0.010	0.1488
22.096	0.00016	0.0000	1.802	0.020	0.2976
28.556	0.00039	0.0000	1.420	0.030	0.4464
32.133	0.00070	0.0000	1.038	0.040	0.5952
33.000	0.00102	0.0000	0.657	0.050	0.7440
32.947	0.00111	0.0016	0.513	0.054	0.8000
31.114	0.00160	0.0572	0.474	0.070	0.8151
26.741	0.00217	0.1897	0.450	0.080	0.8244
19.932	0.00281	0.3960	0.427	0.090	0.8337
18.950	0.00290	0.4258	0.403	0.100	0.8430
			0.379	0.110	0.8523
			0.355	0.120	0.8616
			0.331	0.130	0.8709
			0.307	0.140	0.8802
			0.283	0.150	0.8895
			0.260	0.160	0.8988
			0.236	0.170	0.9081
			0.212	0.180	0.9174
			0.188	0.190	0.9267
			0.164	0.200	0.9360
			0.140	0.210	0.9453
			0.116	0.220	0.9546
			0.093	0.230	0.9639
			0.069	0.240	0.9732
			0.045	0.250	0.9825
			0.000	0.269	1.0000

Other default parameters used when concrete modeling are Dilation angle $38°$, eccentricity 0.1, the ratio of equibi-axial compressive stress to initial uniaxial compressive stress 1.16, k representing the ratio of second stress invariant = 0.667 and viscous parameter $\mu = 0$. Modulus of elasticity of concrete $E_C = 31.480\text{GPa}$ and possion's ratio of $v = 0.2$ is used in elastic condition.

4.2.3.2. Reinforcing Steel Data

Reinforcing steel properties inputted into Abaqus software are modulus of elasticity $E_s = 200GPa$, passion's ratio $v = 0.3$ and yield strength of $f_y = 300MPa$.

5. ANALYSIS AND COMPARISON OF ANALYTICAL AND FINITE ELEMENT NUMERICAL RESULTS

5.1.Finite Element Model Validation

In order to validate the ability of the selected concrete model i.e CDPM to study the tensile and compressive behavior of reinforced concrete deep beams on ultimate load capacity, a benchmark test has been carried out using one of the deep beams, studied by [63] for the evaluation of shear strength of deep beams. This test serves as a source for comparison with the existing experimental results. In the study conducted by [63], simply supported beams were instrumented to measure the mid span deflections and loads. Fig. 20 illustrates the cross section and loading configuration of the tested beam.

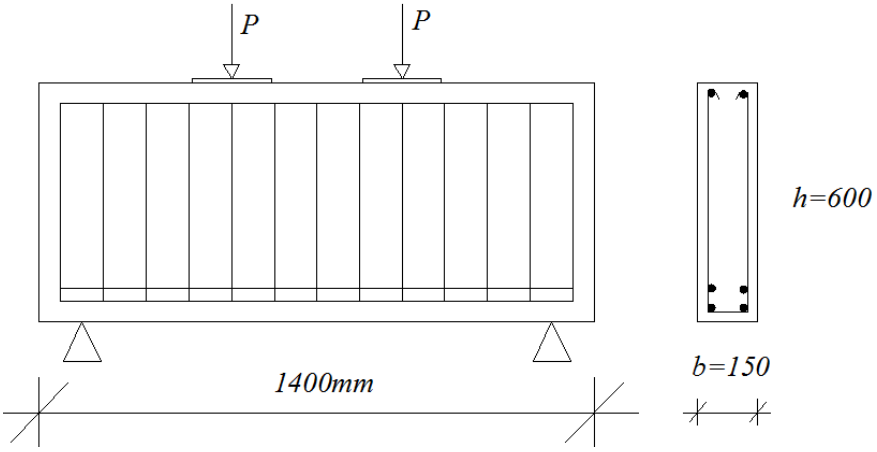

Figure 20: Cross-section and loading configuration of beam SS-1 as in [63]

An 8- node solid element with one point integration was utilized to create the concrete beam mesh. An embedded truss reinforcement a 2-node linear 3D truss element was used to model steel rebars. Fig. 21 illustrates the load–deflection response of the studied beam in comparison with the experimental results obtained by [63]. The material inputs used for the nonlinear finite element analysis using Abaqus are as in the case study.

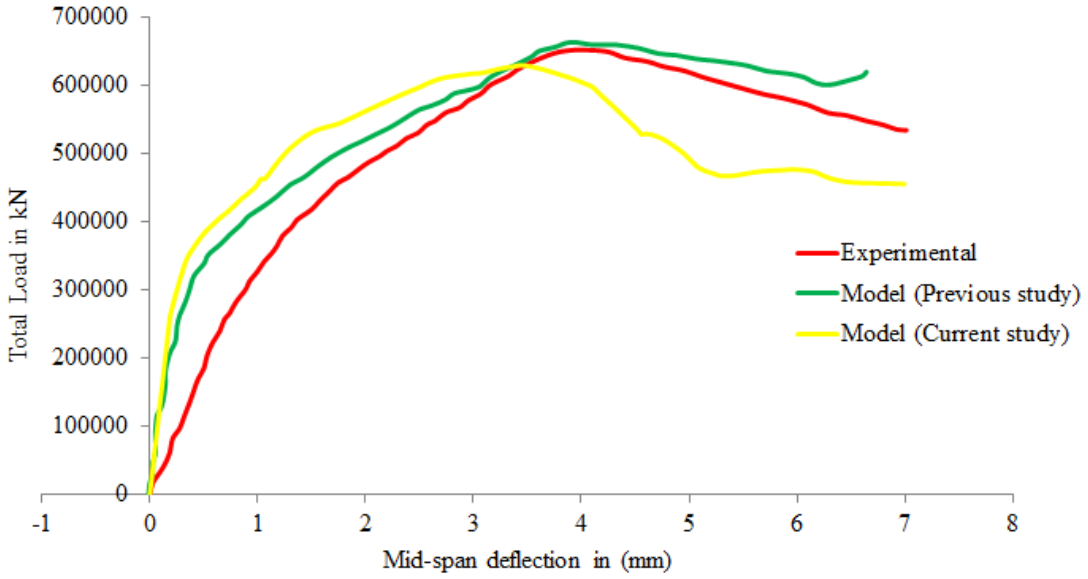

Figure 21: Comparison of load deflection response for the applied material model versus experimental result

As seen in the Fig. (21) above modeled response verifies the ability of the selected model to capture the whole beam's behavior up to failure and shows a good agreement to the experimental results.

The ultimate load obtained in the current study is 628.962kN, and the experimentally determined by [63] and the one with previous study are 651.5kN and 663.0kN respectively. The percentage of difference is also computed as in below to show the method prediction capacity.

$$\text{Difference}(\%)\ \text{to experimental value} = (1 - \frac{628.962}{651.5}) * 100 = 3.5\%$$

$$\text{Difference}(\%)\ \text{to previous study} = (1 - \frac{651.5}{663}) * 100 = 1.74\%$$

A percentage difference of 3.5% and 1.74% of model prediction capacity to experimental and previous study indicates the method can be used as alternative method of analysis.

It is therefore reasonable to conduct a case study on selected deep beam specimens to further investigate the behavior of reinforced concrete deep beams at ultimate load condition as covered in case study part of this work.

5.2. Results with Case Study

A number of researchers are devoted to modify the strut-and-tie method to predict the ultimate load carrying capacity of disturbed reinforced sections, such as deep beams. But due to the inconsistencies in methods followed and the very complex load distribution in deep reinforced sections due to stress localization findings were not so sound. So as technological advancements are made always this field of study requires more refined and accurate problem approaches.

Therefore, in this study to support the modified strut-and-tie method a case study for general applicability of problem solving is required. For this reason a categories of selected deep reinforced concrete beam sections are assessed using the modified analytic method and verified with the help of results from nonlinear finite element analysis.

5.3. Case Study Description

Generally, three Categories of deep beams will be investigated. The basics for the classification of specimens is span condition (simple or continuous span) and point of load application (one or two point). Further the specimens categorized under each Category are with shear span to depth ratios of 1.00, 1.25, 1.50, 1.75 and 2.00 aimed to predict the ultimate load carrying capacity. The notations and details of parameters under each category are discussed as in below.

The reinforcement conditions of each Category's specimen are reinforced to achieve ductile failure so that large deformation of the concrete which occur before yielding of tie reinforcement is mainly avoided. Based on this requirement the ultimate load carrying conditions will be predicted by using analytical model and is validated with results from nonlinear finite element analysis.

Category-I: Simply supported deep beam with one point central concentrated loading

This Category comprises of five deep reinforced concrete beam specimens with shear span to depth ratio of 1.00, 1.25, 1.50, 1.75 and 2.00 all with the same overall span length of 2200mm. For category-I a steel plate sizing 300x200x20mm at loading and support is used. The cross-sections studied under category-I and the details of reinforcing are shown in Fig. (22).

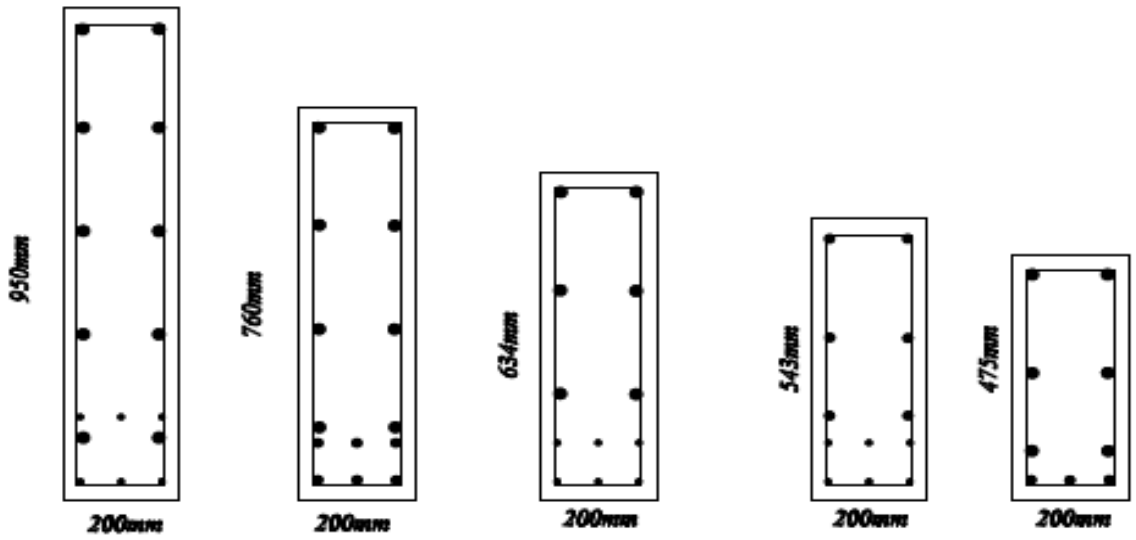

Figure 22: Cross-sections studied in case study of Category I

The detailing of main and web reinforcements for category-I case study is also shown in Table (4) below.

Table 4: Main and web reinforcement detailing for beam specimens under category-I

Shear span to depth ratio	Main reinforcement ratio ρ_s	Vertical web reinforcement ratio ρ_v	Horizontal web reinforcement ratio ρ_h
1.00	0.003	0.019	0.019
1.25	0.0086	0.0157	0.0157
1.50	0.0046	0.019	0.019
1.75	0.0048	0.0157	0.0157
2.00	0.0068	0.0157	0.0157

To validate the principle of Strut-and-tie model based design the main reinforcement should have to yield before the concrete crushes or before the beam reaches its ultimate capacity.

In this research paper this is evidenced by showing a plot of load deformation curve and stress strain curve for main reinforcement, designated as tie reinforcement in strut-and-tie design method.

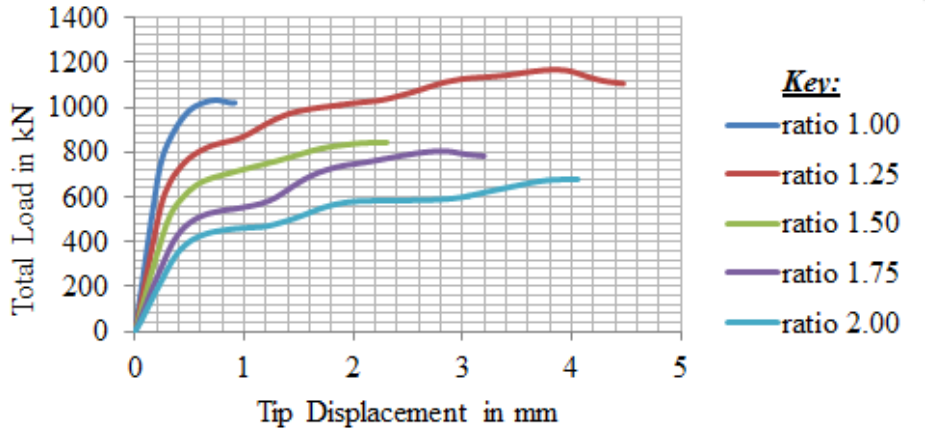

(a)

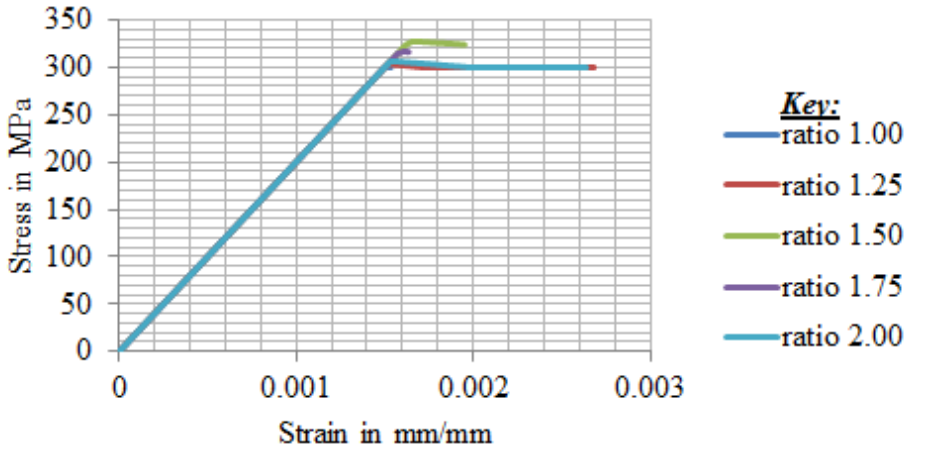

(b)

Figure 23: Load Displacement (a) and Steel Stress Strain (b) curves of Category-I

To illustrate the failure modes and behavior of simply supported reinforced concrete deep beams subjected to one point concentrated loading studied in category-I, the step wise failure progress of following representative deep beam from this category with shear span to depth ratio of 1.00 is shown at different stage of its failure with contour for tensile damage shown at different stage. As shown in Fig. (24) below the failure at the application of small percent of ultimate load as in Fig. (24a), initiation of flexural cracks is seen at the mid span of the beam. These tiny cracks are supposed to be due to flexural stress developed at most bottom extreme fiber of the mid-section and at this stage the stress is fully flexural. After a while or some increment in percent of ultimate loading diagonal cracking of concrete would take place as seen from Fig. (24b) below. After then if a continuation in increment percent of ultimate loading is done the flexural stress in the

bottom (main) steel reaches to its ultimate and the yielding will result as in Fig. (24c) and Fig. (23) The yielding of reinforcement. Due to further increase in percent of ultimate load could not carried by the tie reinforcement, the nodal conditions reach their crushing strength and as a result crushing will takes place as shown in Fig. (24d). As a result of weakening of the web by tension or splitting of diagonal cracks seen in Fig. (24) result in weakening of concrete in compression and full crushing will takes place and the Ultimate capacity the load this step is taking place.

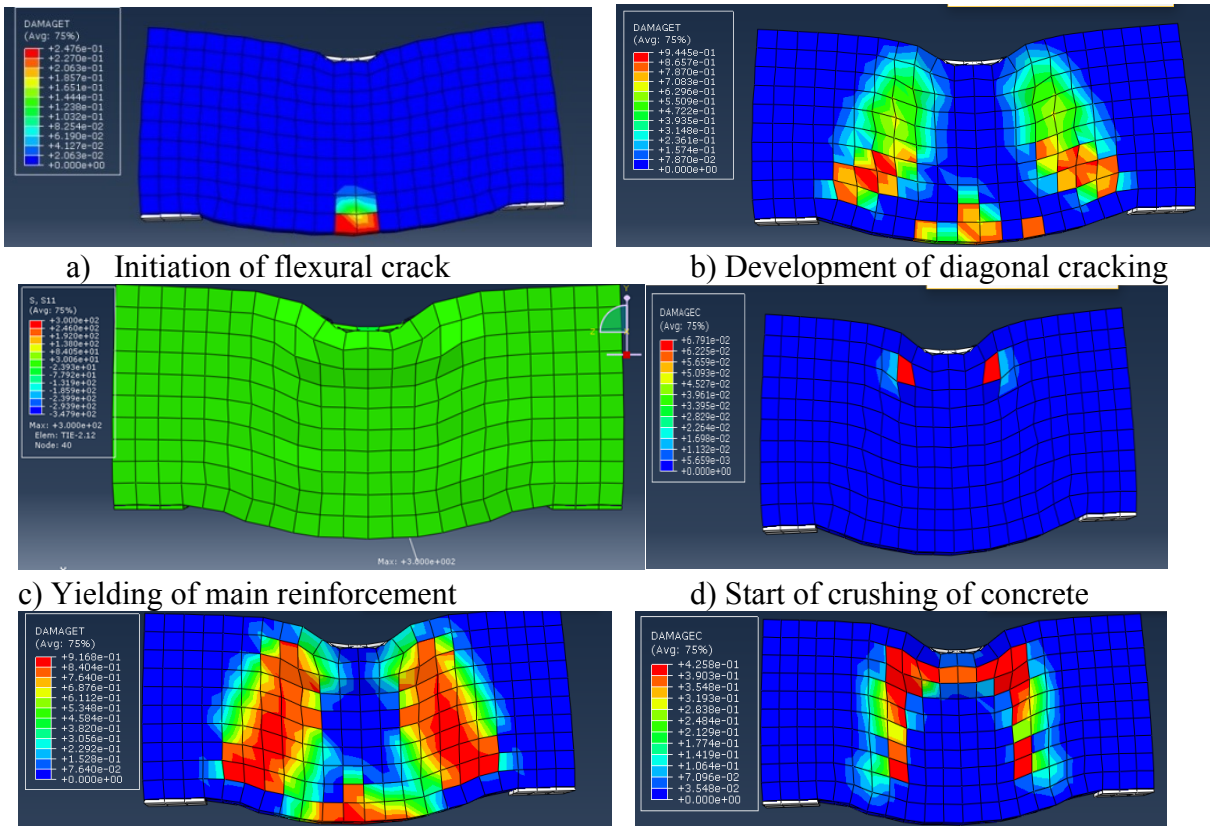

a) Initiation of flexural crack

b) Development of diagonal cracking

c) Yielding of main reinforcement

d) Start of crushing of concrete

e) Overall cracking of concrete diagonally

f) Overall failure of the beam by crushing

Figure 24: Failure progress of one point loaded simply supported deep beam of shear span to depth 1.00

The contour plots of the ABAQUS/Standard output in the form of image as in described above for reinforced concrete deep beam with shear span to depth ratio 1.00 in category-I for the rest of beams in this category is included in the appendix.

[1]**Table 5:** Analytically Predicted and Finite Element Numerical ultimate load results for Category-I

Category	Shear span to depth ratio	$P_{predicted}$[1] (in kN)	P_{FEA} (in kN)	P_{pre}/P_{FEA}
C-I	1.00	1002.508	1030.950	0.972
	1.25	1142.834	1166.210	0.980
	1.50	860.116	842.893	1.020
	1.75	683.330	803.911	0.850
	2.00	556.643	685.476	0.812
Statistical Analysis		Mean		0.927
		SD		0.090
		CV		0.097

Category-II: Simply supported deep beam with two point concentrated loading Category-II also comprises of five deep reinforced concrete beam specimens with shear span to depth ratio of 1.00, 1.25, 1.50, 1.75 and 2.00 all with the same overall span length of 4060mm and breadth 200mm. The same to that of Category-I deep beam specimens in this Category also uses a steel plate with dimensions 400x200x20mm at loading and support points for the same reason. Here to avoid the effect of position of center to center loading position is the same as to the beam overall depth and the notations and the details of reinforcing of cross-sections studied under category-II are shown in Fig.(25).

[1] Analytically derived ultimate load capacity prediction (Eq. 24)

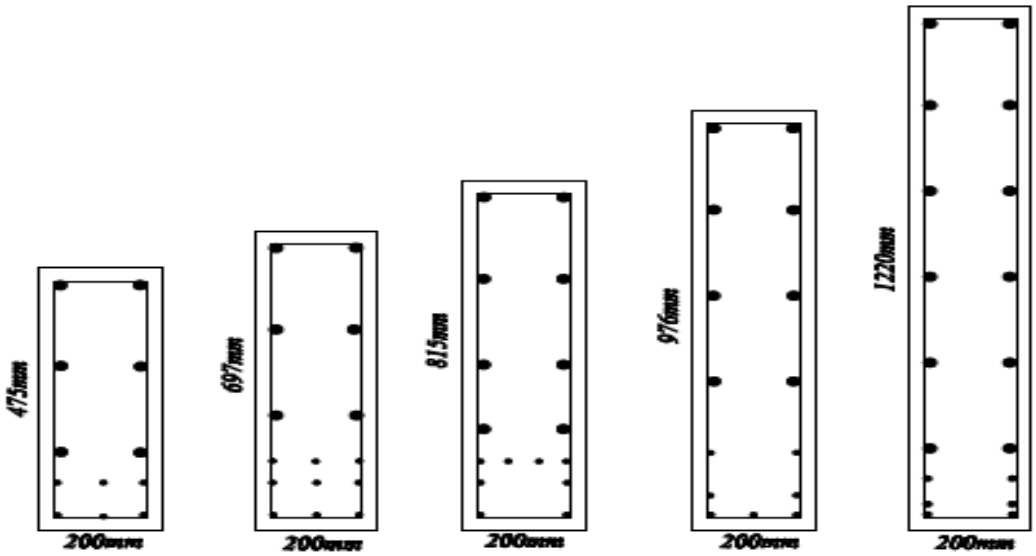

Figure 25: Cross-sections studied in case study of Category II

For category-II the reinforcement (vertical and horizontal) detailing is tabulated as in Table (6) below.

Table 6: Main and web reinforcement detailing for beam specimens under category-II

Shear span to depth ratio	Main reinforcement ratio ρ_s	Vertical web reinforcement ratio ρ_v	Horizontal web reinforcement ratio ρ_h
1.00	0.003	0.019	0.0157
1.25	0.0031	0.0157	0.0157
1.50	0.0044	0.0157	0.0157
1.75	0.0054	0.0157	0.0157
2.00	0.0045	0.0157	0.0157

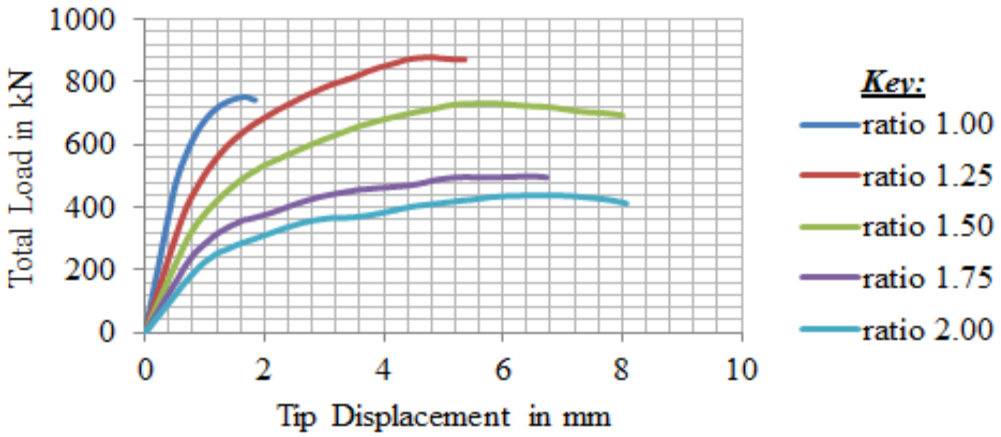

(a)

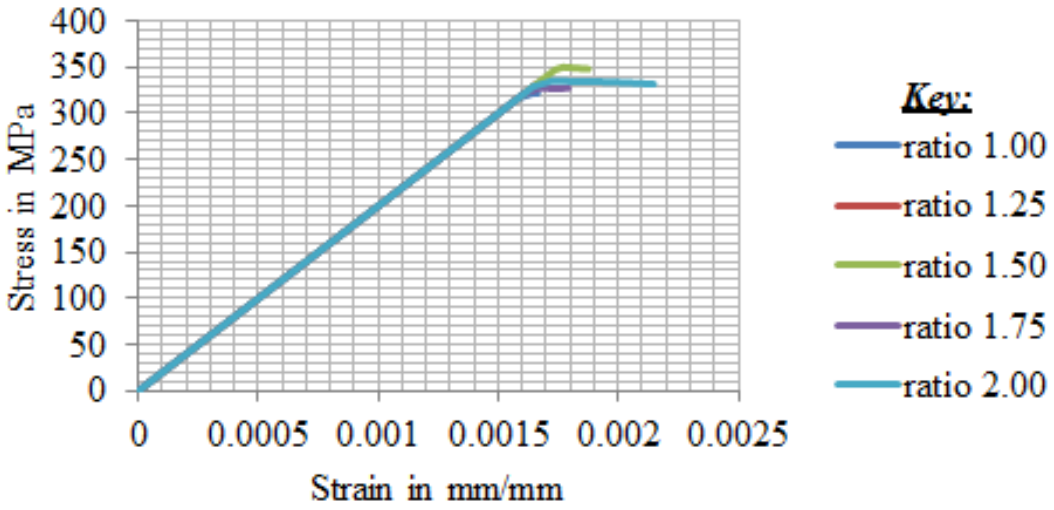

(b)

Figure 26: Load-Displacement (a) and Stress Strain (b) curves of Category-II

To illustrate the failure modes and behavior of simply supported reinforced concrete deep beams studied in category-I loaded two point concentrated load, the step wise failure progress of following representative deep beam from this category with shear span to depth ratio of 1.00 is shown at different stage of its failure with contour for tensile damage shown at different stage. As shown in Fig. (27) below the failure at the application of small percent of ultimate load as in Fig. (27a), initiation of flexural cracks is seen at the mid span of the beam. These tiny cracks are supposed to be due to flexural stress developed at most bottom extreme fiber of the mid-section and at this stage the stress is fully flexural. After a while or some increment in percent of ultimate loading diagonal cracking of concrete would take place as seen from Fig. (27b) below. After then if a continuation in increment percent of ultimate loading is done the flexural stress in the bottom (main) steel reaches to its ultimate and the yielding will result as in Fig. (27c) and Fig. (26) The yielding of reinforcement. Due to further increase in percent of ultimate load could not carried by the tie reinforcement, the nodal conditions reach their crushing strength and as a result crushing will takes place as shown in Fig. (26d). As a result of weakening of the web by tension or splitting of diagonal cracks seen in Fig. (26e) result in weakening of concrete in compression and full crushing will takes place and the Ultimate capacity the load this step is taking place.

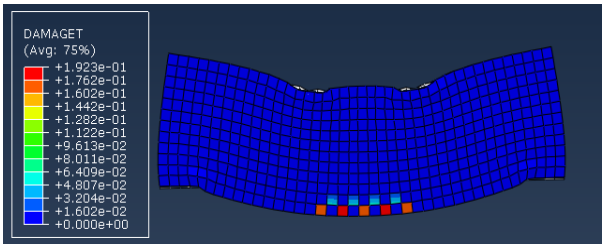

a) Initiation of flexural cracking

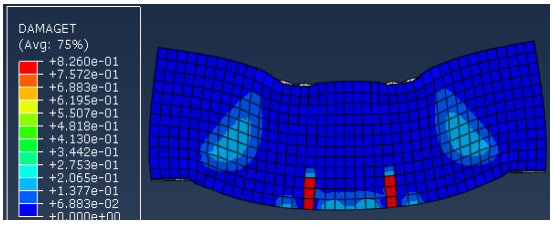

b) Initiation of diagonal cracking

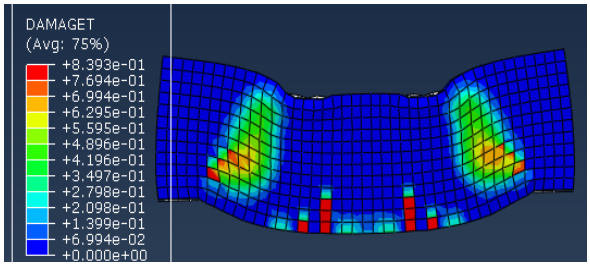

d) Start of crushing at near node

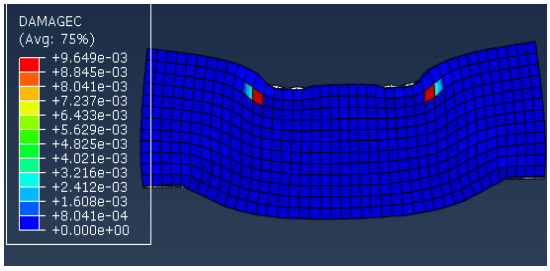

c) Developed diagonal cracking

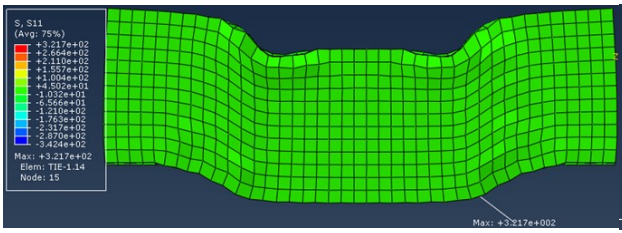

e) Yielding of main reinforcement

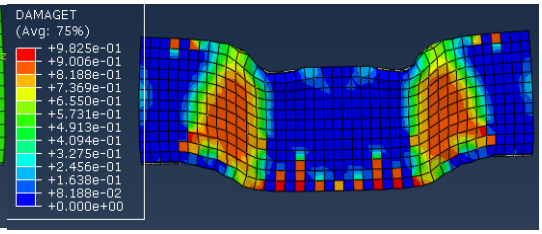

f) totally cracked diagonal strut

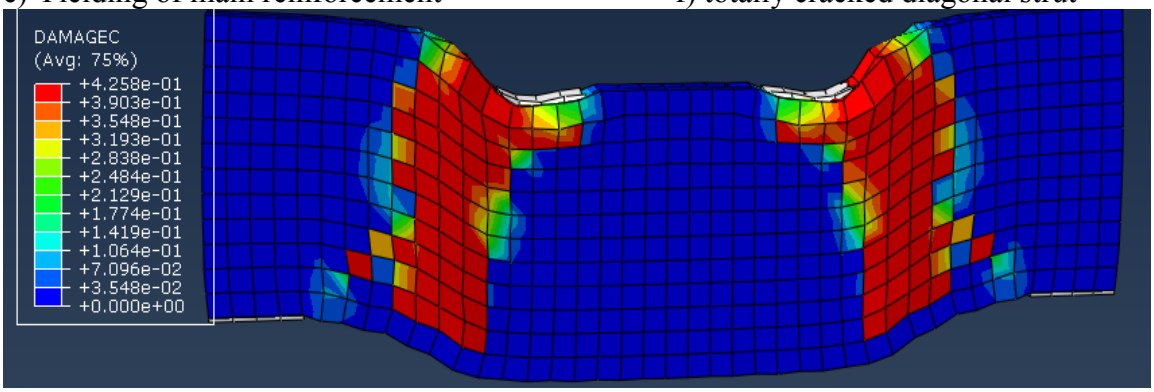

g) Overall failure of the beam by web tension plus compression

Figure 27: Failure progress of two point loaded simply supported deep beam of shear span to depth of 1.00

The contour plots of the ABAQUS/Standard output in the form of image as in described above for reinforced concrete deep beam with shear span to depth ratio 1.00 in category-II for the rest of beams in this category is included in the appendix.

Table 7: Analytically Predicted and Finite Element Numerical ultimate load results for Category-II

Category	Shear span to depth ratio	$P_{predicted}$[2] (in kN)	P_{FEA} (in kN)	$\mathbf{P_{pre}/P_{FEA}}$
C-II	1.00	855.788	751.785	1.138
	1.25	617.168	878.497	0.703
	1.50	534.756	731.213	0.731
	1.75	505.928	498.480	1.015
	2.00	437.043	438.395	0.997
Statistical Analysis		Mean		0.917
		SD		0.191
		CV		0.208

Category-III: The same to that of Category-I and Category-II this Category also comprises of five deep beam specimens with shear span to depth ratio of 1.00, 1.25, 1.50, 1.75 and 2.00 and all specimens are with the same overall span length of 4000mm. For this Category a steel plate with dimensions 200x200x20mm at loading and support is used. The details of reinforcing and the cross-sections studied under Category-III are shown in Fig. (28).

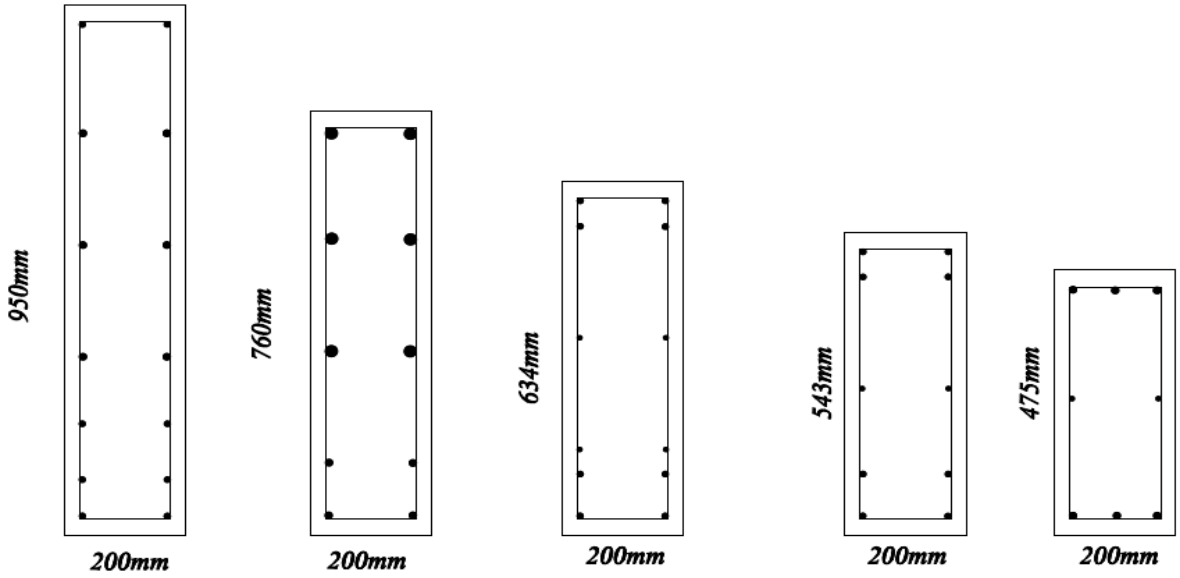

Figure 28: Cross-sections studied in case study of Category III

[2] Analytically derived ultimate load capacity prediction (Eq. 24)

Table 8: Main and web reinforcement detailing for beam specimens under category-III

Shear span to depth ratio	Main reinforcement ratio ρ_s	Vertical web reinforcement ratio ρ_v	Horizontalweb reinforcement ratio ρ_h
1.00	0.0027	0.00565	0.00565
1.25	0.0023	0.00565	0.00565
1.50	0.0027	0.0025	0.0025
1.75	0.0033	0.0025	0.0025
2.00	0.0026	0.0025	0.0025

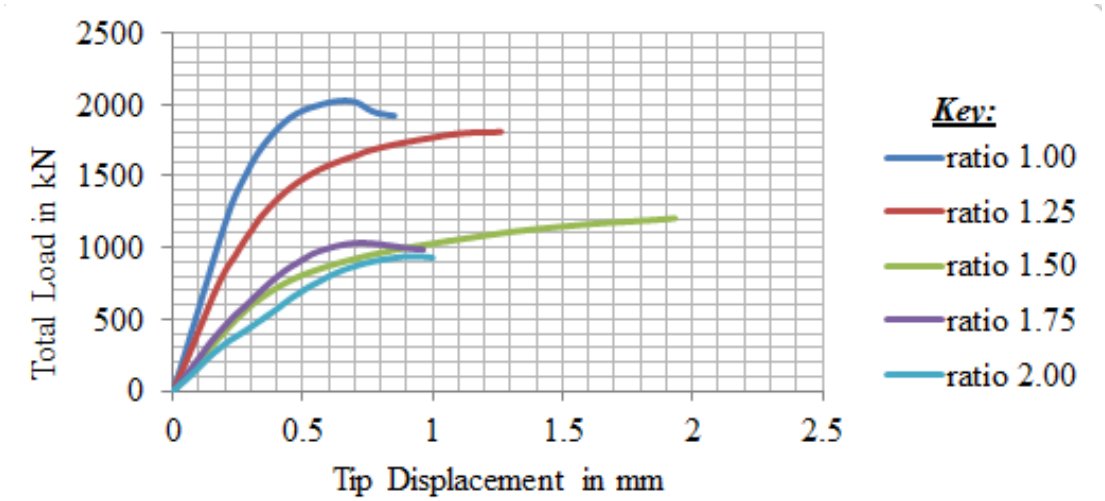

(a)

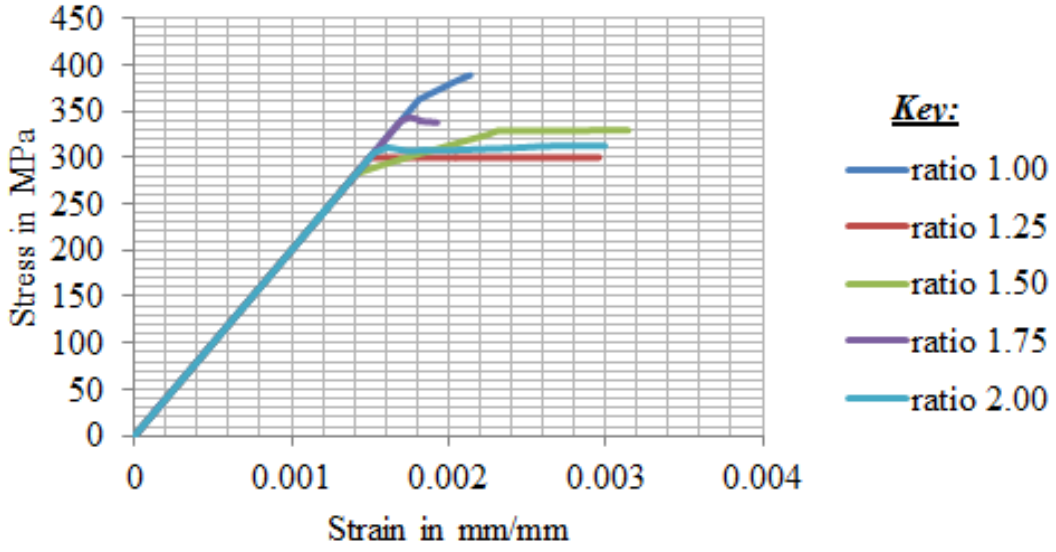

(b)

Figure 29: Load Displacement (a) and Stress Strain (b) curves of Category-III

To illustrate the failure modes and behavior of simply supported reinforced concrete deep beams studied in category-III, the step wise failure progress of following representative deep beam from this category with shear span to depth ratio of 1.00 is shown at different stage of its failure with contour for tensile damage shown at different stage. As shown in Fig. (30) below the failure at the application of small percent of ultimate load as in Fig. (30a), initiation of flexural cracks is seen at the mid span of the beam. These tiny cracks are supposed to be due to flexural stress developed at most bottom extreme fiber of the mid-section and at this stage the stress is fully flexural. After a while or some increment in percent of ultimate loading diagonal cracking of concrete would take place as seen from Fig. (30b) below. After then if a continuation in increment percent of ultimate loading is done the flexural stress in the bottom (main) steel reaches to its ultimate and the yielding will result as in Fig. (30c) and Fig. (30) The yielding of reinforcement. Due to further increase in percent of ultimate load could not carried by the tie reinforcement, the nodal conditions reach their crushing strength and as a result crushing will takes place as shown in Fig. (30d). As a result of weakening of the web by tension or splitting of diagonal cracks seen in Fig. (30e) result in weakening of concrete in compression and full crushing will takes place and the Ultimate capacity the load this step is taking place.

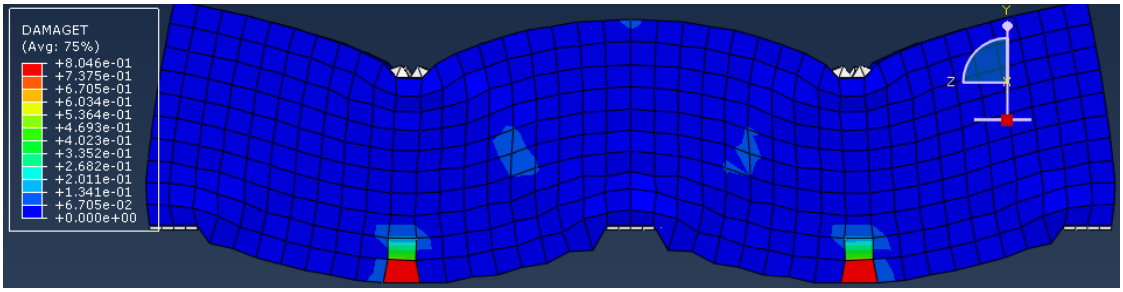

a) Initiation of flexural cracking

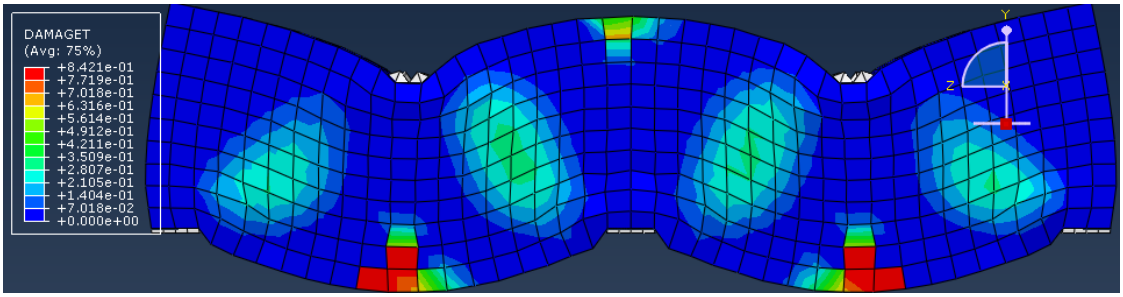

b) initiation of diagonal web cracking

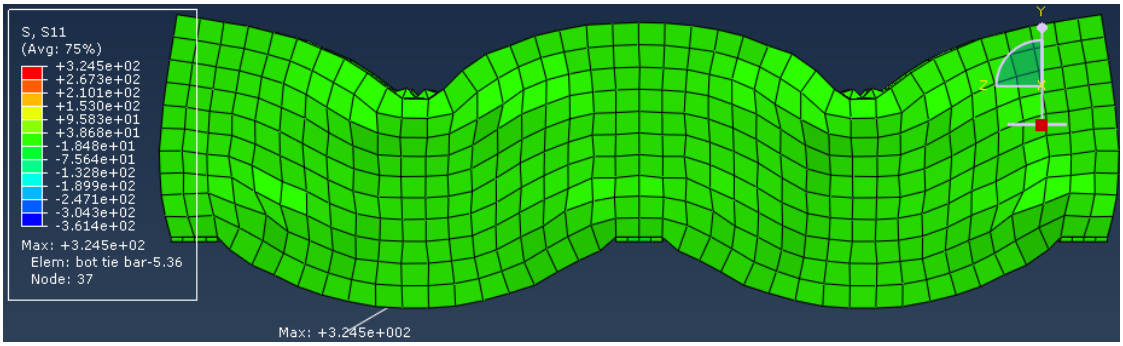

c) Yielding of main reinforcement by flexure

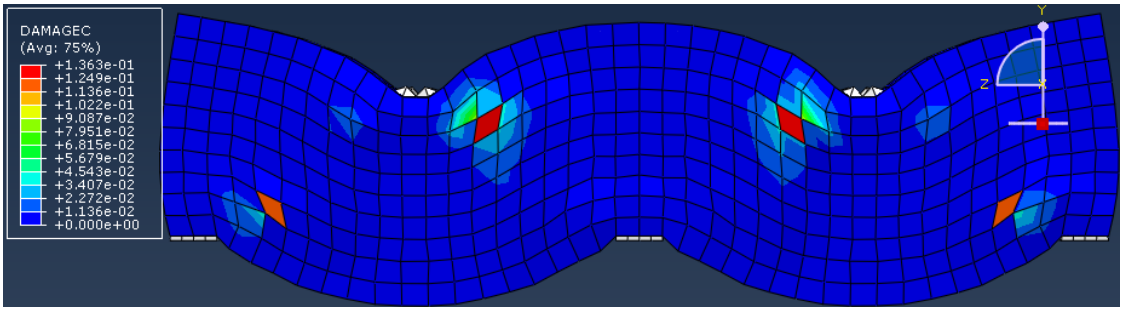

d) starting crushing at node (loading)

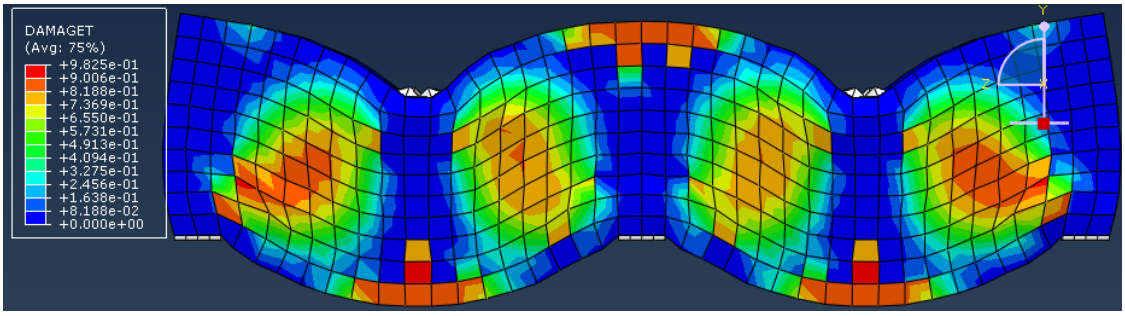

e) Fully developed diagonal web cracking

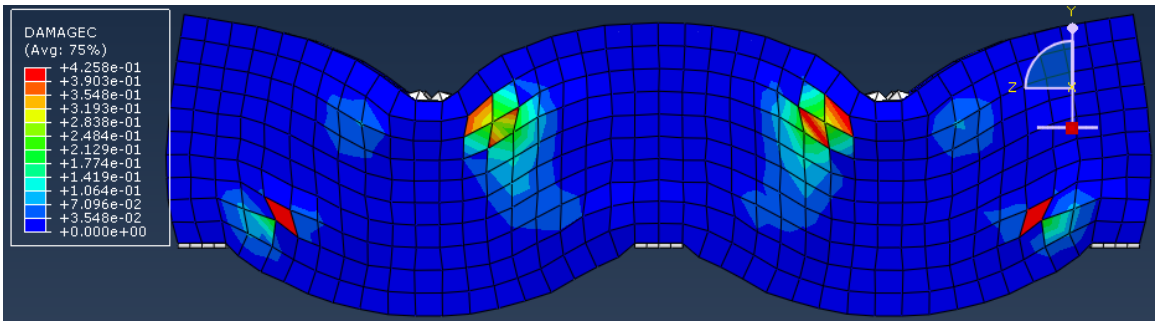

f) Fully crushed nodes both at loading and support by compression

Figure 30: Failure progress of two points symmetrically loaded two span continuous deep beam of shear span to depth of 1.00

The contour plots of the ABAQUS/Standard output in the form of image as in described above for reinforced concrete deep beam with shear span to depth ratio 1.00 in category-III for the rest of beams in this category is included in the appendix.

Table 9: Analytically Predicted and Finite Element Numerical ultimate load results for Category-III

Category	Shear span to depth ratio	$P_{predicted}$[3] (in kN)	P_{FEA} (in kN)	P_{pre}/P_{FEA}
C-III	1.00	1825.767	2026.460	0.900
	1.25	1503.466	1810.500	0.830
	1.50	1241.792	1249.480	0.994
	1.75	860.196	1033.950	0.832
	2.00	670.906	940.320	0.713
Statistical Analysis		Mean		0.854
		SD		0.103
		CV		0.121

5.1.Case Study Results and Discussion

5.1.1. Discussion Based on Statistical Results

As shown in Tables (5), (7) and (9) by the statistical analysis of results predicted by analytic expression derived for the prediction of ultimate load carrying capacity of reinforced concrete deep beams investigated in the case study to that of finite element analysis, above for case studies under categories (I), (II) and (III) respectively statistical parameters such as mean, standard deviation (SD) and coefficient of variance (CV) are calculated and tabulated along with results.

These statistical measures here are used to test accuracy of analytically derived equation compared to nonlinear finite element numerical simulation results. The calculated mean value for ratios of analytically predicted results to nonlinear finite element results in each category I and II are above 90% and 85.4% for category II as shown in respective Tables. This tells us the consistency of analytically predicted results to that of nonlinear finite element results as nonlinear finite element method is recommended by many codes

[3] Analytically derived ultimate load capacity prediction (Eq. 24)

whenever refined analysis approach is required. Mainly the coefficient of variation obtained (0.097), (0.208) and (0.121) respective of category I, II and III tells us good accuracy and consistencies for the values obtained. Especially the lesser values of coefficient of variation for category-I tells us the derived analytical expression from mechanism of reinforced concrete deep beam is most accurate than that of category-II and III. Similarly the coefficient of variation for category-III is also less than that of category-II and this tells the predictability of the analytic expression is more accurate from that of category-II. From this observation we can generalize the results obtained from analytical derived expression are in best agreement with the results from nonlinear finite element analysis than for simple span deep beams to greater accuracy level. But almost for all categories this could be considered as sufficient to use the analytically derived equation as a proper approach for the assessment of ultimate strength of reinforced concrete deep beams made up of different geometrical, material and reinforcement conditions.

5.1.2. Discussion Based on Failure Modes and Progresses of Nonlinear Finite Element and Numerical Simulation Results

5.1.2.1. General Simulated Failure Mode and Behavior

As shown the failure progress of all deep beam specimens studied in the case study under the appendix part all the specimens showed the same response up to failure. This is intentionally achieved to be governed by one mode of failure, that is flexural or by yielding of main reinforcement to prove a ductile design of strut-and-tie method. This is also shown by plotting the stress-strain in main (flexural) reinforcement and it is shown that the reinforcement is fully yielded before or at ultimate load as in shown in Figs. (23), (26) and (29). In addition the plot of ultimate load versus tip mid span displacement shown in the same figures tells a ductile failure mode as the behavior near ultimate load or post ultimate load does not show sudden drop in ultimate load.

In addition, we can see some numerical ultimate load conditions from the plot of the stress contours in the above Figs. (23) and (26); at about 20% 0f ultimate load flexural cracking is noticed. After some increment in load at about 33% of ultimate loading the web of the beam starts to crack and the stress in the flexural reinforcement the rate of

stress increase slightly decreases, this time stress redistribution starts. After the formation of a tiny cracks at the diagonal of the beam the rate of stress in flexural reinforcements once again starts to increase, and large flexural crack develops as in (b) and (c) of Figs. (23) and (26) respectively.

After this large flexural cracking the reinforcement will reach to its yield stress of at about 75% ultimate load capacity of the beam as in (c) and (e) of Figs. (23) and (26) respectively. Later on the concrete near supports starts to crush due to weakening of the diagonal strut by traverse diagonal cracking derived from the increase tensile stress in flexural reinforcement. This is well seen in (d) and (d) of Figs. (23) and (26) for category I and II resp.

Now at this point of about 94% of ultimate load the crushing of concrete near support and later as web weakens by traverse tensile force the beam gets at critical as can be seen in the Figs. (e) and (f) of Figs. (23) and (26) and the beam reach at its collapse load. The mechanism condition of the beams is also shown in (f) and (g) of Figs. (23) and (26) respectively.

The other validness of the proposed analytical approach as simulated by finite element is seen in the Figs. (23) and (26) by load displacement and stress strain plots for categories I and II, the main reinforcement is yielded before the beam reaching its ultimate capacity as in under reinforced section. Therefore failure is seen to be governed by flexure; hence the design results in ductile failure.

Consequently, the plots of load displacement curves and longitudinal (main) steel reinforcement stress strain curves in Figs. (23), (26) and (29) in the above for category (I), (II) and (III) respectively tells us the ultimate load carrying capacity and the main (longitudinal) reinforcement is yielding prior beam collapse as required in strut-and-tie model design method. Hence this helps sufficient stress redistribution to take place before collapse takes place and the assumptions to use strut-and-tie design method such as the formation of arch action between strut and tie and the requirement of sufficient ductility by reinforced concrete member design.

5.2.Parametric Study

5.2.1. Numerical Simulation Case Studies

Generally in this research paper it is required to study the influence of longitudinal (main) reinforcement, web reinforcement namely vertical and horizontal web reinforcement contribution for ultimate load carrying capacities of reinforced concrete deep beams divided in three major categories. This parametric study is designed to be carried out by means of numerical simulation, lets us take a few discussion on why numerical simulation is required as in next subtopic.

5.2.2. Why Numerical Simulation

As mentioned in the preceding section we need numerical simulation to adopt parametric study and this is mainly intended to improve design formulation for wider application.

Moreover there are some other situations stipulate numerical simulations as well. In real construction, there have been many occasions that constructed structures need performance assessment due to changes in design codes, specification, and application as well as occurrence of damage or decay in under service structures. This happens when a constructed building face new condition and needs to be retrofitted or repaired. Important structures such as inshore or offshore platforms, infrastructures such as bridges, lifelines and nuclear containments need continuous and accurate assessments of their performance in their service life [64]. Numerical simulation is one of the answers to all above problems. In this aspect nonlinear finite element method has dominant role in numerical assessments of structures. It is however some advantage and disadvantage here to be mentioned that there are plenty of models have been proposed so far for concrete member modeling. But there is no consensus on one model to cover entire condition of RC members and yield accurate results in all respect. Each model has its own merit and demerit. In essence for each specific problem, specific model should be employed. In other words some preliminary analyses with different constitutive and crack models ought to be performed first and then pick one model best results fit to the experimental observation then perform the final analysis for entire structure or conduct parametric study. This is a rational way in numerical simulation although there are some recommendations to use certain model for certain problem [64].

5.2.3. Effect of Main Reinforcement Ratio on Ultimate Shear Strength

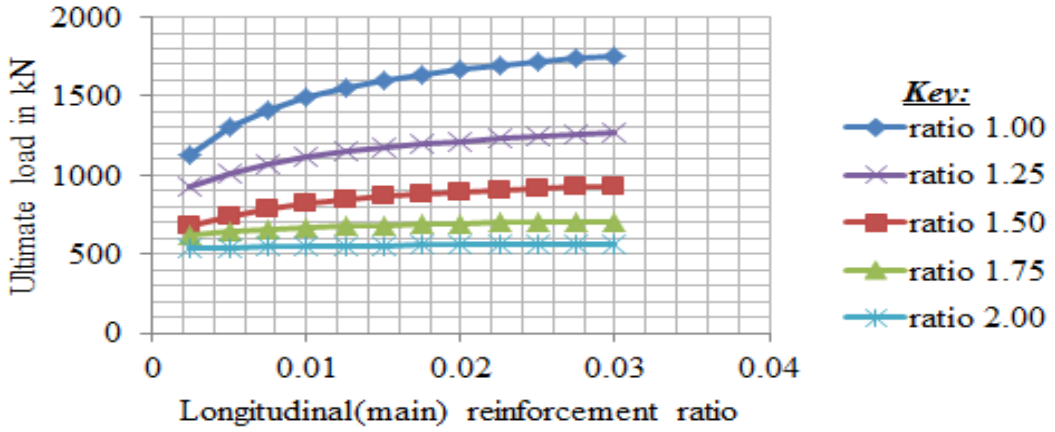

Figure 31: Effect of main reinforcement ratio on ultimate load carrying of Category-I

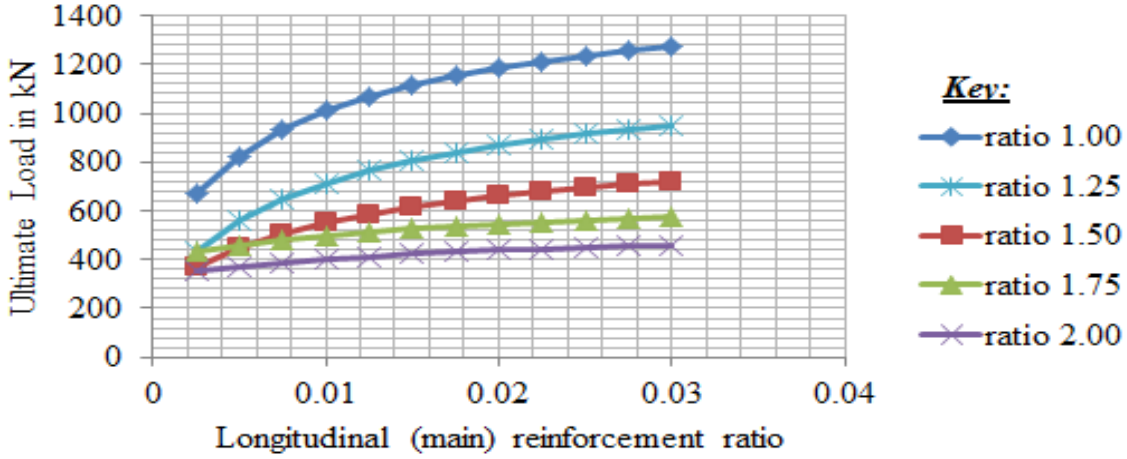

Figure 32: Effect of main reinforcement ratio on ultimate load carrying of Category-II

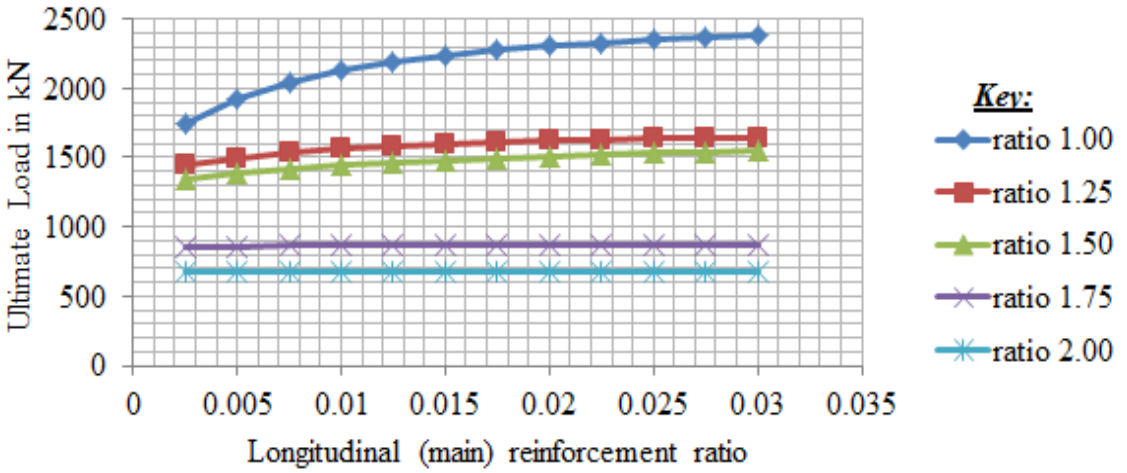

Figure 33: Effect of main reinforcement ratio on ultimate load carrying of Category-III

As seen in the above plots of longitudinal (main) reinforcement versus ultimate load capacity in Figs. (31), (32) and (33) for reinforced concrete deep beams categories of category (I), (II) and (III) is aimed to predict or assess the ultimate load conditions for varying reinforcement ratios. The study is carried out for varying ratios of longitudinal reinforcement ratios and provision of minimum web reinforcement ratio. It is seen that regardless of shear span to depth ratio the increase in longitudinal reinforcement ratio results in the increase in ultimate load. The increase in ultimate load is significant for reinforced concrete deep beams with shear span to depth ratios of 1.5 and less than 1.5. But for the remaining that means that of 1.75 and 2.00 the increase in longitudinal reinforcement ratio has no considerable effect on ultimate load, of course to give conclusion it is expected to increase in a very smaller rate than seen in with shear span to depth ratios of 1.5 and below it.

Generally, the effect of main reinforcement ratio on ultimate load gives increase in ultimate load, and this increase is more effective for deep beams with smaller shear span to depth ratios than any of deep beam above to that of with larger shear span to depth ratios. But after reaching to ultimate load the plots in the above figures tells us the ultimate load capacity goes to constant ultimate load value and any further increase in reinforcement ratio does not increase the ultimate load carrying capacities.

5.2.4. Effect of Web Reinforcement Ratio on Ultimate Shear Strength

The parametric study for web reinforcement in this research is conducted separately for vertical and horizontal web reinforcement keeping the longitudinal (main) reinforcement constant. This separately studying is specially intended to determine which method of web reinforcing is significantly influencing variable the ultimate load carrying capacity of reinforced concrete deep beams belonged under each category. Therefore it is presented as in Figs. (34), (35), and (36) below.

5.2.4.1.Effect of Vertical Web Reinforcement on Ultimate Shear Strength

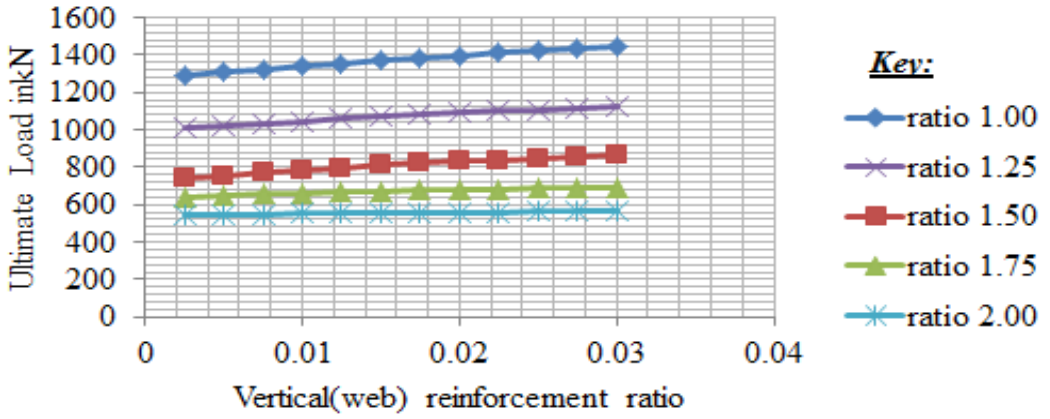

Figure 34: Effect of vertical reinforcement ratio on Ultimate load carrying of category-I

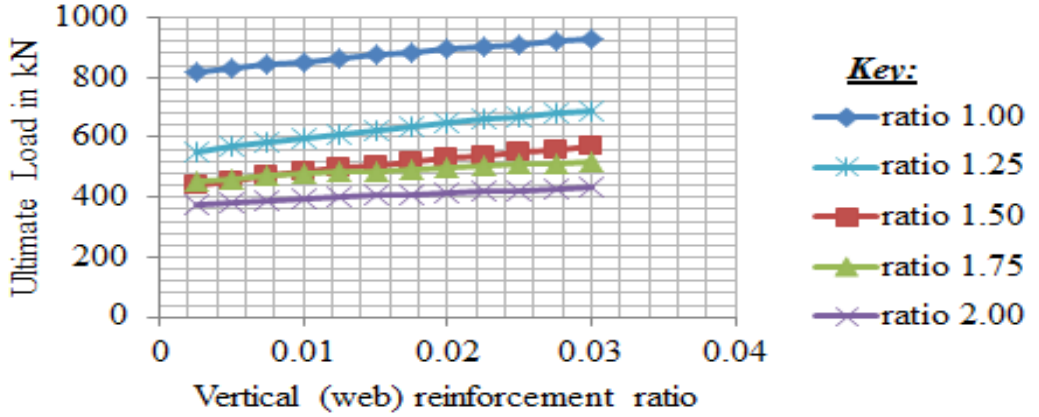

Figure 35: Effect of vertical reinforcement ratio on Ultimate load carrying of category-II

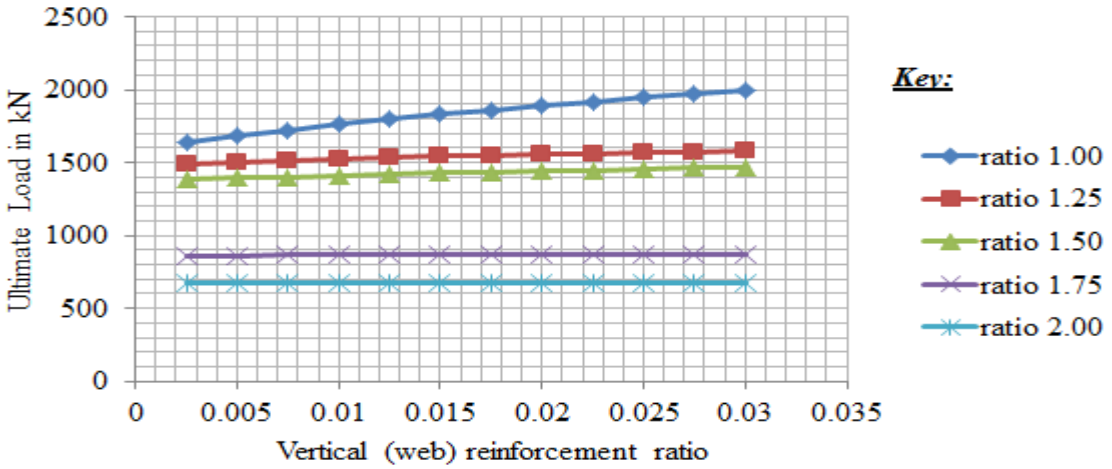

Figure 36: Effect of vertical reinforcement ratio on Ultimate load carrying of category-III

The plots of Figs. above (34), (35), and (36) of vertical web reinforcement ratio versus ultimate load curves indicate that the ultimate load capacity is increasing linearly for any increase in vertical reinforcement ratio. It is evident that for deep beams under category I and II the increase in ultimate load is linear in especially for deep beams with shear span to depth ratios of 1.5 and less than 1.5. This is expected to be resulted from the higher depth geometry of the beams and the shear span to depth ratio is the main responsible parameter. In addition for beams with shear span to depth ratios of 1.75 and 2.00 in the same category the increase in vertical shear reinforcement has little effect on ultimate load unlikely to that of 1.00, 1.25 and 1.50. But for deep beams category-III only a significant ultimate load increase is seen for beams with shear span to depth ratios of 1.00, 1.25 and 1.50 and for the rest of the beams the increase in vertical web reinforcement resulted in a slight linear increase in ultimate load. Unlikely deep beams with the same shear span to depth ratios in the other categories this insignificant effect in deep beams for category-III is expected to be resulted from continuity of span which allows more internal redistribution of stresses is taking place and this has led to the major redistribution of stresses before reaching ultimate load stage and parametric variation could not cause any more capacity changes once ultimate capacity is reached.

5.2.4.2.Effect of Horizontal Web Reinforcement on Ultimate Shear Strength

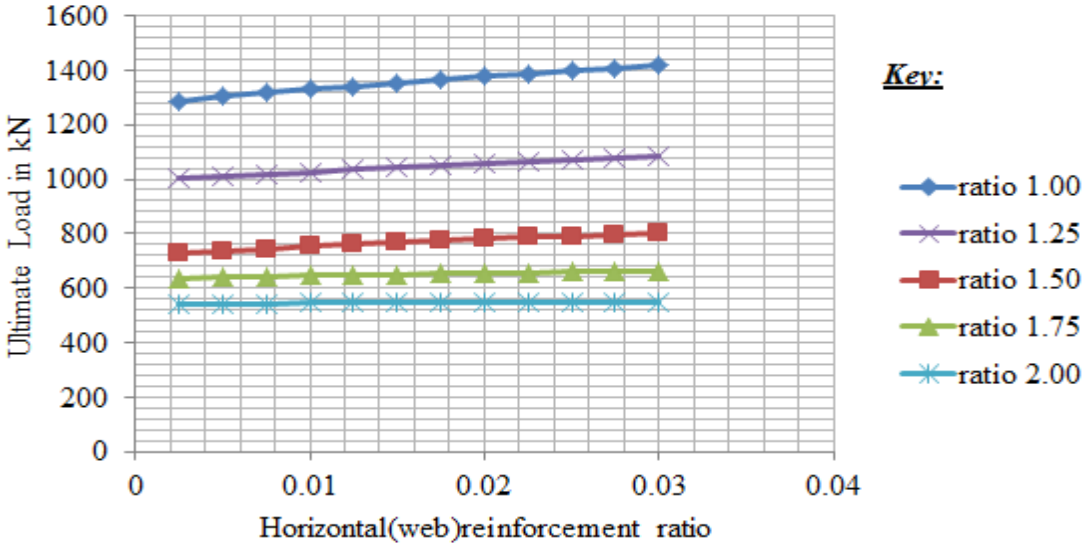

Figure 37: Effect of Horizontal reinforcement ratio on Ultimate load carrying of category-I

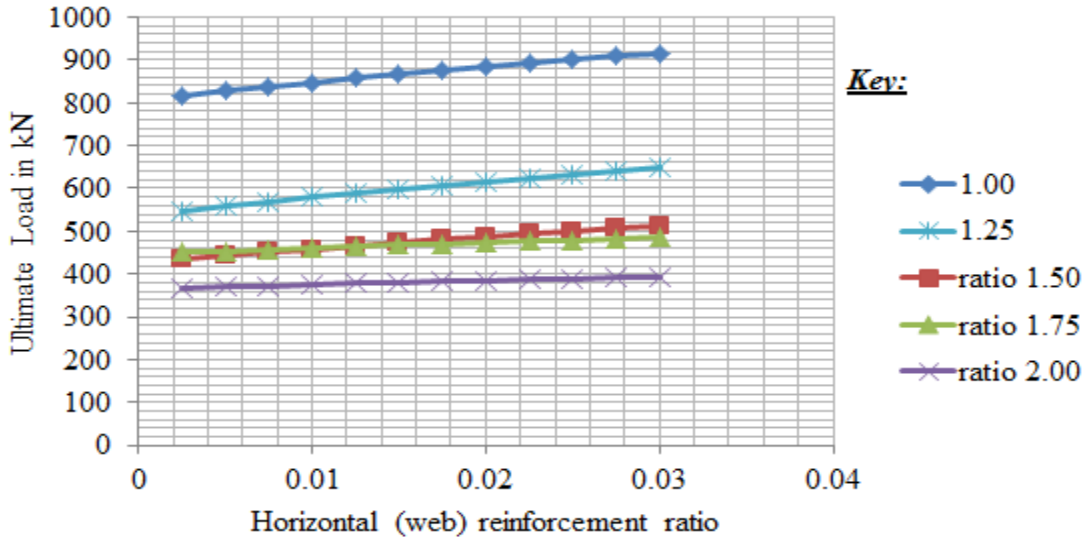

Figure 38: Effect of Horizontal reinforcement ratio on Ultimate load carrying of category-II

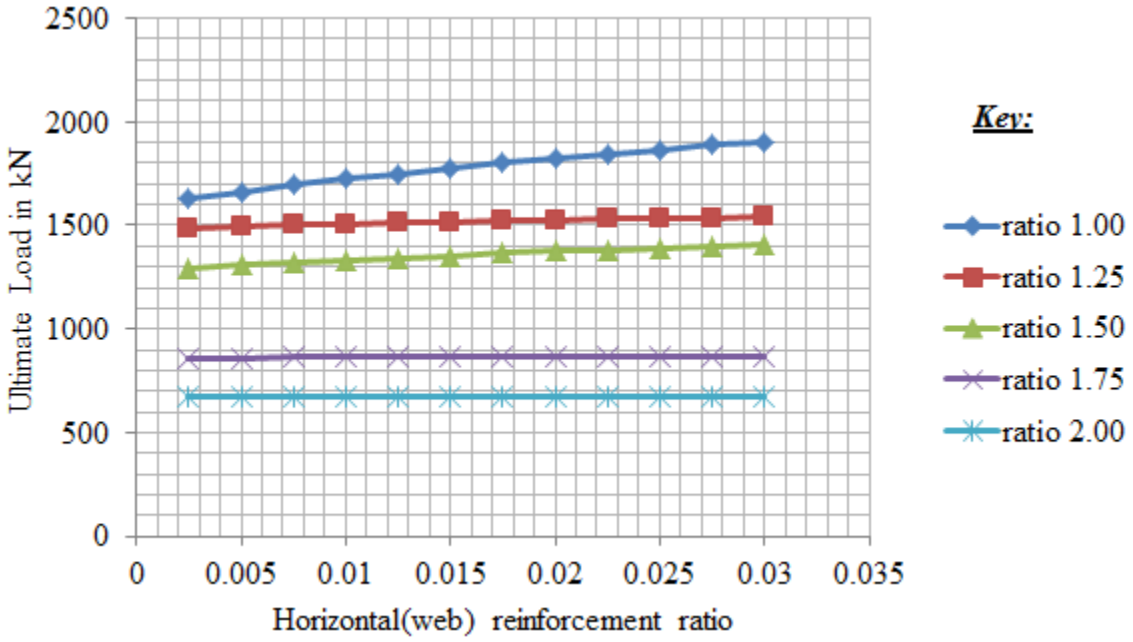

Figure 39: Effect of Horizontal reinforcement ratio on Ultimate load carrying of category-III

As seen from the plots of Figs. (37), (38), and (39) above horizontal web reinforcement versus ultimate load the increase in horizontal reinforcement showed a less moderate effect than vertical web reinforcement. The increase in ultimate load is also seen to be linear and this is seen to be more significant for deep beams of category-I and II with shear span to depth ratio 1.00 and 1.25 and similar trends in increase in ultimate load for

corresponding increase in horizontal reinforcement ratios but for category-III of deep beams with shear span to depth ratios of 1.00, 1.25 and 1.50 analogous increase in ultimate load is seen. For the remaining deep beams that means for deep beams of with shear span to depth ratios 1.75 and 2.00 the increase in ultimate load is less significant for any increase in horizontal web reinforcement.

6. CONCLUSION AND RECOMMENDATION

Based on observations and findings made in this research paper in the evaluation of the strut-and-tie method for reinforced concrete deep beams by analytical procedures to establish analytic expression that predicts the ultimate load carrying capacity and validated with the help of nonlinear finite element numerical simulation case studies, later on by parametric study the conclusion and recommendation is drawn respectively as in below.

6.1. Conclusions

The study on deep reinforced concrete section is considered to be interesting especially when nonlinear behavior of constituting materials mainly that of concrete is taken into account. It is the stand point of this research paper to take account the nonlinear behavior of concrete by manipulating some assumptions of equilibrium and mechanism of shear resistance of reinforced concrete deep beams and to evaluate the strut-and-tie method analytically and validating analytical results with that of nonlinear finite element numerical simulation.

Therefore, it is interesting to conclude the main findings from analytic study covered and the result of parametric studies as follow.

i. The analytically derived equation from equilibrium configuration of the proposed truss model for the application and evaluation of strut-and-tie method is in good agreement for predicting the ultimate load condition of reinforced concrete deep beams studied in the case study, as validated and correlated with results from nonlinear finite element numerical simulations.

ii. The mode of failure is seen to be flexural failure and this result in ductile design of deep beams in which yielding of the main reinforcement takes place prior collapse. This is shown by Figs. (23b), (26b) and (29b) for categories I, II and III resp.

iii. Consideration of concrete softening effect as in Mohr-Coulomb criteria is seen important and it is appropriate to include its effect on post cracking behavior

of concrete members and its effect due in the prediction of ultimate load carrying capacity of deep reinforced concrete beams.

Further, based on the parametric studies and the effect parameters studied in this work as the effect of longitudinal or main reinforcement and the effect of web reinforcement which constitutes vertical and horizontal web reinforcements ratio are treated alternatively and results are presented in respective analysis. To conclude web reinforcement ratios on ultimate strength that means the vertical and horizontal web reinforcement vertical web reinforcement one in the absence of the other alternatively studied by case study and both has the same effect on the ultimate load capacities with differing magnitude. But based on the independent study conducted the following observations are drawn.

a) Main reinforcement ratio has a direct effect on ultimate load carrying capacity of reinforced concrete deep beams of all categories. The increase in main reinforcement ratio has resulted in increase in ultimate load and once the ultimate capacity reached further increase in reinforcement ratio does not bring about any contribution.
b) The increase vertical reinforcement ratio linearly increases the ultimate load capacity and it is most effective especially for deep beams with smaller shear span to depth ratio as shear failure is responsible for failure. But for beams with larger shear span to depth ratio the effect of vertical reinforcement diminishes and this is expected to be the result of slenderness effect is introduced and the load carrying is approaching to be dependent on its flexural capacity.
c) The effect is seen for increasing the horizontal web reinforcement ratios but with smaller rate of increase in ultimate load capacity for any increase in horizontal web reinforcement ratios. Even though the effect is with in slow rate unlike to the beams for shear span to depth ratio 1.50 and greater than 1.50 the effect after slight increase tend to null.

6.2.Recommendations for Future Work

Analysis of reinforced structure requires great effort due to the nonlinear behavior of concrete and study of load carrying behavior is seen to be interesting, especially where

post-cracking behavior is assumed significant contribution to load carrying capacity of the structural member under consideration.

Therefore the following points should be considered as recommended future task in the area of the study.

- The findings in this paper would be better if experimental studies are carried out to determine the general applicability of the method.
- Further study on parameters such as concrete grade and others other than studied in the parametric study subtopic using the method used by this paper is recommended.
- The ultimate load prediction equation derived in this research is confined to only two dimensional strut-and-tie truss configurations; the work for three dimensional is left as a gap for future work.

7. BIBLIOGRAPHY

[1] Russo, G. Venir, R. and auletta, M. Reinforced concrete deep beams – shear strength model and design formula. Journal of Structural Eng. 102(3) :(2005), pp429-437

[2] Ashraf R.M., Mohie S. Shoukry, Janet M.Saeed, Prediction of the behavior of reinforced concrete deep beams with web openings using the finite element method. Alexandria 2014.

[3] ACI Committee 446; Fracture mechanics of concrete: Concept, models and determination of material properties, ACI 446.1R-91 (Re-approved 1999, Third printing, july 2002), 1989

[4] Ashour, A. F., "Upper Bound Analysis for Reinforced Concrete Deep Beams with Fixed End Supports", ACI Structural Journal, 96,2, 1999, pp.167-173.

[5] Abolfazl A., Reza A. and Ali R.R. Investigation of experimental and analytical shear strength of reinforced concrete deep beams. Journal of Str.Engg. (2011), pp.1-19.

[6] AASHTO, Bridge Design Specification, Customary US units, with 2008 Interim Revisions, American Association of State Highway and Transportation Officials, Washington, DC, 2008.

[7] CSA-S806-02, Design of Concrete Structures, Canadian Standards Association, 2004.

[8] Vecchio F. J. and Collins M. P., "Compression Response of Cracked Reinforced Concrete", Journal of Structural Engineering, ASCE, 119,12, 1993, pp3590-3610.

[9] ACI 318-08, Building Code Requirements for Structural Concrete and Commentary.

[10] Eurocode2: Design of concrete structures – Part 1-1 EN1992

[11] De Pavia, H.A. R et al.; Strength and behavior of Deep Beams in shear

[12] Leonhardt, F., and Walther, R.; Wall type beams (Wandartige Trager), Bulletine No.178, Deutscher ausschuss fur stahlbeton, Berlin, pp.159

[13] Asin, M.; The behavior of reinforced concrete continuous deep beams, Delft University press, The Netherlands, 1999

[14] Ngo, D. and Scordelis, A. D.; Finite element analysis of reinforced concrete beams, ACI Journal, V.66, No.3, pp.152-163, 1967

[15] Rashid, Y. R.; Analysis of prestressed concrete pressure vessels, Nuclear Engineering and Design, V.7, No.4, pp. 334-355, 1968

[16] Bazant, Z. P. and Oh, B. H.; Crack band theory for fracture of concrete, J. of Materials and Structures, V.16, No.93, pp. 155-177, 1983

[17] Bazant, Z. P. and Lin, F. B.; Nonlocal smeared cracking model for concrete fracture, ASCE, J. of Structural div., V.114, No.11, pp. 2493-2510, 1988

[18] Vecchio, F. and Collins, M. P.; The modified compression field theory for reinforced concrete elements subjected to shear, ACI Structural Journal V.3, No.4, pp.219-231, 1986

[19] Hsu, T. T. C.; Unified Theory of Reinforced Concrete, CRC press,1993

[20] Lin, C. S., and Scordelis, A. C.; Nonlinear analysis of RC shells of general forms, J. of structural Div., ASCE, V.102, pp. 523, 1975

[21] ACI Committee 446; Fracture mechanics of concrete: Concept, models and determination of material properties, ACI 446.1R-91 (Re-approved 1999, Third printing, july 2002), 1989

[22] Kong, F. K.; and Chemrouk, M. (2002) Reinforced concrete deep beams university of Newcastle

[23] Sciarmmarella, C. A. (1963). Effect of holes in deep beams with reinforced vertical edges, engineering progress, university of Fla, 17, No.12.

[24] Quanfeny, W., Hoogenboom, P. C. J. (2004). Nonlinear Analysis of Reinforced Concrete Continuos Deep Beams using stringer – panel model. Asian journal of Civil Engineering (Building and Housing), 5(1-2), 25.

[25] Ashour, A. F. and Morley, C. T., “Effectiveness Factor of Concrete in Continuous Deep Beams”, Journal of Structural Engineering, ASCE, 122,2, 1996, pp 169-178.

[26] Mohammad R.S., Hiroshi K. and Shigeki U.; Experimental and analytical study on rc deep beams behavior under monotonic load. Minamihara, Tsukuba-shi, Ibaraki-ken: Earthquake Engg. Research institute pp.305-329.

[27] AASHTO. Design specifications, customaryU.S.units:2012interimrevisions. 4ed.Washington: American Association of State Highway and Transportation Officials; 2012. 4.

[28] CAN/CSA-S6-06.CanadianhighwaybridgedesigncodeandS6.1–06 Commentary on CAN/CSA-S6- 06, Canadian Highway Bridge Design Code: Association canadiennede normalization; 2006.

[29] ACI 318-08, Building Code Requirements for Structural Concrete and Commentary.

[30] Pereta R., Vique J. Strut-and Tie modeling of reinforced concrete beam using genetic algorithms optimization. Construction and Building Materials. 2009; 23(8):2914-25.doi10.1016/j.conbuildmat.2009.02.016

[31] Alam MA., Jumaat MZ. Experimental Investigation on U-and L-Shaped End Anchorage FRP Laminate strengthened Reinforced Concrete Beams. The Arabian Journal for Science and Engineering (AJSE) 2012 ;(37-4 :):905-19.

[32] Belarbi A., Hsu TTC. Constitutive laws of softened concrete in biaxial tension compression. ACI, Structure Journal.1995; 92(5):562–73.

[33] AS3600. Australian standard for concrete structures. Standard association of Australia. North Sydney 2009, pp.198.

[34] Oesterle, R. G., Aristizabal-Ochoa, J. D., Shiu, K. N. and Corley, W. G., “Web Crushing of Reinforced Concrete Structural Walls”, ACI Strucural Journal, 81,3, 1984, pp 231-241.

[35] Vecchio F. J. and Collins M. P., “Compression Response of Cracked Reinforced Concrete”, Journal of Structural Engineering, ASCE, 119,12, 1993, pp.3590-3610.

[36] Oesterle, R. G., Aristizabal-Ochoa, J. D., Shiu, K. N. and Corley, W. G., "Web Crushing of Reinforced Concrete Structural Walls", ACI Strucural Journal, 81,3, 1984, pp.231-241.

[37] Rogowsky, D. M. and MacGregor, J. G., "Design of Reinforced Concrete Deep beams", Concrete international: Design and Construction, 1986, pp.49-56.

[38] Ashour, A. F., "Upper Bound Analysis for Reinforced Concrete Deep Beams with Fixed End Supports", ACI Structural Journal, 96,2, 1999, pp.167-173.

[39] Vecchio F. J. and Collins M. P., "Compression Response of Cracked Reinforced Concrete", Journal of Structural Engineering, ASCE, 119,12, 1993, pp.3590-3610.

[40] ASCE-ACI Committee 445 on Shear and Torsion, "Recent Approaches to Shear Design of Structural Concrete", Journal of Strucural Engineering, ASCE, 124, 12, 1998, pp 1375-1417.

[41] Bazant Z. P., and Kim J. K., "Size Effect in Shear Failure of Longitudinally Reinforced Beams", ACI Journal, 81, 5, 1984, pp.456-468.

[42] K. H Yang, H.C. Eun, H.S. Chung, The influence of web openings on the structural behavior of reinforced high-strength concrete deep beams, Eng. Struct. 28(13) (2006) pp.1825-1834.

[43] K.H. Tan, K. Tong, C.Y. Tang, Consistent strut-and-tie modeling of deep beams with web openings, Mag. Conc. Res.55 (1) (2003) pp.572-582.

[44] Ashour A. and Yang K.H. Application of Plasticity Theorem to Reinforced Concrete Deep Beams. 2007; 3: pp4.

[45] F.B.A. Beshara, I.G. Shaaban and T.S. Mustafa. Behavior and analysis of Reinforced Concrete Continuous Deep Beams. Journal of Str.Engg. Pp.9-11

[46] ABAQUS User Manual, version 6.13, ABAQUS Inc., pawtuket, Rhode Island, 2007.

[47] J.M. Saeed, Modeling of the Mechanical Behavior of Concrete, MSc. Thesis, Structural Eng. Dept., Faculty of Engineering, Alexandria University, 2012, pp163.

[48] Tomasz J., Tomasz L, Identification of parameters of concrete damage plasticity constitutive model

[49] Devis J., Observation of fracture path development in mortar beam specimens, Adv. Cem. Bas. Mat., 3(1996)31-36.

[50] Green S.J., Swanson S.R., Static constitutive relations for concrete, AWFL-TR-72-244, U.S. Air Force Weapon Laboratory, Kirtland Air Force Base, NM, 1973.

[51] Schlangen E., Experimental and numerical analysis of fracture processes in concrete, Ph.D. Thesis, Delft University of Technology, 1993.

[52] CBE-FIP, CEB-FIP Model Code 1990; Design Code, Committee Euro-international, 1993.

[53] Lubliner J.J., Oliver S.O., Onate E., A plastic-damage model for concrete, International Journal of Solids and Structures, 25,3(1989)229-326.

[54] Ammar N. Hanoon, M.S. Jaafar, Farzad H. and F.N.A. Abd Aziz; Strut effectiveness factor for reinforced concrete deep beams under dynamic loading conditions, Department of civil engineering, university putra Malaysia and the engineering affairs department,Baghdad university, Iraq. Case studies in str.Eng. 6(2016) pp.84-102.

[55] K. Tan, K. Tong, C. Tang, Direct strut-and-tie model for prestressed deep beams, Journal of Structural Engineering 127(9) (2001) 1076-1084.

[56] Zeng. L.H., and Tan, K.H, (1999). Singapore Patent No.: N.T.U. National Undergraduate Research Project.

[57] R.D. Cook, W.C. Young, Advanced Mechanics of Materials, vol.2, prentice Hall Upper Saddle River, NJ, 1999.

[58] ASCE-ACI445, Recent Approaches to Shear Design of Structural Concrete, Journal of Structural Engineering 124(12) (1998) 1374.

[59] CBE-FIP, CEB-FIP Model Code 1990; Design Code, Committee Euro-international, 1993.

[60] S.J. Foster, A.R. Malik, Evaluation of efficiency factor model in strut-and-tie modeling of non-flexural members, Journal of Structural Engineering 128(5) (2002) pp.569-577.

[61] K. Tan, K. Tong, C. Tang Direct strut-and-tie model for prestressed deep beams, Journal of Structural Engineering 127(9) (2001) pp.1076-1084.

[62] AASHTO. Design specifications, customaryU.S.units:2012interimrevisions. 4ed.Washington: American Association of State Highway and Transportation Officials; 2012. 4.

[63] S. Hong, D.Kim, S. Kim, N. Hong, Shear strength of reinforced concrete deep beams with end anchorage failure, ACI Structural Journal 99(1) (2002) 12-22.

[64] Mohammad R.S., Hiroshi K. and Shigeki U.; Experimental and analytical study on rc deep beams behavior under monotonic load. Minamihara, Tsukuba-shi, Ibaraki-ken: Earthquake Engg. Research institute pp.305-329.

8. APPENDIX

I) Finite Element Simulations and Failure Stages of Beams Under Category-**I**

1) Shear span to depth ratio 1.25

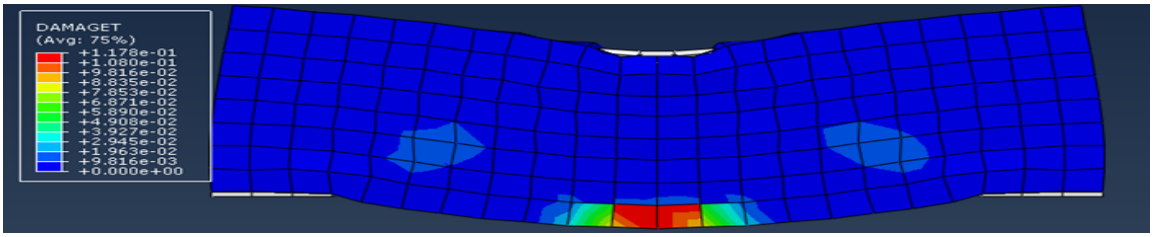

(a) Start of flexural cracking

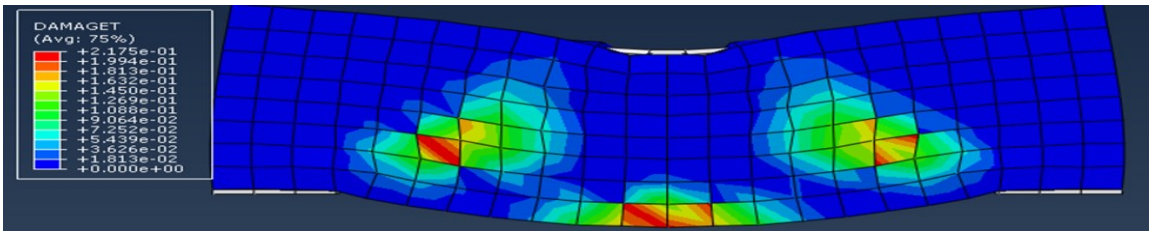

(b) Diagonal web cracking started

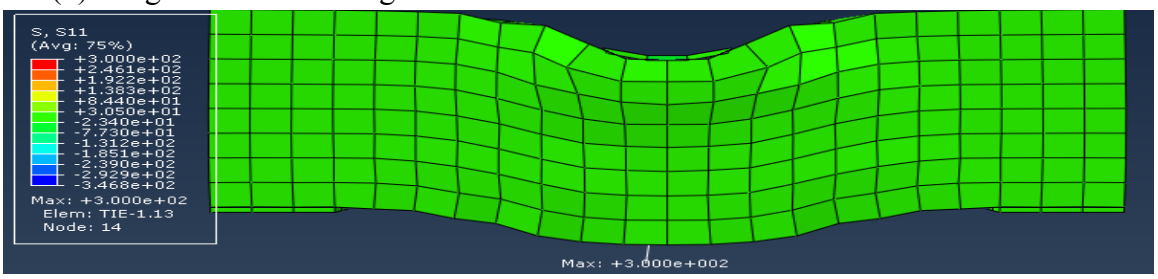

d) Yielding of main reinforcement by flexure

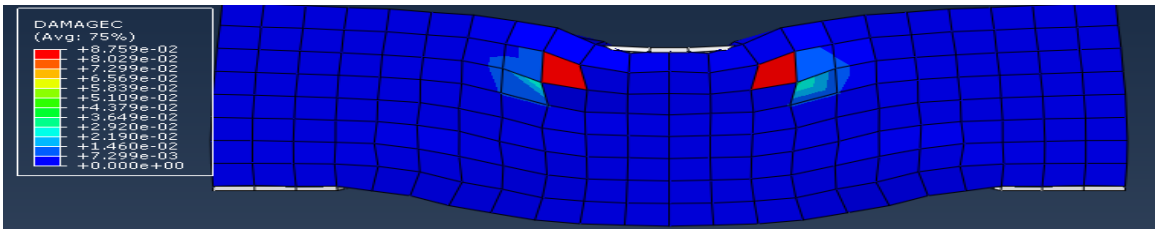

e) Crushing of concrete at loading

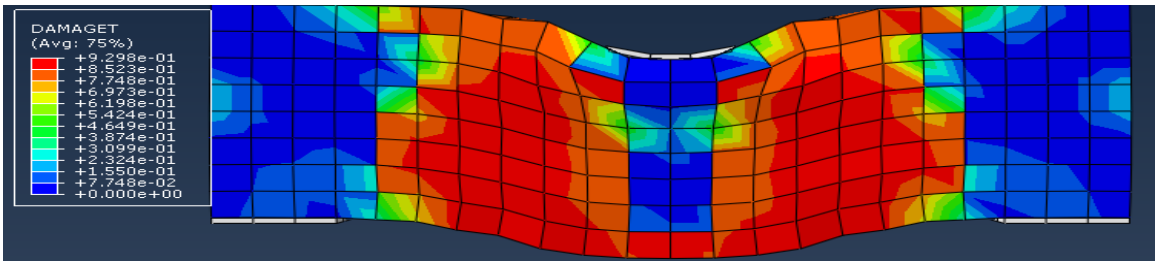

f) Fully developed diagonal cracking

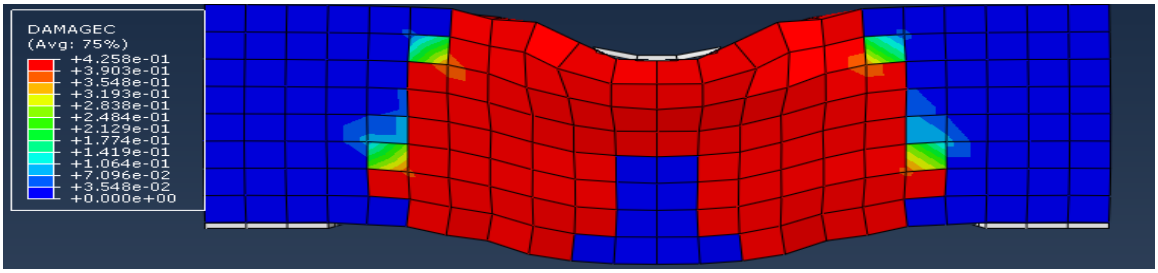

g) Fully failed by web tension plus compression

2) Shear span to depth ratio 1.50

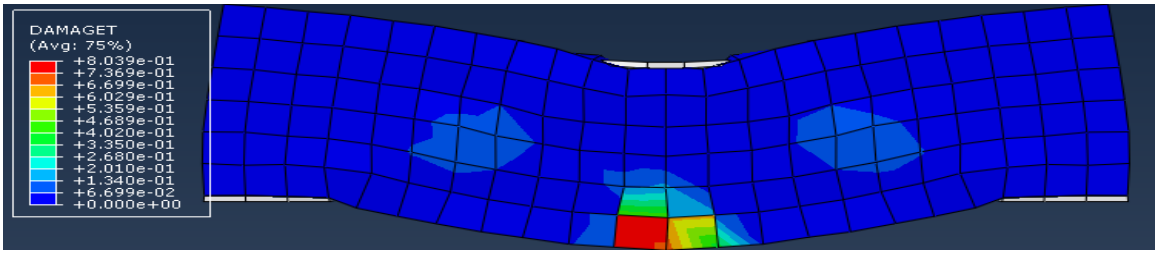

(a) Start of flexural cracking

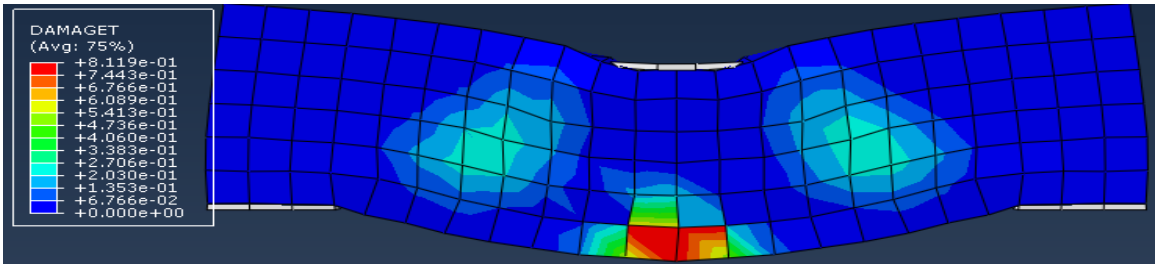

(b) Diagonal web cracking started

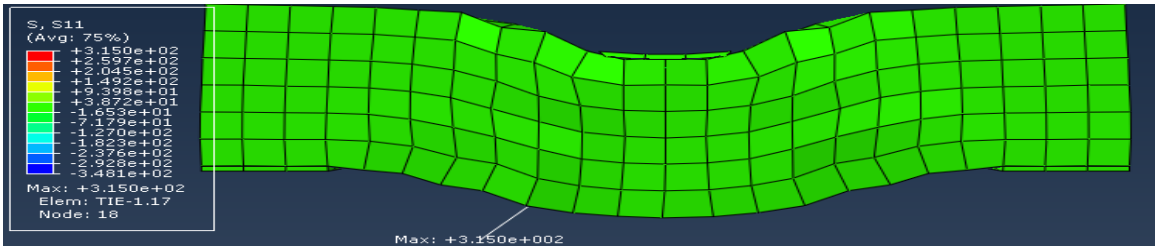

(c) Yielding of main reinforcement by flexure

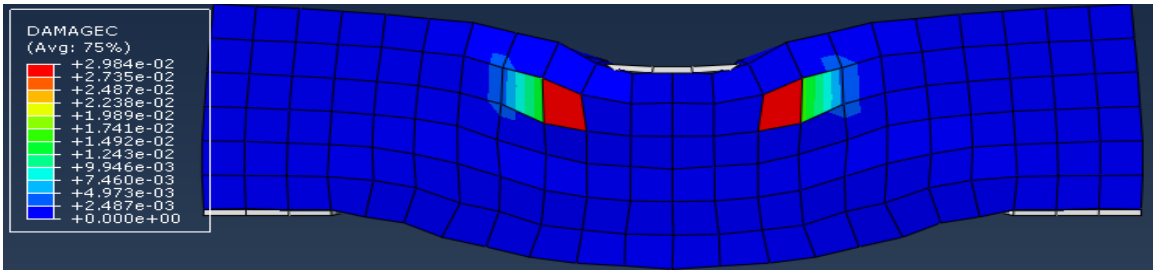

e) Crushing of concrete at loading

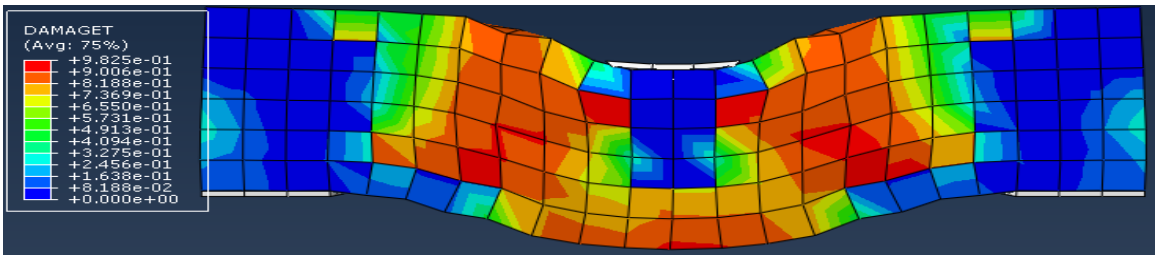

f) Fully developed diagonal cracking

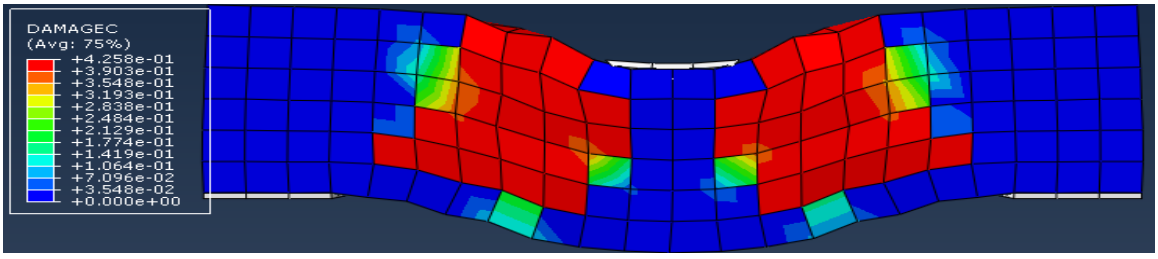

g) Fully failed by web tension plus compression

3) Shear span to depth ratio 1.75

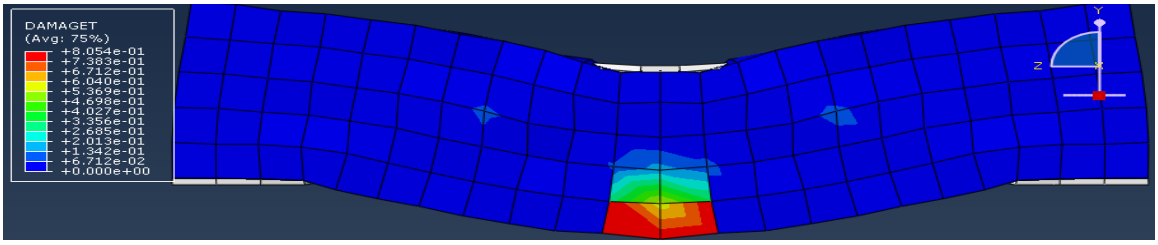

a) Start of flexural cracking

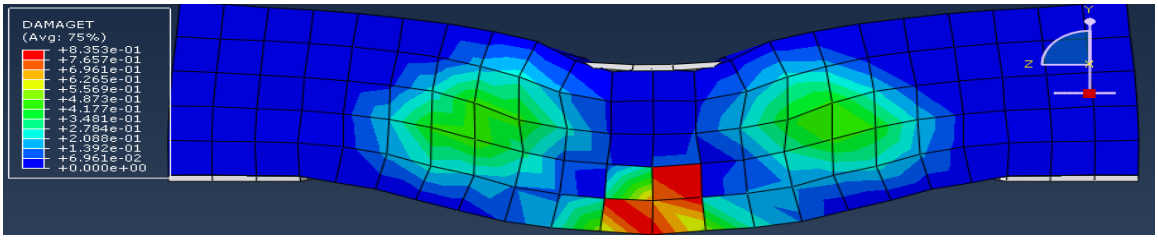

b) Diagonal web cracking started

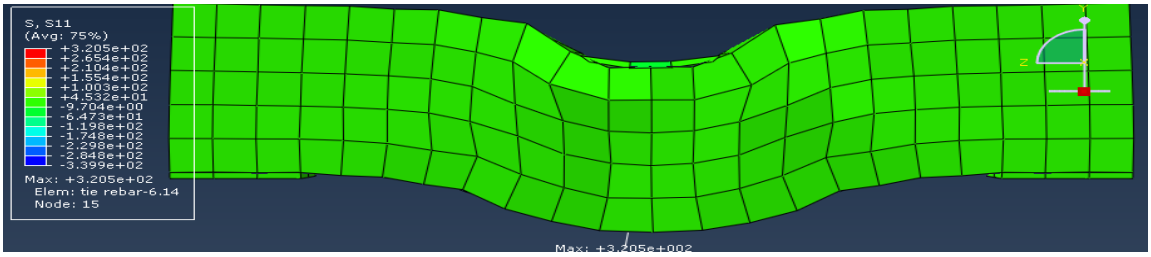

c) Yielding of main reinforcement by flexure

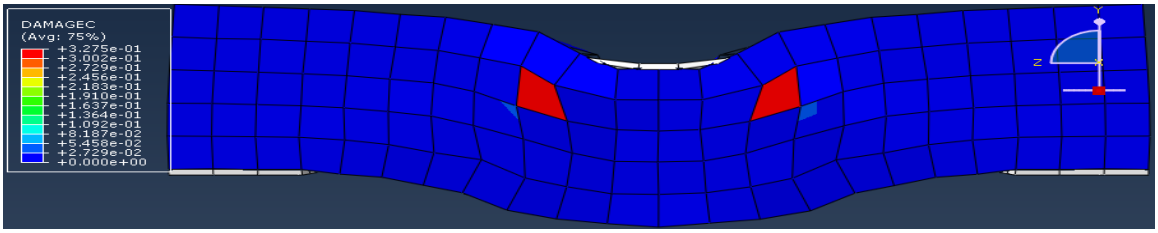

d) Crushing of concrete at loading

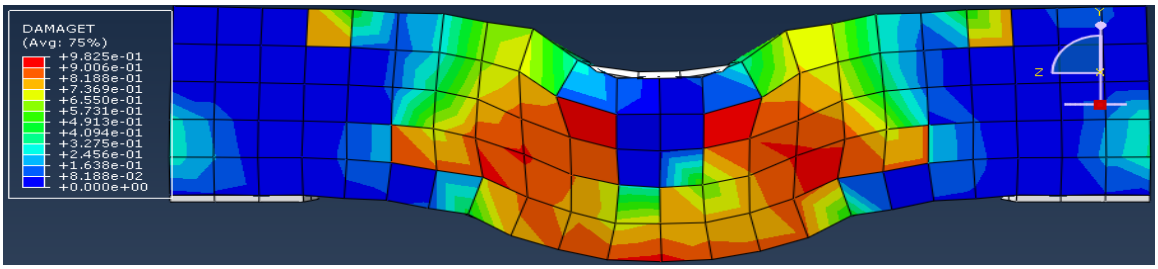

e) Fully developed diagonal cracking

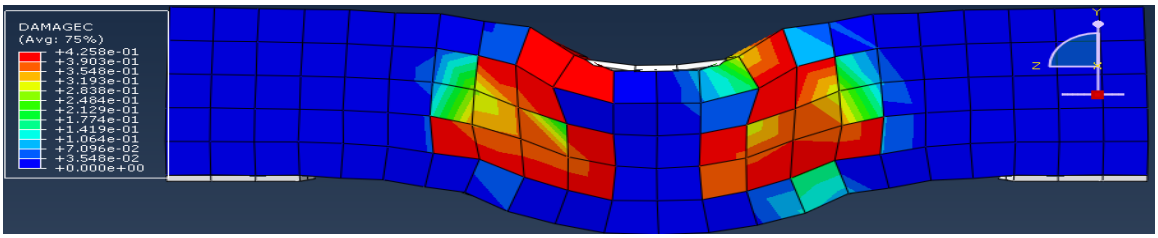

f) Fully failed by web tension plus compression

4) Shear span to depth ratio 2.00

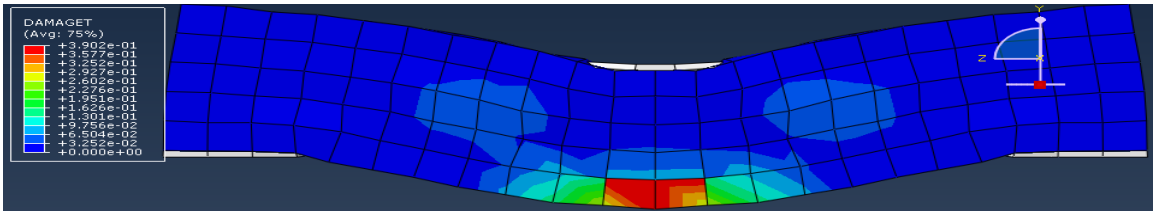

a) Start of flexural cracking

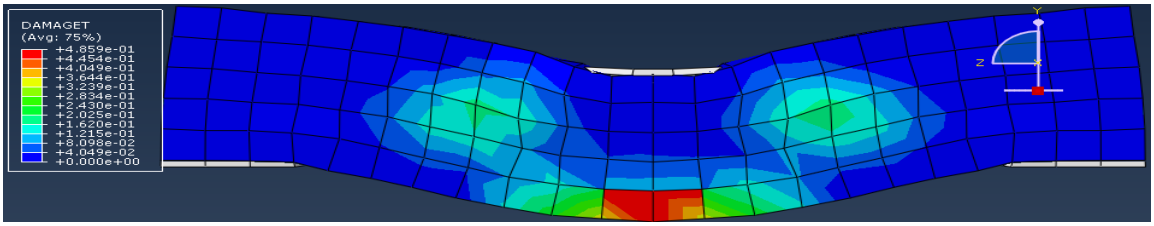

b) Diagonal web cracking started

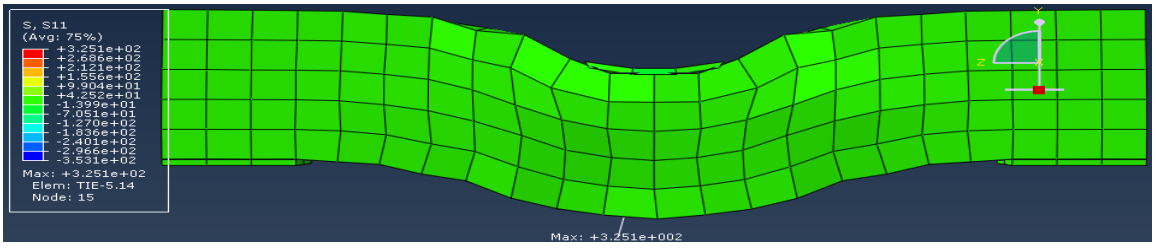

c) Yielding of main reinforcement by flexure

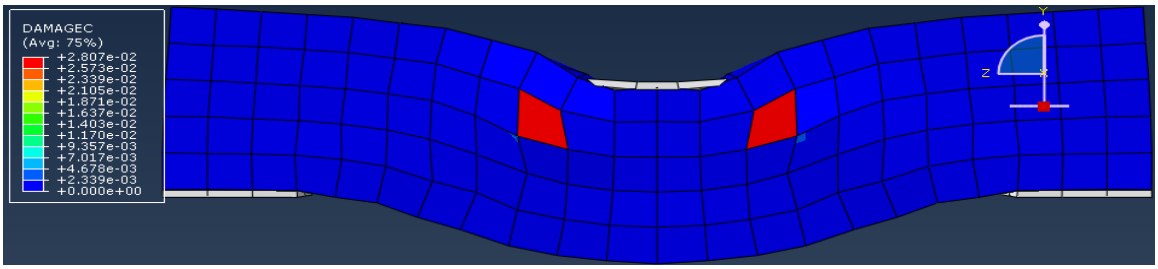

d) Crushing of concrete at loading

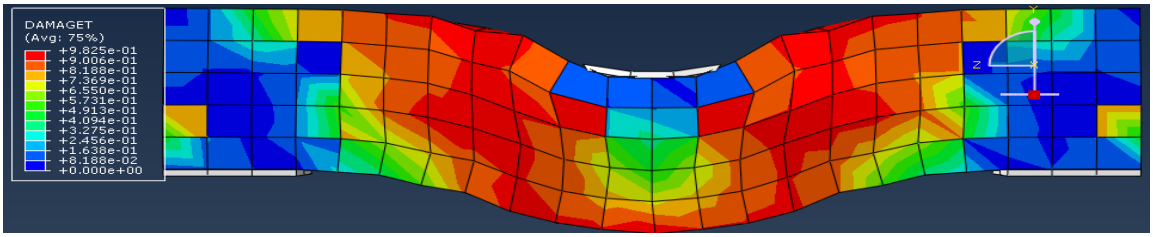

e) Fully developed diagonal cracking

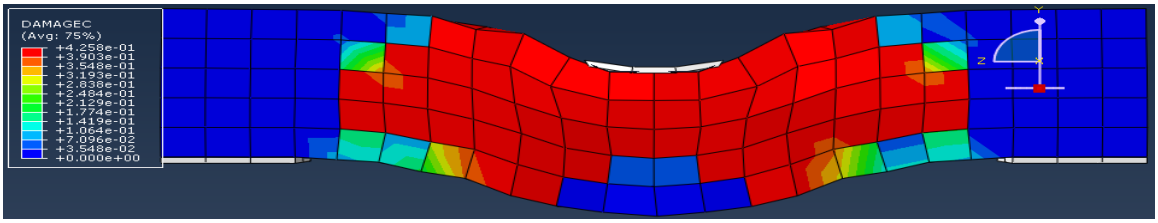

f) Fully failed by web tension plus compression

II) Finite Element Simulations and Failure Stages of Beams Under Category-II

1) Shear span to depth ratio 1.25

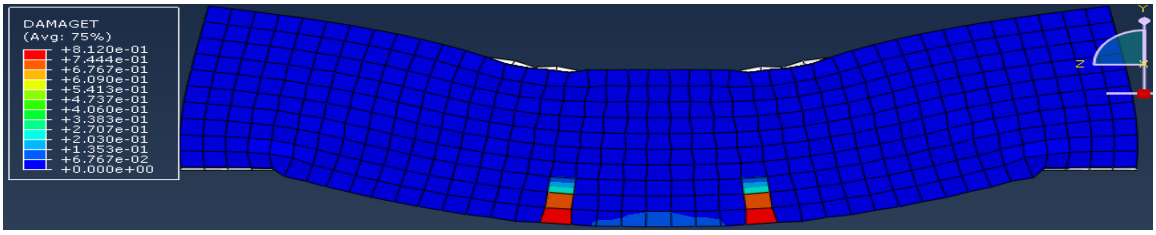

a) Start of flexural cracking

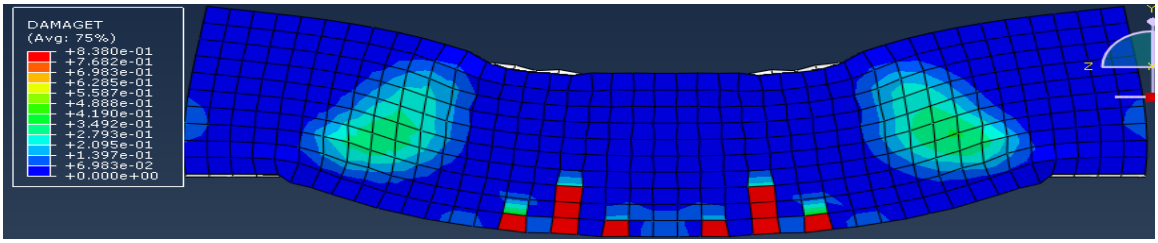

b) Diagonal web cracking started

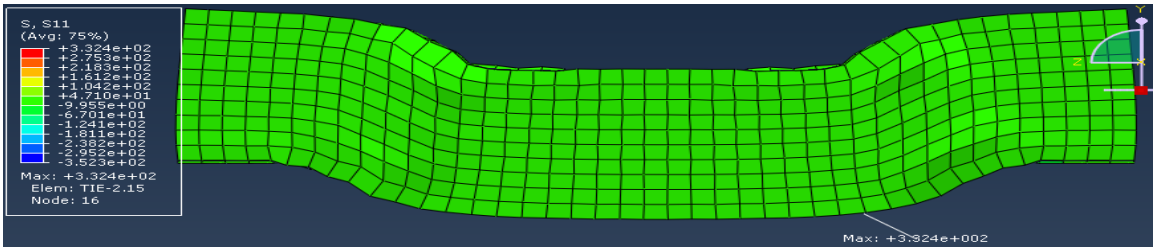

c) Yielding of main reinforcement by flexure

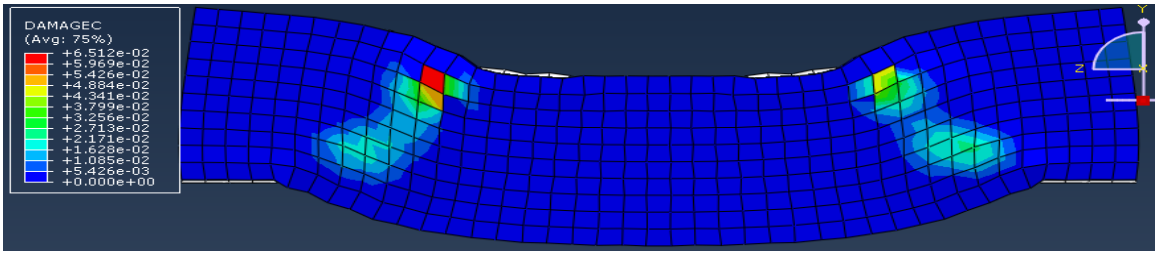

d) Crushing of concrete at loading

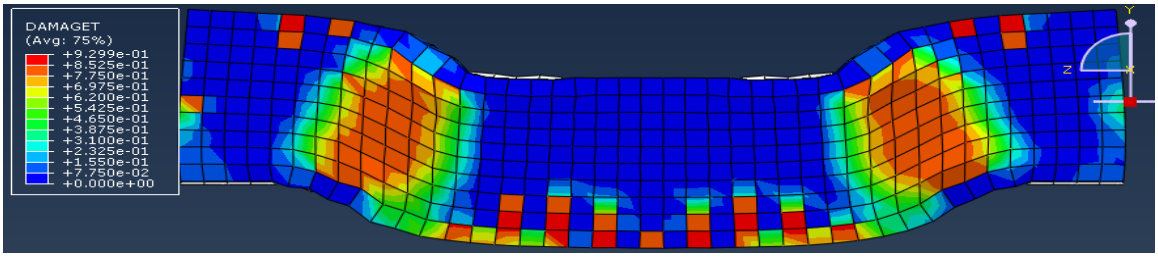

e) Fully developed diagonal cracking

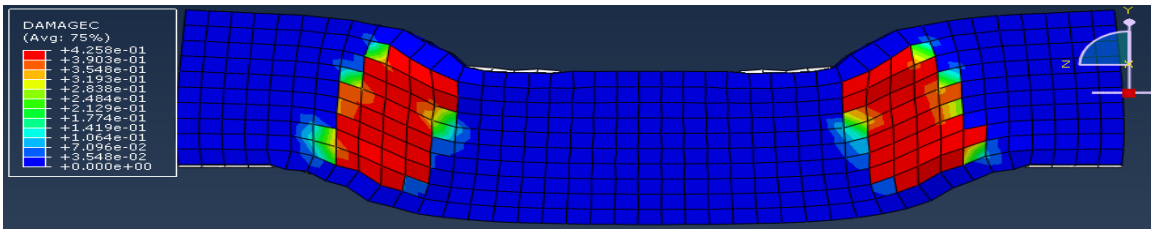

f) Fully failed by web tension plus compression

2) Shear span to depth ratio 1.50

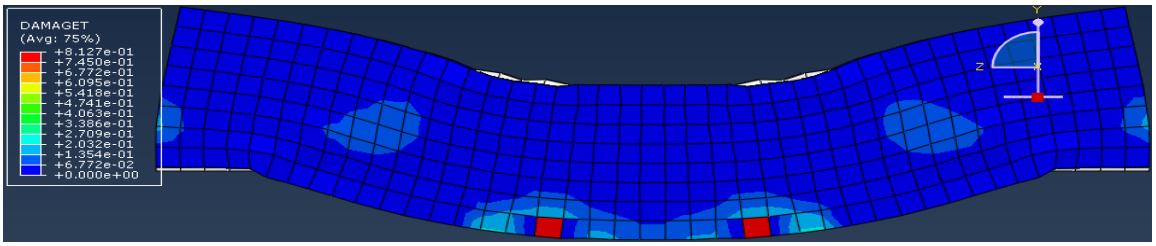

a) Start of flexural cracking

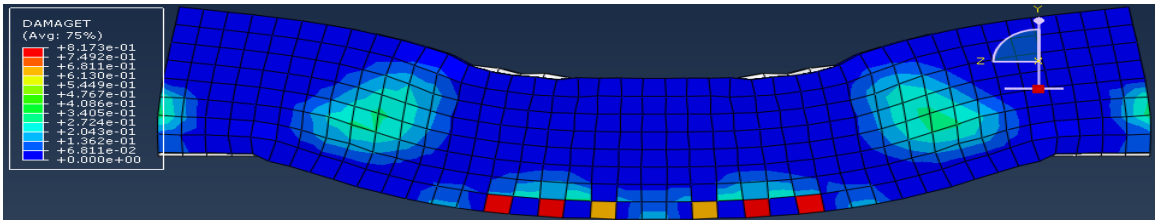

b) Diagonal web cracking started

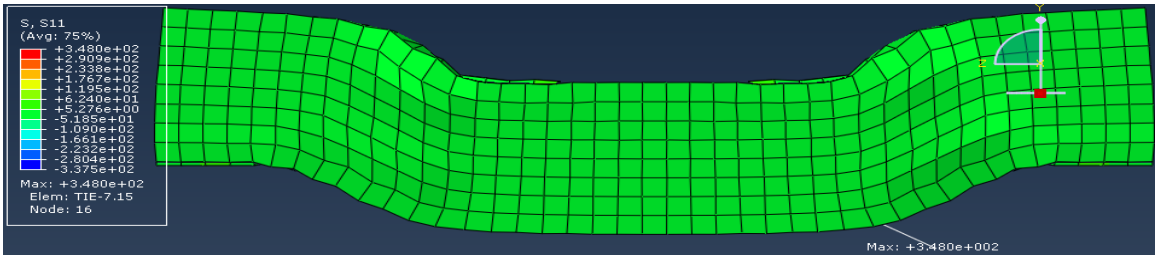

c) Yielding of main reinforcement by flexure

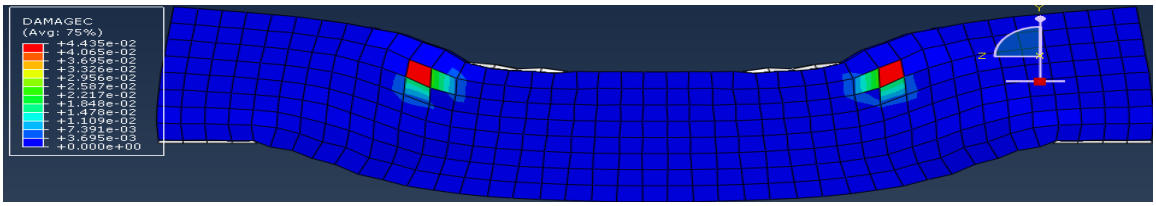

d) Crushing of concrete at loading

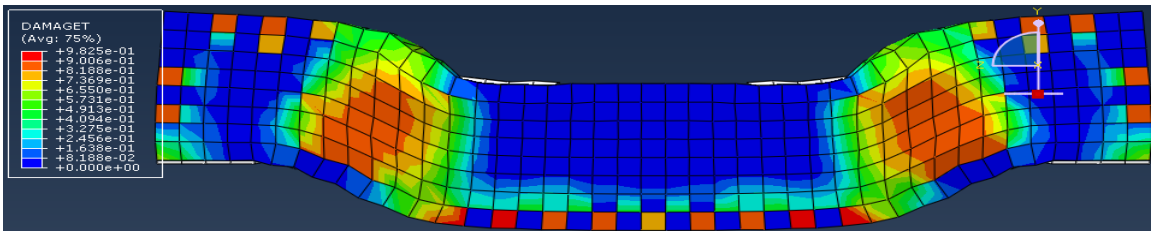

e) Fully developed diagonal cracking

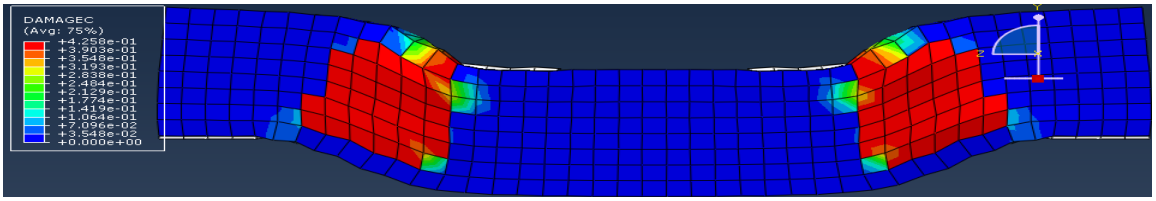

f) Fully failed by web tension plus compression

3) Shear span to depth ratio 1.75

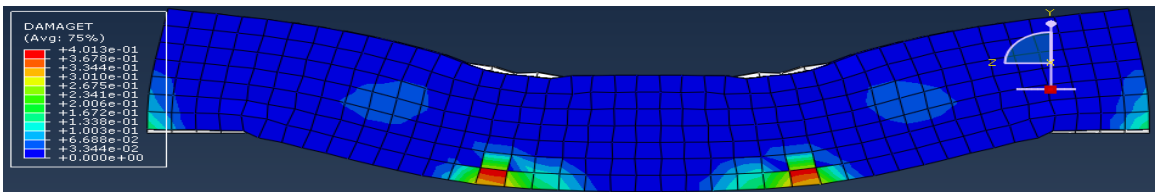

a) Start of flexural cracking

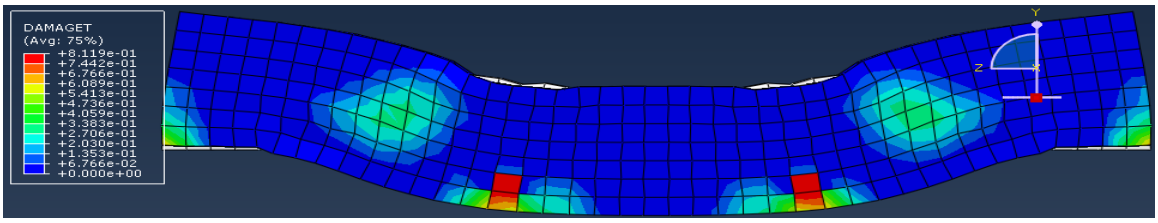

b) Diagonal web cracking started

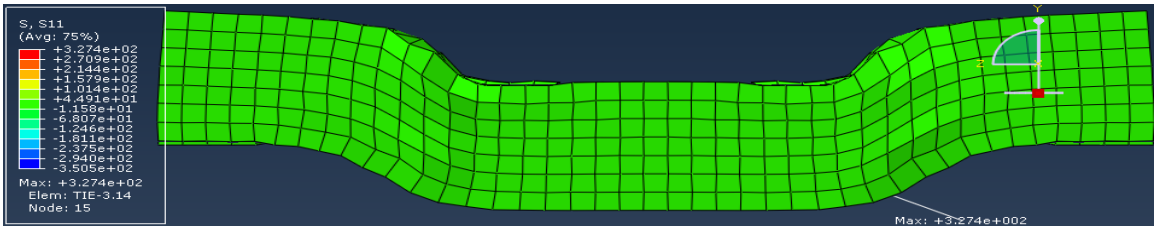

c) Yielding of main reinforcement by flexure

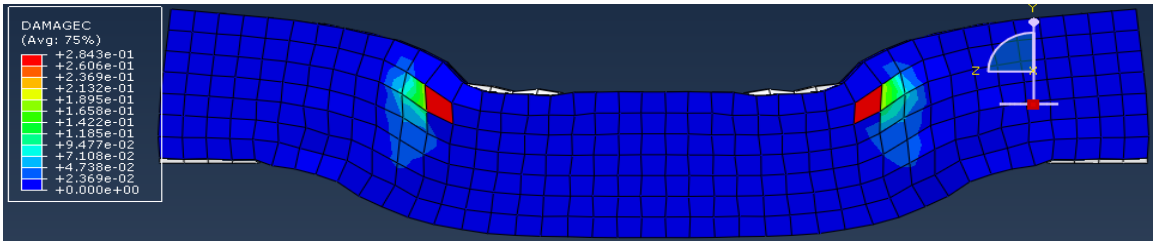

d) Crushing of concrete at loading

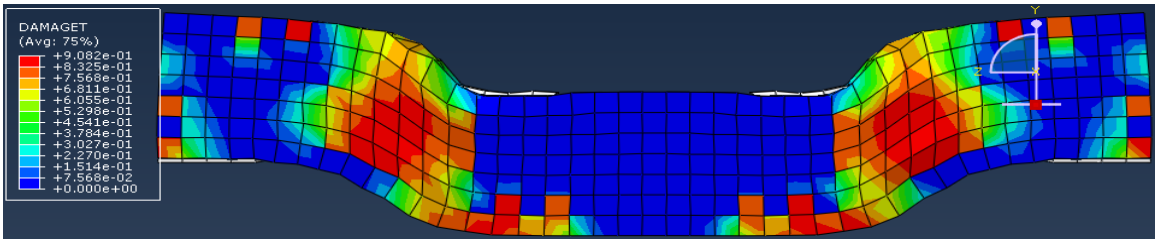

e) Fully developed diagonal cracking

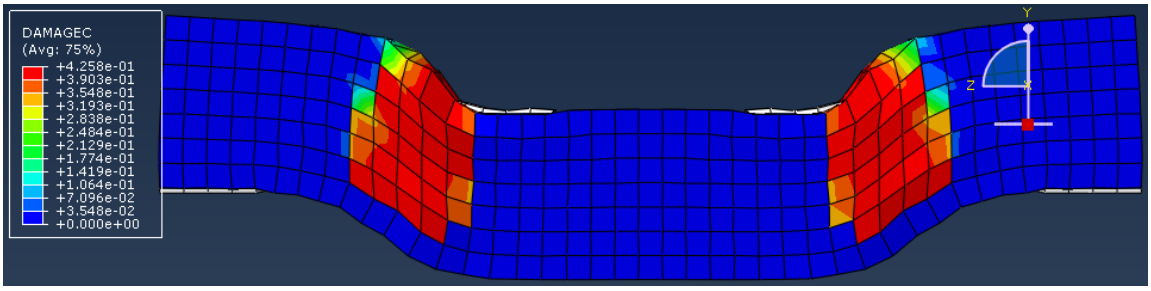

f) Fully failed by web tension plus compression

4) Shear span to depth ratio 2.00

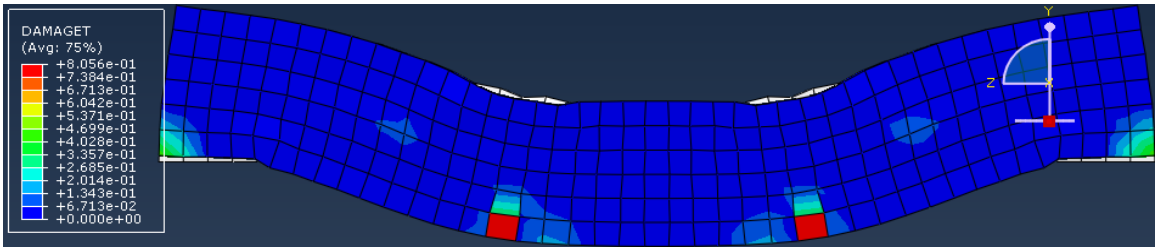

a) Start of flexural cracking

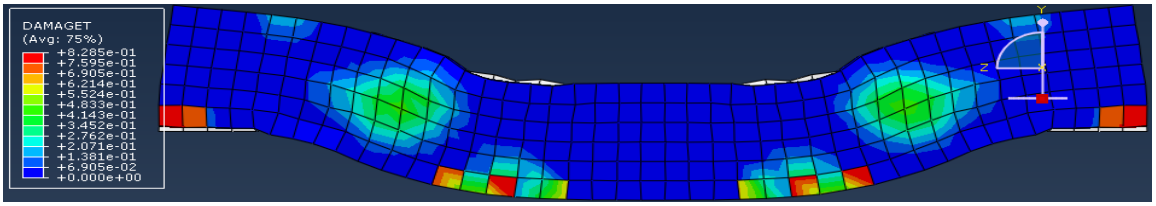

b) Diagonal web cracking started

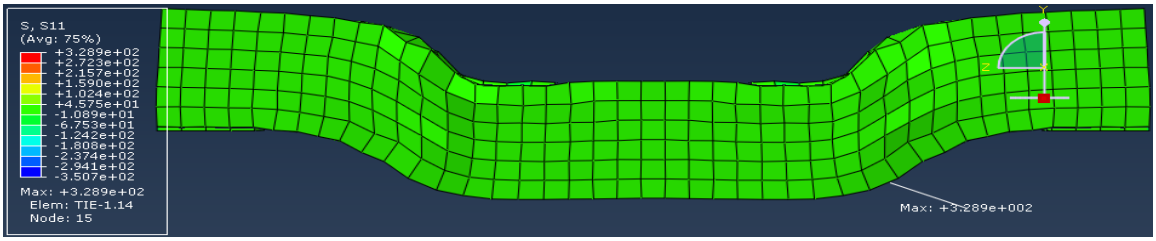

c) Yielding of main reinforcement by flexure

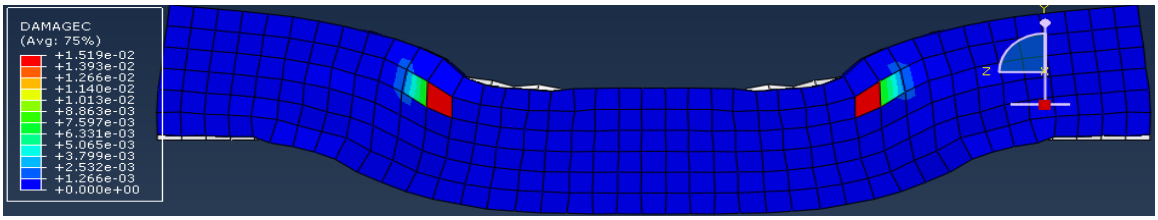

d) Crushing of concrete at loading

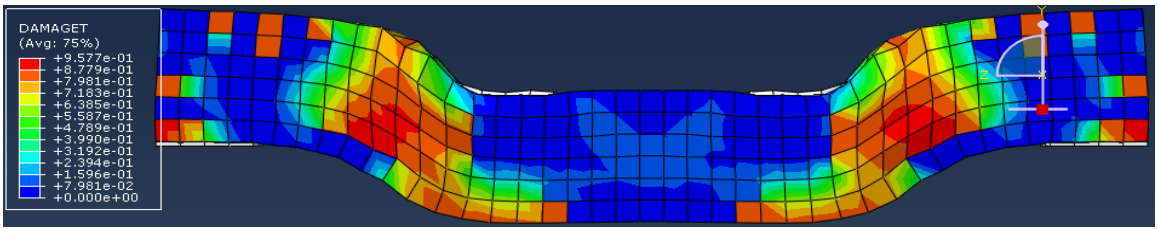

e) Fully developed diagonal cracking

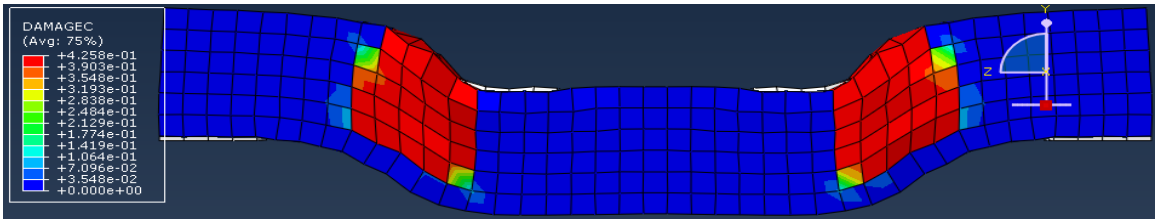

f) Fully failed by web tension plus compression

III) Finite Element Simulations and Failure Stages of Beams Under Category-III

1) Shear span to depth ratio 1.25

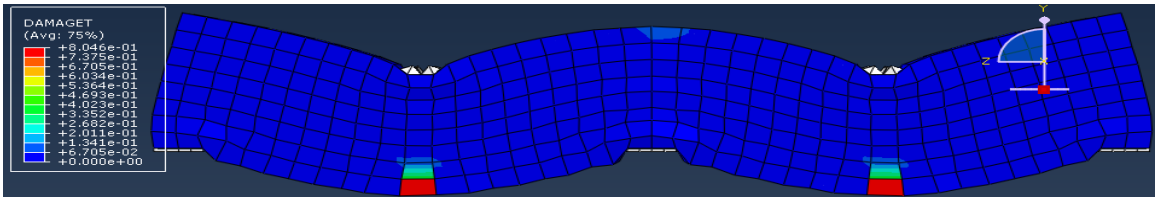

a) Start of flexural cracking

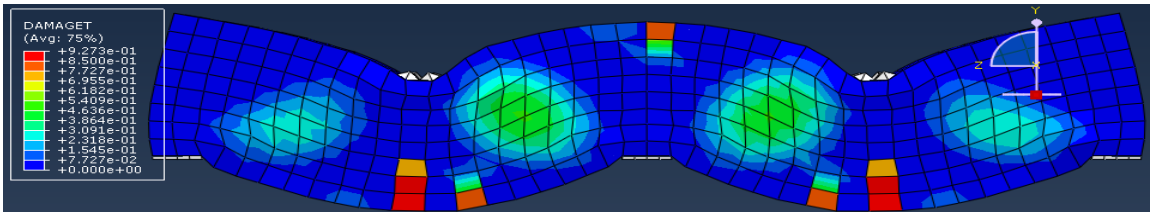

b) Diagonal web cracking started

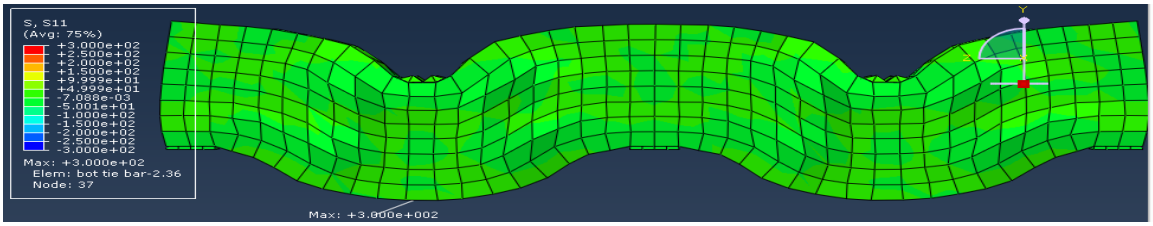

c) Yielding of main reinforcement by flexure

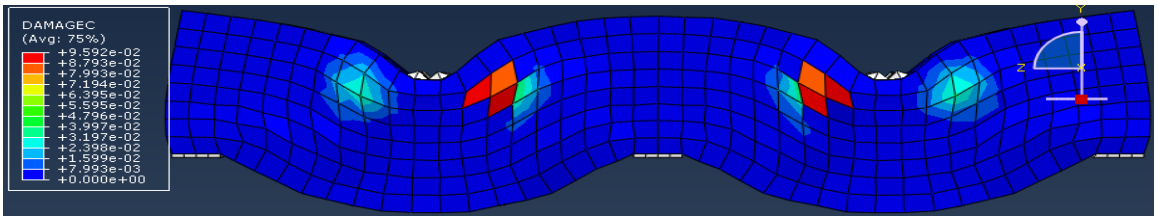

d) Crushing of concrete at loading

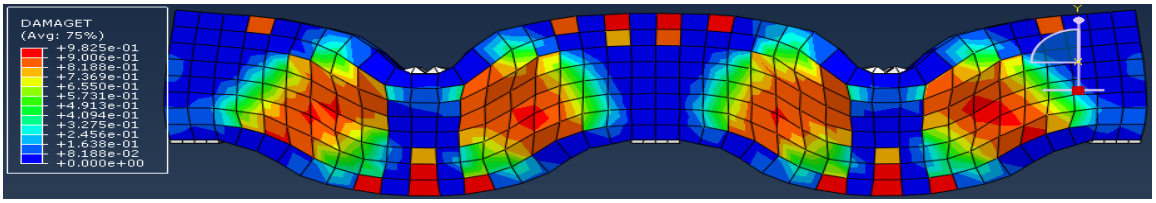

e) Fully developed diagonal cracking

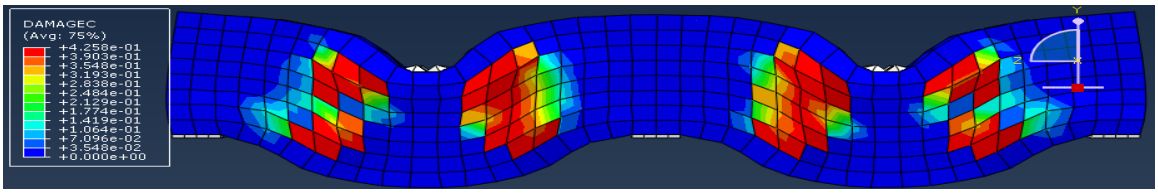

f) Fully failed by web tension plus compression

2) Shear span to depth ratio 1.50

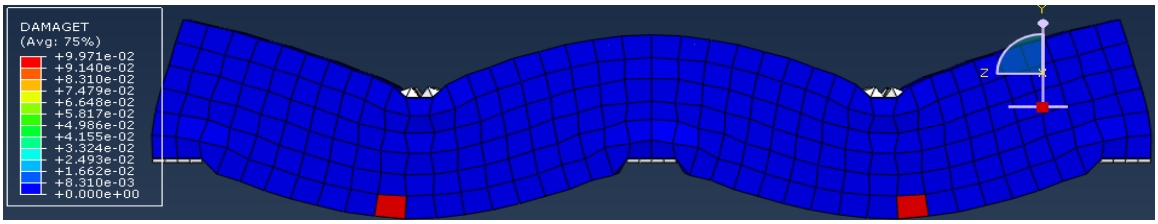

a) Start of flexural cracking

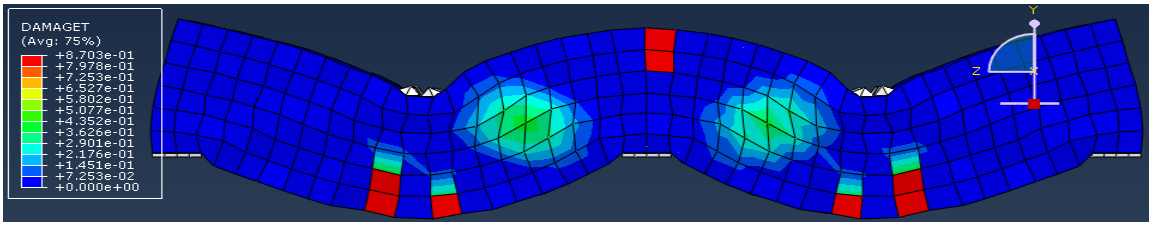

b) Diagonal web cracking started

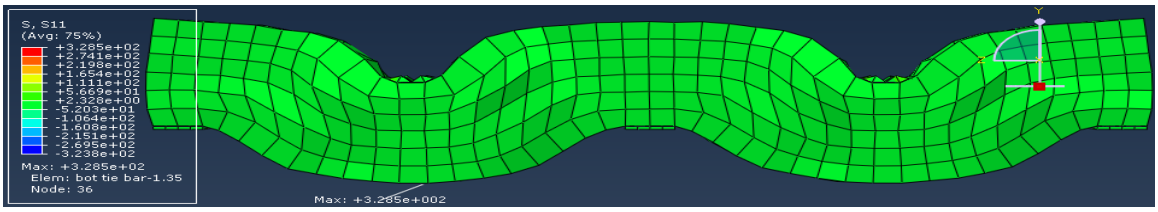

c) Yielding of main reinforcement by flexure

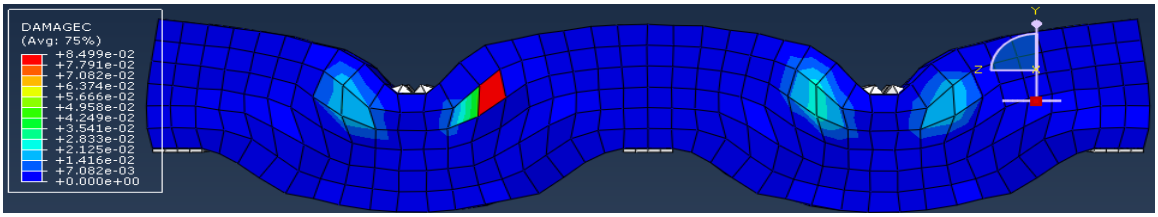

d) Crushing of concrete at loading

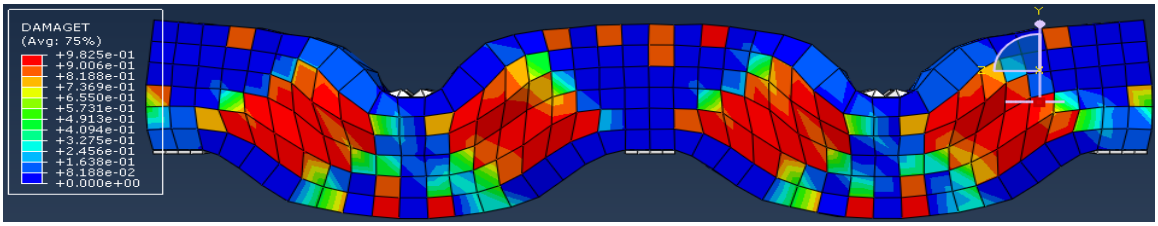

e) Fully developed diagonal cracking

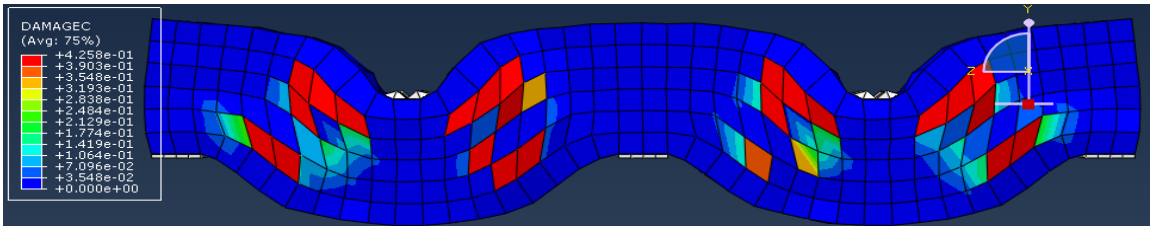

f) Fully failed by web tension plus compression

3) Shear span to depth ratio 1.75

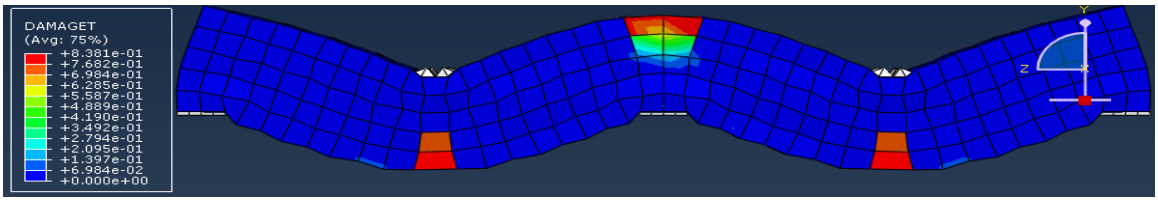

a) Start of flexural cracking

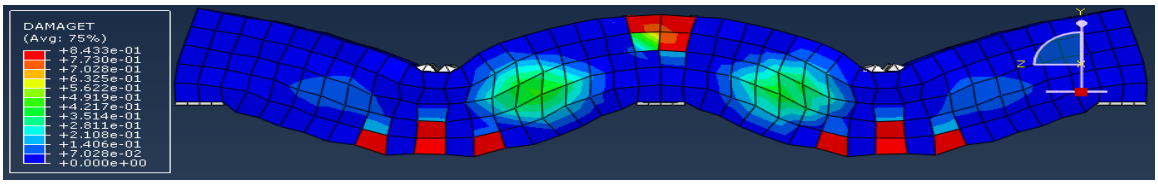

b) Diagonal web cracking started

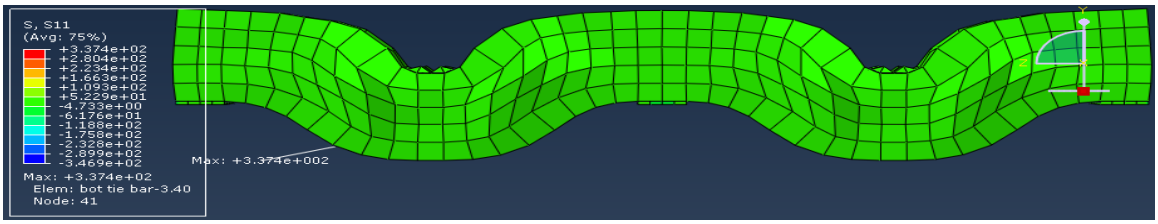

c) Yielding of main reinforcement by flexure

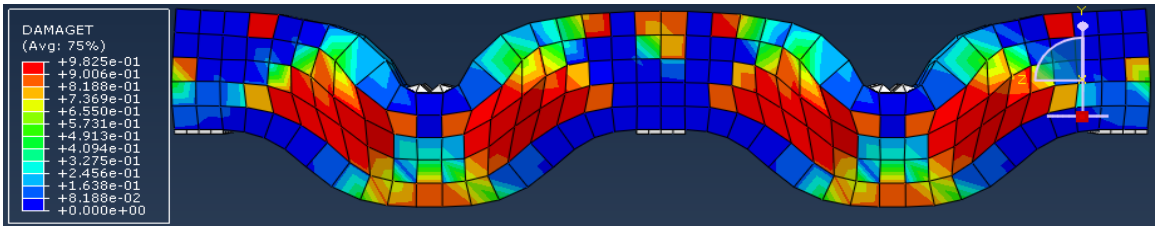

d) Crushing of concrete at loading

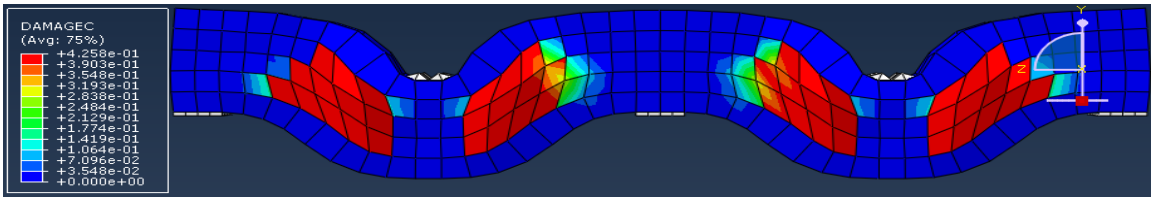

e) Fully developed diagonal cracking

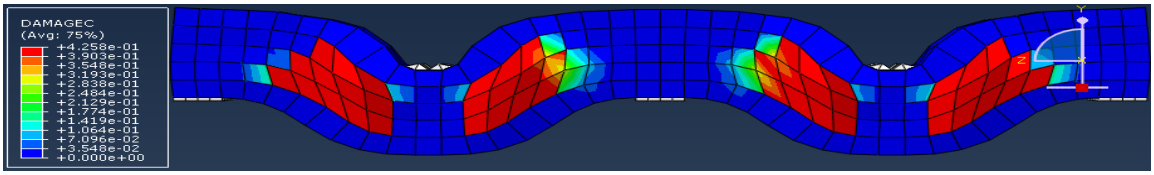

f) Fully failed by web tension plus compression

4) Shear span to depth ratio 2.00

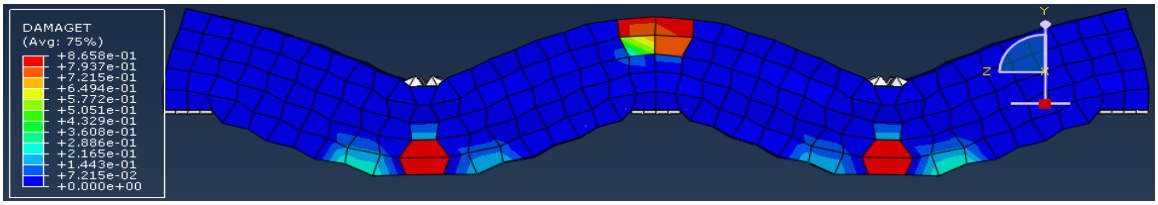

a) Start of flexural cracking

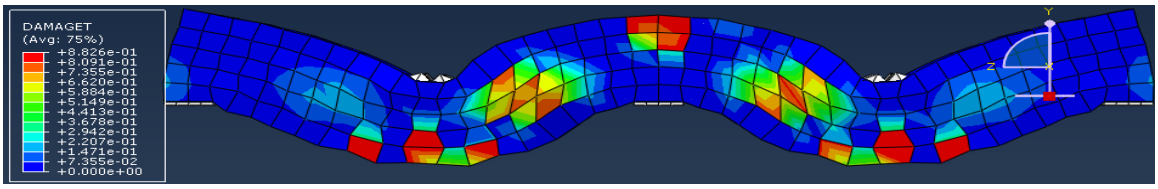

b) Diagonal web cracking started

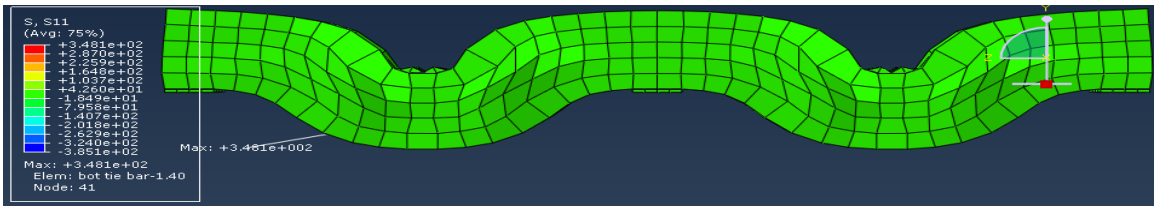

c) Yielding of main reinforcement by flexure

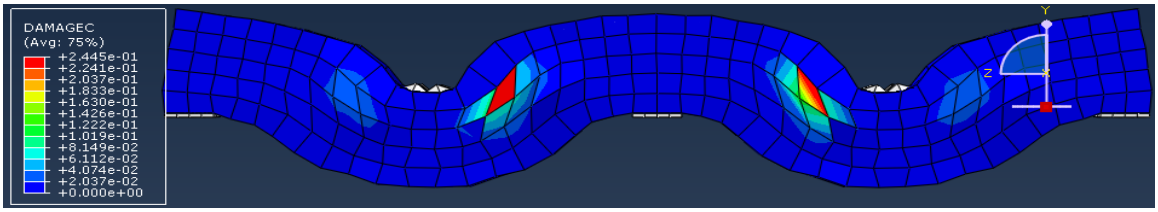

d) Crushing of concrete at loading

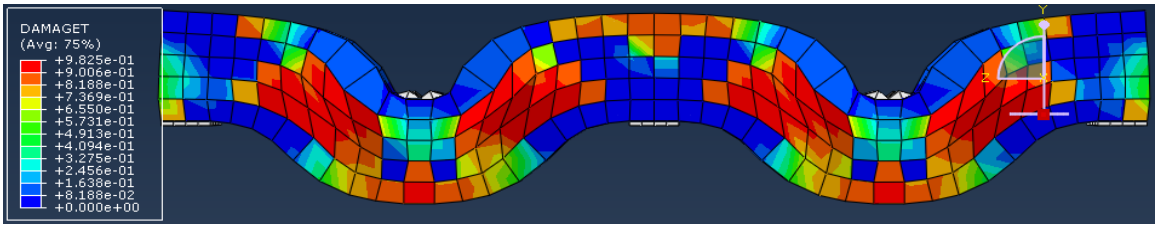

e) Fully developed diagonal cracking

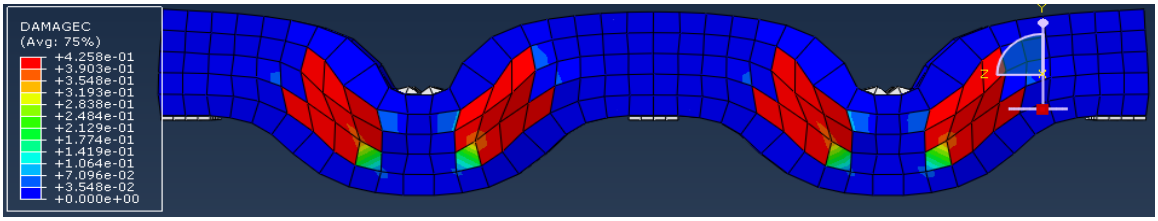

f) Fully failed by web tension plus compression